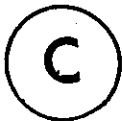


THE SPECTROSCOPY AND PHOTOPHYSICS OF STYRENE

by



DAVID ANTHONY CONDIRSTON, B.Sc.

A Thesis

Submitted to the School of Graduate Studies

in Partial Fulfillment of the Requirements

for the Degree

Doctor of Philosophy

McMaster University

September, 1979

THE SPECTROSCOPY AND PHOTOPHYSICS OF STYRENE



DOCTOR OF PHILOSOPHY
(Chemistry)

McMaster University
Hamilton, Ontario

TITLE: The Spectroscopy and Photophysics of Styrene

AUTHOR: David Anthony Condirston, B.Sc. (Brock University)

SUPERVISOR: Dr. J.D. Laposa

NUMBER OF PAGES: xi, 162

ABSTRACT:

The infrared and Raman spectra of liquid styrene, styrene-d₃, styrene-d₅ and styrene-d₈ have been analyzed. Assignments have been made for the 42 normal modes of vibration in each molecule. The fluorescence and fluorescence excitation spectra of solutions of the four isotopic styrenes have been studied in a polycrystalline methylcyclohexane matrix at 77 K. Vibrational analysis of the fluorescence spectra indicate that the \bar{A} state of styrene is planar. The $\bar{A}-\bar{X}$ transition moment is a-axis polarized, in contrast to what has been found in several other monosubstituted benzenes. The fluorescence excitation spectra have also been vibrationally analyzed, and several excited state fundamental frequencies have been assigned.

The fluorescence decay time and quantum yield of each of the four styrenes have been determined, in cyclohexane at room temperature and in 3-methylpentane at room temperature and at 77 K. The radiative rate constant is essentially independent of isotope, solvent and temperature. The non-radiative rate constant decreases only very slightly upon deuteration and by about 50% upon cooling. These results are compared with similar data of a related compound, trans-stilbene.

Triplet-triplet electronic energy transfer studies at 77K using acetophenone as sensitizer indicate the presence of a rapid non-radiative decay pathway from triplet styrene.

ACKNOWLEDGEMENTS

I would like to thank my research director, Dr. J.D. Laposa, for the guidance and helpful advice that he was only too happy to give. I wish him success in all his future endeavors.

To my colleagues Halvidar Singh, Vince Morrison, Bob Nalepa and Dave Evans, I extend my gratitude for their willingness to impart the fruits of their experience to me, and also for their friendship.

I am grateful to the Department of Chemistry for their financial support during my stay at McMaster.

Finally to my wife Kerry, who skilfully typed this thesis and whose constant encouragement helped me to get the damn thing finished, I owe a lasting debt of gratitude.

TABLE OF CONTENTS

		Page
CHAPTER 1	INTRODUCTION	1
	1.1 General.....	1
	1.2 Previous Spectroscopic and Phtotphys- ical Work on Styrene.....	2
	1.3 Aims of the Present Work.....	7
CHAPTER 2	THEORY AND BACKGROUND	10
	2.1 The Wave Equation.....	10
	2.2 Spectroscopic Transitions.....	10
	2.3 The Theory of Electronic Spectra.....	11
	2.3.1 Allowed Transitions.....	11
	2.3.2 Vibronic Interactions.....	13
	2.4 Theory of Vibrational Spectra.....	15
	2.4.1 Normal Co-ordinates, Vibrational Wavefunctions and Symmetry Considerations.....	15
	2.4.2 Depolarization Ratios.....	20
	2.4.3 Teller-Redlich Product Rule.....	20
	2.5 The Fate of Absorbed Energy.....	21
	2.6 Fluorescence Excitation.....	24
	2.7 Fluorescence Quantum Yields.....	25
	2.8 Singlet Decay Times.....	27
	2.9 Polycrystalline Matrices and the Shpol'skii Effect.....	30
	2.10 Triplet-Triplet Energy Transfer in Rigid Solution.....	30

	Page
CHAPTER 3 EXPERIMENTAL	32
3.1 Chemicals.....	32
3.2 Spectra.....	35
3.2.1 Infrared Spectra.....	35
3.2.2 Raman Spectra.....	36
3.2.3 Fluorescence and Fluorescence Excitation Spectra.....	36
3.2.4 Absorption Spectra.....	40
3.3 Measurement of Singlet Lifetimes.....	40
3.4 Determination of Fluorescence Quantum Yields.....	47
3.5 Triplet-Triplet Energy Transfer Work..	51
CHAPTER 4 ANALYSIS OF THE INFRARED AND RAMAN SPECTRA	52
4.1 Introduction.....	52
4.2 Normal Vibrations of Styrene.....	52
4.3 Analysis.....	55
4.3.1 Vibrations Common to Monosubsti- tuted Benzenes.....	61
4.3.2 Vinyl Group Modes.....	76
4.4 Teller-Redlich Product Ratios.....	81
CHAPTER 5 ANALYSIS OF THE FLUORESCENCE AND FLUOR- ESCENCE EXCITATION SPECTRA	98
5.1 Vibrational Analysis of the Fluores- cence of the Styrenes.....	98
5.2 Analysis of the Fluorescence Excita- tion Spectra and the Symmetry of the First Excited Singlet State of Styrene	118
5.3 Discussion of the Fluorescence of the Styrenes.....	131

	Page
CHAPTER 6 PHOTOPHYSICS OF THE STYRENES	136
CHAPTER 7 SUMMARY	147
BIBLIOGRAPHY	151

LIST OF TABLES

		Page
Table 3.1	Singlet Decay Times of some Standard Substances.....	46
Table 4.1	Previously Assigned Ground State Fundamentals of Styrene-h ₈	53
Table 4.2	Approximate Descriptions of the Normal Vibrations of Styrene.....	56
Table 4.3	Expected Frequency Regions for the Normal Vibrations of Monosubstituted Benzenes....	67
Table 4.4	Vibrational Analysis of the Infrared and Raman Spectra of C ₆ H ₅ CHCH ₂ and C ₆ H ₅ CDCD ₂ ..	82
Table 4.5	Vibrational Analysis of the Infrared and Raman Spectra of C ₆ D ₅ CHCH ₂ and C ₆ D ₅ CDCD ₂ ..	88
Table 4.6	Ground State Fundamentals of the Styrenes.	93
Table 4.7	Teller-Redlich Product Ratios for a' Modes in the Styrenes.....	96
Table 4.8	a _{1g} b ₂ Teller-Redlich Product Ratios for Some Monosubstituted Benzenes.....	96
Table 5.1	Vibrational Analysis of the Fluorescence Spectra of 10 ⁻⁴ M C ₆ H ₅ CHCH ₂ and C ₆ H ₅ CDCD ₂ in Polycrystalline Methylcyclohexane at 77 K.....	104
Table 5.2	Vibrational Analysis of the Fluorescence Spectra of 10 ⁻⁴ M C ₆ D ₅ CHCH ₂ and C ₆ D ₅ CDCD ₂ in Polycrystalline Methylcyclohexane at 77 K.....	113
Table 5.3	0,0 Shifts from Vapor to Solid Solution in Some Substituted Benzenes.....	124
Table 5.4	Vibrational Analysis of the Fluorescence Excitation Spectra of 10 ⁻⁵ M C ₆ H ₅ CHCH ₂ and C ₆ H ₅ CDCD ₂ in Polycrystalline Methylcyclohexane at 77 K.....	126
Table 5.5	Vibrational Analysis of the Fluorescence Excitation Spectra of 10 ⁻⁵ M C ₆ D ₅ CHCH ₂ and C ₆ D ₅ CDCD ₂ in Polycrystalline Methylcyclohexane at 77 K.....	127

	Page
Table 5.6 . Excited State Fundamental Frequencies of Some Monosubstituted Benzenes.....	128
Table 6.1 . Fluorescence Lifetimes, Quantum Yields and Rate Constants for the Styrenes.....	137

LIST OF FIGURES

		Page
Figure 2.1	Jablonski Diagram Showing Principal Photophysical Processes in Complex Molecules.....	23
Figure 3.1	Block Diagram of Emission Apparatus.....	37
Figure 3.2	Block Diagram of Fluorescence Lifetime Apparatus.....	41
Figure 3.3	Nanosecond Discharge Lamp used for Measurement of Fluorescence Lifetimes.....	42
Figure 3.4	Optical System in Fluorescence Lifetime Apparatus.....	44
Figure 3.5	Sensitivity Correction Curve for Photomultiplier-Monochromator Combination.....	50
Figure 4.1	Some Normal Vibrations of Monosubstituted Benzenes.....	58
Figure 4.2	Some Normal Vibrations of Monosubstituted Ethylenes.....	59
Figure 4.3	The Infrared Absorption Spectra of Liquid $C_6H_5CHCH_2$ and $C_6H_5CDCD_2$	62
Figure 4.4	The Infrared Absorption Spectra of Liquid $C_6D_5CHCH_2$ and $C_6D_5CDCD_2$	63
Figure 4.5	The Raman Spectra of Liquid $C_6H_5CHCH_2$ and $C_6H_5CDCD_2$	64
Figure 4.6	The Raman Spectra of Liquid $C_6D_5CHCH_2$ and $C_6D_5CDCD_2$	65
Figure 5.1	The Uncorrected Fluorescence Spectra of 10^{-4} M $C_6H_5CHCH_2$ and $C_6H_5CDCD_2$ in Polycrystalline Methylcyclohexane at 77 K.....	103
Figure 5.2	The Uncorrected Fluorescence Spectra of 10^{-4} M $C_6D_5CHCH_2$ and $C_6D_5CDCD_2$ in Polycrystalline Methylcyclohexane at 77 K.....	112
Figure 5.3	The Uncorrected Fluorescence Excitation Spectra of 10^{-3} M $C_6H_5CHCH_2$, $C_6H_5CDCD_2$, $C_6D_5CHCH_2$ and $C_6D_5CDCD_2$ in Polycrystalline Methylcyclohexane at 77 K.....	120

	Page
Figure 5.4 The $\tilde{A}+\tilde{X}$ Vapor Phase Absorption Spectra of $C_6H_5CHCH_2$ and $C_6H_5CDCD_2$	122
Figure 5.5 The $\tilde{A}+\tilde{X}$ Vapor Phase Absorption Spectra of $C_6D_5CHCH_2$ and $C_6D_5CDCD_2$	123
Figure 6.1 Plot of $1/\tau_p$ for Acetophenone <u>vs</u> Styrene Concentration.....	145

CHAPTER ONE

INTRODUGTION

1.1 General

Molecular spectroscopy is the study of the absorption or emission of electromagnetic radiation by molecules. Spectroscopy is one of the most powerful tools that a chemist has at his disposal for the elucidation of molecular structure. There are several different branches of spectroscopy, depending on the amount of energy involved in the absorption or emission process. Microwave spectroscopy deals with transitions between the various rotational levels of the molecule and can yield, for suitable molecules, precise information on internuclear distances and bond angles. Infrared spectroscopy, complemented by the Raman scattering process, enables one to gain knowledge of molecular symmetry, bond and angle force constants, and moments of inertia. Electronic spectroscopy can give qualitative or quantitative information on the structure of the various excited electronic states of molecules.

One particularly useful type of emission process is photoluminescence, which can be described as the process of light emission subsequent to light absorption. Usually the energy of light used for excitation of the sample is in the ultraviolet or visible range, making the sample molecules electronically excited. In addition to obtaining emission spectra, spectroscopists, as well as those in other fields such as physics and biochemistry, are also interested in the kinetics of photoluminescent process. Excited state

lifetimes and luminescence quantum yields are the most important photophysical parameters that one needs in order to elucidate the processes involved in the deactivation of an excited electronic state.

Since the luminescence studies of Stark⁽¹⁾ on liquid benzene and Stark and Meyer⁽²⁾ on benzene derivatives at the beginning of this century, these and other aromatic molecules have been the subject of continuing investigation into their luminescent and photophysical properties. A particularly interesting class of monosubstituted derivatives of benzene are those in which the substance is a multiply-bonded species directly attached to the aromatic ring. Recently there have been several spectroscopic studies done on the three isoelectric molecules benzonitrile ($C_6H_5C\equiv N$), phenylacetylene ($C_6H_5C\equiv CH$), and phenylisocyanide ($C_6H_5N\equiv C$), both gas phase electronic absorption⁽³⁻⁷⁾ and luminescence from polycrystalline matrices at low temperature⁽⁸⁻¹⁰⁾. A molecule which is similar to these, but which is also the simplest aromatic molecule that can undergo both luminescence and geometric isomerization subsequent to excitation, is the styrene molecule ($C_6H_5CH=CH_2$). It is the spectroscopy and photophysics of this compound that is the subject of the present work.

1.2 Previous Spectroscopic and Photophysical Work On Styrene

The first attempt at an analysis of the vibrational spectra of styrene was made by Pitzer et al⁽¹¹⁾ using the infrared spectra recorded by Stair and Coblentz⁽¹²⁾ and

Williams⁽¹³⁾ and the Raman Spectra of Bourguel^(14,15) and Mizushima et al⁽¹⁶⁾. Roy⁽¹⁷⁾ reported the Raman spectrum of styrene but did not attempt to assign any observed bands to specific normal vibrations. More recently, Fateley and co-workers⁽¹⁸⁾ and Moss and Zundel⁽¹⁹⁾ have made fairly complete analyses of the $C_6H_5CHCH_2$ vibrational spectra, each group assigning at least 35 of the 42 normal modes of vibration. The latter authors also recorded the infrared and Raman spectra of styrene- d_8 ($C_6D_5CDCD_2$). No data seems to exist on the vibrational spectra of any other deuterated styrene analogue.* A broad band centered at $\sim 125\text{ cm}^{-1}$ has been observed in the laser Raman spectrum of gas phase styrene⁽²²⁾. The four weak maxima superimposed on this band have been assigned as the (2+0), (3+1), (4+2), and (5+3) overtones of the torsional mode, ν_{42} . A barrier height of 623 cm^{-1} was calculated by fitting the observed frequencies to a potential function of the form $V(\phi) = \sum_{i=1}^{\infty} V_i (1 - \cos i\phi)$.

The 2877 Å system of styrene has been studied in absorption by Robertson, Matsen and Music⁽⁵⁾, Morgan⁽²³⁾, Lombardi and co-workers^(24,25), Hui and Rice⁽²⁶⁾ and very recently by Hollas et al⁽²⁷⁾. Both Robertson et al and Morgan assigned

* Very recently, an analysis of the vibrational spectra of styrene- β - d_2 ($C_6H_5CHCD_2$), based on the work appearing in Chapter 4, has appeared in the literature⁽²⁰⁾. In addition, Green and Harrison⁽²¹⁾ have recently made revisions to some of the previously existing $C_6H_5CHCH_2$ vibrational assignments, and have reanalyzed Moss and Zundel's $C_6D_5CDCD_2$ infrared and Raman spectra. Both of these works were published after the analysis of the vibrational spectra appearing in this work was completed.

the strong band at 2877 Å as the electronic origin. The former group of workers found four upper state fundamental frequencies but did not suggest any interpretation. Morgan⁽²³⁾ found these and five other active excited state vibrational frequencies but again no analysis of the spectrum was put forward. Hartford and Lombardi⁽²⁴⁾ photographed the 2877 Å band under high resolution and found that it is predominantly A-type in character. The changes in the rotational constants upon excitation were consistent with a planar excited state structure. Parker and Lombardi⁽²⁵⁾ observed Stark splittings of some of the rotational features of the 2877 Å band. The small change in dipole moment ($|\Delta\mu| = 0.13D$) was interpreted to show that only slight intramolecular charge transfer takes place upon excitation. Hui and Rice⁽²⁶⁾ have re-examined the vibronic structure in the $\tilde{A}+\tilde{X}$ absorption system of styrene, trans- β -styrene- d_1 , and styrene- d_8 , and by comparison of their spectra with those of phenylacetylene, obtained by King and So⁽⁶⁾, have made the first attempt at assigning some excited state fundamental frequencies to specific normal modes. Very recently, Hollas, Khalilipour, and Thakur⁽²⁷⁾ have performed a more complete vibrational analysis of the $\tilde{A}+\tilde{X}$ absorption spectra of $C_6H_5CHCH_2$ and $C_6H_5CHCD_2$ *.

The fluorescence spectrum of styrene had been obtained by Marsh⁽²⁸⁾ as early as 1923, and by Titeica⁽²⁹⁾ in 1936. In more recent times, the gas phase fluorescence of styrene

*The analysis of the fluorescence excitation spectra appearing in Chapter 5 was completed and had appeared in the literature before the work by Hollas et al was published.

has been studied by Morgan⁽²³⁾, who used optical excitation, and by Singh⁽³⁰⁾, who employed an electrical discharge to excite the sample. Both workers assigned the band near $34\,760\text{ cm}^{-1}$ as the electronic origin, and analyzed the emission in terms of a number of ground state fundamental frequencies. Korschin, Sundholm and Sundholm⁽³¹⁾ and Penchev and Simeonov⁽³²⁾ have each reported the fluorescence spectrum of styrene in ethanol at 77 K. Whereas the former group observed only five maxima in the spectrum, the latter reported seeing 25 bands. Their spectrum was not presented, however. Grajcar and Baudet⁽³³⁾ have given a vibronic analysis of the fluorescence spectrum of styrene in crystalline pentane solution at 77 K*. In this solvent, 38 vibronic bands were obtained, and the origin of the transition was assigned to a weak band at $34\,323\text{ cm}^{-1}$.

Salisbury and Phillips and co-workers, using the techniques of fluorescence decay and time-resolved emission spectroscopy⁽³⁴⁻³⁶⁾, fluorescence excitation⁽³⁷⁾ and time-resolved fluorescence excitation spectroscopy⁽³⁸⁾, have put forward convincing evidence that styrene and trans- β -methylstyrene vapors, when excited into the \tilde{B} state, undergo relaxation to a "twisted" singlet state which is emissive. Briefly, their major finding was that these molecules exhibited a variation in their fluorescence spectra with the time the photons were observed relative

* The analysis of the fluorescence spectra appearing in Chapter 5 was completed and had been submitted for publication before the work of Grajcar and Baudet appeared in the literature.

6

to the excitation pulse, and a variation in their fluorescence decay rates with emission wavelength. The importance of rotation about the olefinic double bond in causing these effects was inferred from a study of 2-phenylnorborn-2-ene by the time-resolved technique. It was observed for this compound that early and late gated spectra were identical, and the fluorescence decay times were independent of the wavelength of observation.

Gas phase fluorescence quantum yields and lifetimes as a function of excess vibrational energy in the 287.7 nm band system have been obtained Hui and Rice⁽²⁶⁾. Salisbury and Phillips and co-workers⁽³⁶⁾ have determined the fluorescence lifetime of styrene vapor excited at 285.0 nm and have in effect extended the study of Hui and Rice by determining quantum yield and lifetime parameters as a function of excitation wavelength from 287 to 255 nm⁽³⁸⁾. On moving from A state to B state excitation, the fluorescence decay becomes non-exponential, with a weak long-lived component being introduced. This long-lived decay was attributed to emission from the twisted excited state.

The fluorescence quantum yield and lifetime of styrene in cyclohexane solution have been reported by Crosby and Salisbury⁽³⁹⁾ and by Lyons and Turro⁽⁴⁰⁾. Basile⁽⁴¹⁾ and Berlman⁽⁴²⁾ have also reported styrene's fluorescence lifetime in cyclohexane.

1.3 Aims of the Present Work

In recent years there has been some controversy concerning the nature of styrene's first excited electronic state. The problem first arose when Hartford and Lombardi's rotational band contour analysis of the 2877 Å band⁽²⁴⁾ (the origin band, as assigned by Robertson et al⁽⁵⁾ and Morgan⁽²³⁾ in absorption and by Morgan⁽²³⁾ and Singh⁽³⁰⁾ in emission) showed that it is type A in character. That is to say, the direction of the electronic transition moment is almost parallel to the a axis, and the transition is ${}^1A_1 \rightarrow {}^1A_1$ (C_{2v} language is used to indicate styrene's similarity to other monosubstituted benzenes). This result is at variance with the fact that in all other monosubstituted benzenes for which the corresponding 0,0 band has been rotationally analyzed the band has been shown to be type B, indicative of a ${}^1B_2 \rightarrow {}^1A_1$ electronic transition^(6, 43-48). In fact, it has been suggested by King and van Putten⁽⁴⁹⁾ and by Muirhead et al⁽⁷⁾ that the band originally assigned as the 0,0 band is in reality a vibronic band involving one quantum of a b_2 (in C_{2v}) vibration. More recent theoretical calculations^(33,50) have predicted nearly long axis polarization for the $\tilde{A}-\tilde{X}$ transition, however. It was hoped that a study of the fluorescence spectroscopy of styrene at low temperature would shed some light on the nature of the first excited singlet state. To this end, spectra were obtained in a polycrystalline methylcyclohexane matrix. Since the spectra were well resolved, vibrational analysis of the spectrum was possible, but only after the fundamental

vibrational frequencies of styrene were known to a good degree of certainty. All of the previous attempts to identify the fundamental frequencies of styrene resulted in incomplete assignments. Thus, the infrared and Raman spectra of $C_6H_5CHCH_2$, styrene- $\alpha,\beta,\beta-d_3$ ($C_6H_5CDCD_2$), styrene- d_5 ($C_6D_5CHCH_2$), and $C_6D_5CDCD_2$ were recorded and analyzed.

The effect of deuterium isotope substitution on the luminescence characteristics of aromatic hydrocarbon molecules has been of considerable interest for some time. It has been a valuable aid in the understanding of radiationless electronic transitions⁽⁵¹⁾. While the phosphorescence process shows marked increases in quantum yield and lifetime upon deuteration, there is a lack of a significant isotope effect on fluorescence^(42,52,53). Styrene, with its exocyclic vinyl group, is known to photoisomerize in solution⁽²⁶⁾. It was of interest to see whether partial and complete deuteration of styrene, with its additional non-radiative pathway, has any more than the very minor effect on fluorescence quantum yield and lifetime which is the case for other aromatic hydrocarbons.

Temperature effects on fluorescence quantum yields and lifetimes continue to play an important role in elucidating the mechanisms of excited state deactivation. The cis-trans isomerization of trans-stilbene has recently been the subject of intensive experimental⁽⁵⁴⁻⁶²⁾ and theoretical⁽⁶³⁻⁶⁶⁾ study. In particular the singlet lifetimes have been obtained as a function of temperature from room temperature to 77 K^(67,68).

Also, the fluorescence quantum yield of trans-stilbene shows a drastic increase with decreasing temperature^(69,70). With styrene's obvious structural similarities to trans-stilbene the same type of behaviour might be expected. Fluorescence quantum yields and lifetimes of styrene and the three deuterated styrenes at liquid nitrogen temperature were obtained and compared to room temperature results in an attempt to understand the processes which are depopulating styrene's first excited singlet state. Styrene is also known to be a non-phosphorescent molecule. The deuterium and temperature work, as well as studies involving the deliberate population of styrene's triplet manifold by electronic energy transfer, would hopefully make more clear the reasons why styrene does not emit from its first triplet state.

CHAPTER TWO

THEORY AND BACKGROUND

2.1 The Wave Equation

The non-relativistic time-independent Schroedinger equation for a molecule can be written as

$$\hat{H}(q,Q) \psi (q,Q) = E \psi (q,Q) \quad (2.1)$$

where \hat{H} is the Hamiltonian operator and ψ and E are the stationary state wavefunctions and energies, and q and Q are the complete sets of electronic and nuclear co-ordinates, respectively.

2.2 Spectroscopic Transitions

A spectroscopic transition may occur between two stationary states a and b , with energies E_a and E_b respectively, at a wavenumber $\bar{\nu}$ if

$$\bar{\nu} = \frac{|E_b - E_a|}{hc} \quad (2.2)$$

where h is Planck's constant and c is the speed of light. The probability of an electric dipole transition between these two states is proportional to the transition moment

$$\vec{R}_{ab} = \langle \psi_b | \vec{M} | \psi_a \rangle \quad (2.3)$$

where ψ_a and ψ_b are the stationary state eigenfunctions of the two states involved in the transition, and \vec{M} is the electric dipole moment operator. Equation 2.3 does not hold for Raman scattering. In the Raman effect, the operator \vec{M} is replaced by the induced dipole moment vector \vec{P} . The magnitude of \vec{P} is equal to $\alpha |\vec{E}|$, where \vec{E} is the electric vector of the incident radiation and α is the polarizability.

2.3 The Theory of Electronic Spectra

2.3.1 Allowed Transitions

The transition moment for an electric dipole transition between two non-degenerate vibronic states $\psi_{e',v'}$ and $\psi_{e'',v''}$ is given, from Equation 2.3, by

$$\vec{R}_{e',v',e'',v''} = \langle \psi_{e',v'} | \vec{M} | \psi_{e'',v''} \rangle \quad (2.4)$$

Application of the Born-Oppenheimer Approximation⁽⁷¹⁾ to separate the motion of the electrons and of the nuclei enables the total wavefunction (neglecting rotation) to be written as

$$\psi_{e'v'}(q, Q) = \psi_{e'}(q, Q) \psi_{v'}(Q) \quad (2.5)$$

where ψ_e and ψ_v are the electronic and vibrational wavefunctions respectively. Since \vec{M} is a vector, it can be resolved into an electronic and a nuclear part,

$$\vec{M} = \vec{M}_e + \vec{M}_n \quad (2.6)$$

The vibronic transition moment (Equation 2.4) then becomes

$$\begin{aligned} \vec{R}_{e',v',e'',v''} = & \langle \psi_{v'}(Q) | \langle \psi_{e'}(q, Q) | \vec{M}_e | \psi_{e''}(q, Q) \rangle | \psi_{v''}(Q) \rangle \\ & + \langle \psi_{v'}(Q) | \vec{M}_n | \psi_{v''}(Q) \rangle \langle \psi_{e'}(q, Q) | \psi_{e''}(q, Q) \rangle \end{aligned} \quad (2.7)$$

The second term in Equation 2.7 vanishes due to the orthogonality of the electronic wavefunctions. Equation 2.7 then simplifies to

$$\vec{R}_{e',v',e'',v''} = \langle \psi_{v'}(Q) | \vec{R}_{e',e''}(Q) | \psi_{v''}(Q) \rangle \quad (2.8)$$

where the pure electronic transition moment

$$\vec{R}_{e',e''}(Q) = \langle \psi_{e'}(q, Q) | \vec{M}_e | \psi_{e''}(q, Q) \rangle \quad (2.9)$$

has a parametric dependence on the nuclear co-ordinates. To eliminate all dependence of $\vec{R}_{e'e''}(Q)$ on the nuclear co-ordinates, the Condon approximation is applied. $\psi_e(Q)$ is approximated by $\psi_e(q, Q_0)$, i.e. ψ_e is evaluated only at the equilibrium nuclear configuration of the state from which the transition originates. Equation 2.9 then becomes

$$\vec{R}_{e'e''}(0) = \langle \psi_{e'}(q, Q_0) | \vec{M}_e | \psi_{e''}(q, Q_0) \rangle \quad (2.10)$$

where Q_0 represents the equilibrium nuclear configuration of the initial state (the lower state for absorption, the upper state for emission). Equation 2.8 then simplifies to

$$\vec{R}_{e'v'e''v''} = \vec{R}_{e'e''}(0) \langle \psi_{v'}(Q) | \psi_{v''}(Q) \rangle \quad (2.11)$$

An electronically allowed transition is one in which $\vec{R}_{e'e''}(0) \neq 0$.

Group theoretically, the condition that must be fulfilled is that $\Gamma_{\psi_{e'}} \otimes \Gamma_{\psi_{e''}} \otimes \Gamma_{\vec{M}}$ is totally symmetric under all symmetry operations of the point group to which the molecule belongs for at least one of the vector components of \vec{M} . The vibrational transitions which will be observed as fine structure in the electronic transition will be those for which $\langle \psi_{v'}(Q) | \psi_{v''}(Q) \rangle \neq 0$, i.e. $\Gamma_{\psi_{v'}} \otimes \Gamma_{\psi_{v''}}$ is totally symmetric of all symmetry operations of the molecule's point group. Therefore, for an allowed transition between two non-degenerate vibronic levels, vibrational quantum number changes

$$\Delta v = v' - v'' = 0, \pm 1, \pm 2, \dots \quad (2.12)$$

are allowed for transitions between all totally symmetric vibrational modes, and

$$\Delta v = 0, \pm 2, \pm 4, \dots \quad (2.13)$$

are allowed for transitions between non-totally symmetric vibrational modes.

2.3.2 Vibronic Interactions

To a good approximation (the Born-Oppenheimer approximation), Equation 2.5 represents the vibronic wavefunction for a molecular system. There is an exact separation of nuclear and electronic motion, and so in this approximation there can be no "intensity borrowing" and the transition moment will be zero for a transition which is formally forbidden by the electronic selection rules. Vibronic interactions, then, are made possible because ψ_e and ψ_v are not exactly separable, i.e. there is a dependence of the electronic wavefunction upon the nuclear co-ordinates.

The Herzberg-Teller theory⁽⁷²⁾ of vibronic intensity borrowing is often invoked to explain the appearance of a formally forbidden transition (or the appearance of a forbidden component in an electronically allowed transition). In this theory the Condon approximation is relieved by expanding the electronic Hamiltonian H_e (or the transition moment) in terms of the normal co-ordinates of the molecule, Q_i :

$$\hat{H}_e = (\hat{H}_e)_0 + \sum_i \left(\frac{\partial \hat{H}_e}{\partial Q_i} \right)_0 Q_i + \dots \quad (2.14)$$

where Q_i represents the co-ordinates of the nuclei for the i^{th} normal vibration evaluated relative to their equilibrium values in the vibrationless ground state, and the subscript zero refers to the equilibrium nuclear configuration in the

ground electronic state. The second term in Equation 2.14 is the perturbation which takes into account the interaction of electronic and nuclear motions. It is assumed that there exist a number of zeroth order wavefunctions $\psi_k^{\circ}(q, Q)$, which represent the pure electronic wavefunctions of the molecule without regard to nuclear motion. These wavefunctions will be solutions of the zeroth order Hamiltonian $(\hat{H}_e)_{\circ}$, i.e.

$$(\hat{H}_e)_{\circ} \psi_k^{\circ}(q, Q) = E_k^{\circ} \psi_k^{\circ}(q, Q) \quad (2.15)$$

The perturbing term(s) in the electronic Hamiltonian is used to "mix" into a formerly zeroth order state ψ_k° , contributions from other states ψ_j° , in the manner

$$\psi_k = \psi_k^{\circ} + \sum_{k \neq j} c_{kj} \psi_j^{\circ} \quad (2.16)$$

The values of c_{kj} will be given, from perturbation theory, by

$$c_{kj} = \frac{\langle \psi_j^{\circ} | \hat{H}' | \psi_k^{\circ} \rangle}{|E_k^{\circ} - E_j^{\circ}|}, \quad j \neq k \quad (2.17)$$

where \hat{H}' is the perturbing term in the electronic Hamiltonian. For c_{kj} to be non-vanishing, the symmetry condition that must be obeyed is that

$$\Gamma_{\psi_j^{\circ}} \otimes \Gamma_{\psi_k^{\circ}} = \Gamma_{Q_i} \quad (2.18)$$

since $(\frac{\partial H_e}{\partial Q_i})_{\circ} Q_i$ has the same symmetry in electronic space as Q_i does in nuclear space⁽⁷³⁾.

The perturbed wavefunctions described by Equation 2.14 can now be used in evaluating $\vec{R}_{e', v' e'' v''}$. This transition moment is now decomposable into two parts, an allowed component,

$\langle \psi_g^0 | \vec{M} | \psi_k^0 \rangle$ and a forbidden component $\sum_{k \neq j} \langle \psi_g^0 | \vec{M} | \psi_j^0 \rangle$, where ψ_g^0 represents the zeroth order ground state wavefunction. Because the magnitude of the mixing coefficient c_{kj} is inversely proportional to the energy gap between the perturbed and the perturbing states, in conventional Herzberg-Teller theory perturbation of the ground state is considered to be small compared to those of the zeroth order excited states.

The emphasis of the Herzberg-Teller theory of vibronic intensity borrowing is normally on the role of non-totally symmetric vibrations in forbidden transitions. Symmetry arguments dictate that only non-totally symmetric vibrations can bring intensity to symmetry-forbidden transitions. However, it has been recognized, in the case of the S_0 - S_1 transition of phenanthrene^(74,75) and in azulene⁽⁷⁶⁾, that perturbations due to totally symmetric vibrations can contribute intensity in allowed transitions. In molecules whose symmetry is low, vibronic coupling via totally symmetric vibrations may contribute a significant amount to the spectral intensity.

2.4 Theory of Vibrational Spectra

2.4.1 Normal Co-ordinates, Vibrational Wavefunctions and Symmetry Considerations

A molecule with N atoms has $3N-6$ ($3N-5$ for linear molecules) vibrational, three translational and three rotational degrees of freedom. In the classical description of molecular vibrations, the equations of motion for the N nuclei consist of the $3N$ Lagrangian equations

$$\frac{d}{dt} \left(\frac{\partial L}{\partial \dot{\xi}_i} \right) - \frac{\partial L}{\partial \xi_i} = 0, \quad i=1, 2, \dots, 3N \quad (2.19)$$

where the ξ_i are a set of generalized co-ordinates, and

$$L = T - V \quad (2.20)$$

T is the kinetic energy of the nuclei, given by

$$T = \frac{1}{2} \sum_{i=1}^{3N} m_i \dot{\xi}_i^2 \quad (2.21)$$

and V is the potential energy of the nuclei. Potential energy is a function of nuclear displacement; expanded in a power series form (valid for small values of the displacements⁽⁷⁷⁾),

$$2V = 2V_0 + 2 \sum_{i=1}^{3N} \left(\frac{\partial V}{\partial \xi_i} \right)_0 \xi_i + \sum_{i,j=1}^{3N} \left(\frac{\partial^2 V}{\partial \xi_i \partial \xi_j} \right)_0 \xi_i \xi_j + \dots \quad (2.22)$$

The expansion is about the equilibrium positions of the nuclei. If the zero of energy is chosen as the value at the equilibrium configuration, then $V_0 = 0$; also, when the nuclei are in their equilibrium positions, the potential energy is minimized. Therefore, the second term on the right hand side of Equation 2.22 vanishes. For sufficiently small amplitudes of vibrations (i.e., in the harmonic approximation) cubic and higher terms can be neglected, so that

$$V = \frac{1}{2} \sum_{i,j=1}^{3N} \left(\frac{\partial^2 V}{\partial \xi_i \partial \xi_j} \right)_0 \xi_i \xi_j \quad (2.23)$$

The solution of the Lagrangian equations in generalized or even mass-weighted co-ordinates is rather complicated due to the presence of cross terms in the resulting secular equation. To circumvent this problem, and in order to carry out

a quantum mechanical treatment of molecular vibrations, a new set of co-ordinates Q_k , called normal co-ordinates, are used. Both the kinetic and potential energies can now be expressed as the sum of squared terms:

$$T = \frac{1}{2} \sum_{k=1}^{3N} \dot{Q}_k^2, \quad V = \frac{1}{2} \sum_{k=1}^{3N} \lambda_k Q_k^2 \quad (2.24)$$

The quantity $\lambda = 4\pi^2 \nu^2$, where ν is the classical vibration frequency. There is one normal co-ordinate for each normal mode of vibration, and vice versa. The vibrational wave equation has the form⁽⁷⁷⁾

$$-\frac{\hbar^2}{2} \sum_{k=1}^{3N-6} \frac{\partial^2 \psi_v}{\partial Q_k^2} + \frac{1}{2} \sum_{k=1}^{3N-6} \lambda_k Q_k^2 \psi_v = E_v \psi_v \quad (2.25)$$

where E_v is the vibrational energy. By making the substitution

$$\psi_v(Q) = \psi(Q_1) \psi(Q_2) \dots \psi(Q_{3N-6}) \quad (2.26)$$

Equation 2.25 can be factorized into $3N-6$ equations of the type

$$-\frac{\hbar^2}{2} \frac{d^2 \psi(Q_k)}{dQ_k^2} + \frac{1}{2} \lambda_k Q_k^2 \psi(Q_k) = E(k) \psi(Q_k), \quad k=1, 2, \dots, \quad (2.27)$$

$3N-6$

The eigenfunctions $\psi(Q_k)$ in Equation 2.27 are the ordinary harmonic oscillator eigenfunctions, with eigenvalues

$$E_k = h\nu_k(v_k + \frac{1}{2}), \quad v_k = 0, 1, 2, \dots \quad (2.28)$$

v_k is the vibrational quantum number corresponding to normal vibration k . The eigenfunctions themselves have the form

$$\psi_{v_k}(Q_k) = N_{v_k} e^{-\frac{1}{2}\gamma_k Q_k^2} H_{v_k}(\gamma_k^{1/2} Q_k) \quad (2.29)$$

where N_{v_k} is a normalizing factor, $\gamma_k = \frac{4\pi^2 \nu_k}{h}$, and $H_{v_k}(\gamma_k^{1/2} Q_k)$

is the Hermite polynomial of degree v_k . The total vibrational energy is given by the sum of the $3N-6$ individual harmonic oscillator eigenvalues:

$$E_v = \sum_{k=1}^{3N-6} E_k = \sum_{k=1}^{3N-6} h\nu_k (v_k + \frac{1}{2}) \quad (2.30)$$

The Hermite polynomials in the vibrational wavefunction determine the behaviour of the wavefunctions with respect to the symmetry operations that are permitted in the point group to which the molecule belongs. A non-degenerate vibration can only be symmetric or antisymmetric with respect to these symmetry operations⁽⁷⁸⁾. If v_k is even, $\psi_{v_k}(Q_k)$ remains unchanged irrespective of whether or not the sign of Q_k changes upon performing the symmetry operation. If v_k is odd, the sign of the wavefunction changes when the sign of Q_k changes. Hence, assuming that $v=0$ for all other vibrations,

$$\Gamma_{\psi_v} = \Gamma_{Q_k}^{v_k} \quad (2.31)$$

Anharmonicity perturbations do not change the symmetry properties of the vibrational wavefunction⁽⁷⁸⁾.

In order for a normal vibration to absorb infrared radiation the transition moment integral $\langle \psi_v, | \vec{M} | \psi_{v''} \rangle$ must be non-zero. The dipole moment operator can be resolved into Cartesian co-ordinates \vec{M}_x , \vec{M}_y , and \vec{M}_z , which transform in the same manner as do the translation co-ordinates T_x , T_y , and T_z respectively. $\psi_{v''}$, if it is the vibrational ground state, always transforms as the totally symmetric irreducible representation. In the infrared, then, the symmetry condition

in non-degenerate point groups that must be fulfilled for a vibrational transition to occur is then

$$\Gamma_{\psi_{v'}} = \Gamma_{\vec{M}_x} \text{ or } \Gamma_{\vec{M}_y} \text{ or } \Gamma_{\vec{M}_z} \quad (2.32)$$

A similar condition holds for Raman transitions. A vibration is active as a fundamental in the Raman effect if

$$\Gamma_{\psi_{v'}} = \Gamma_{\alpha_{ij}}, \quad i, j = x \text{ or } y \text{ or } z \quad (2.33)$$

where the α_{ij} are the components of the polarizability tensor.

The gas phase Raman study by Carreira and Towns⁽²²⁾ indicated that styrene is planar in its equilibrium ground state. In addition, microwave methods applied to p-fluoro⁽⁷⁹⁾ and p-chlorostyrene⁽⁸⁰⁾ have indicated that these molecules have a planar ground state geometry. Therefore, styrene and the deuterated styrenes belong to the C_s point group. Since each are 16-atom molecules, they have 42 normal modes of vibration. The number of normal vibrations belonging to each symmetry species can be obtained from group theoretical considerations. For the styrenes, the 42 normal modes are subdivided into 29 of symmetry species a' and 13 of species a'' . The character table for the C_s point group is the following:

	E	$\sigma(xy)$		
a'	1	1	T_x, T_y, R_z	$\alpha_x^2, \alpha_y^2, \alpha_z^2, \alpha_{xy}$
a''	1	-1	T_z, R_x, R_y	α_{xz}, α_{yz}

Since the translation vectors and the polarizability tensor components each span both the irreducible representations, all of the vibrational modes of styrene and its deuterated analogues are both infrared and Raman active.

A more detailed treatment of the theory of molecular vibrations can be found in References (77) and (78).

2.4.2 Depolarization Ratios

The depolarization ratio of a Raman band is defined as

$$\rho = \frac{I_{\perp}}{I_{\parallel}} \quad (2.34)$$

where I_{\perp} and I_{\parallel} are the intensities of the Raman bands polarized perpendicular to and parallel to the plane of polarization of the incident radiation. For linearly polarized incident radiation, as was the case for the laser source used to obtain the Raman spectra, this ratio lies between 0 and 0.75 for totally symmetric vibrations and is equal to 0.75 for non-totally symmetric vibrations⁽⁷⁸⁾.

2.4.3 Teller-Redlich Product Rule

The Teller-Redlich product rule⁽⁸¹⁾ relates the ratio of frequencies of all vibrations of a given symmetry type in a pair of isotopic molecules to the molecule's geometry and atomic masses. It is based on the assumption that the fields of force of two isotopic molecules are identical. The rule is rigorously upheld for the zeroth order frequencies ω_i and is a good approximation for the observed fundamentals ν_i .

As applied to the $C_6H_5CDCD_2/C_6H_5CHCH_2$ isotopic pair, for example, the product ratios are.

$$\prod_i \frac{\omega_i^D}{\omega_i^H} = \sqrt{\frac{m_H^3}{m_D^3} \frac{M_D}{M_H} \left(\frac{I_x^D}{I_x^H}\right) \left(\frac{I_y^D}{I_y^H}\right)} \quad \text{a'' modes (2.35)}$$

$$\prod_j \frac{\omega_j^D}{\omega_j^H} = \sqrt{\frac{m_H^6}{m_D^6} \frac{M_D^2}{M_H^2} \left(\frac{I_z^D}{I_z^H}\right)} \quad \text{-a' modes (2.36)}$$

Similar expressions apply for other isotopic pairs.

2.5 The Fate of Absorbed Energy

Unless formed in the vibrationless level of an excited singlet state, an excited species in solution is created with excess vibrational energy. This excess energy is rapidly dissipated by collisions with solvent molecules. The rate constant for this process, called vibrational relaxation is $>10^{12} \text{ s}^{-1}$. If the initially excited electronic state is not S_1 , a process known as internal conversion can occur. This process is a radiationless transition between isoenergetic states of the same multiplicity. The molecule passes from a low vibrational level of the upper state to a high vibrational level of the lower state, from which level vibrational relaxation can again occur. Eventually, these processes will take the excited molecules to a thermally equilibrated vibrational distribution in the first excited singlet state S_1 . The number of molecules which have been found to fluoresce with appreciable efficiency from upper excited singlet states is

small, but growing⁽⁸²⁻⁸⁶⁾.

Some of the radiative and non-radiative processes available to polyatomic molecules are illustrated by the Jablonski diagram in Figure 2.1. From the ground vibrational state of S_1 , several photophysical processes are possible: (i) fluorescence, or a radiative transition involving no change in spin multiplicity; (ii) internal conversion, followed by vibrational relaxation to the S_0 potential surface; (iii) intersystem crossing, which is a radiationless passage from a singlet electronic state to an isoenergetic level in a triplet electronic state (or vice versa), followed by vibrational relaxation. In addition to these processes, the excited molecules can also transfer its energy to other molecules or undergo photochemical reaction. A molecule in the lowest triplet state T_1 , can undergo intersystem crossing back to the S_0 surface, followed by vibrational relaxation, or it can phosphoresce. Phosphorescence is defined as the emission of light between two states of different spin multiplicity.

For the situation when an excited species A^* is subject to several first order or pseudo-first order deactivating processes (for example fluorescence, internal conversion and intersystem crossing if A^* is an excited singlet), the rate of disappearance of A^* is given by

$$-\frac{d\{A^*\}}{dt} = \sum_i k_i \{A^*\} \quad (2.37)$$

where the k_i are the rate constants for the processes that

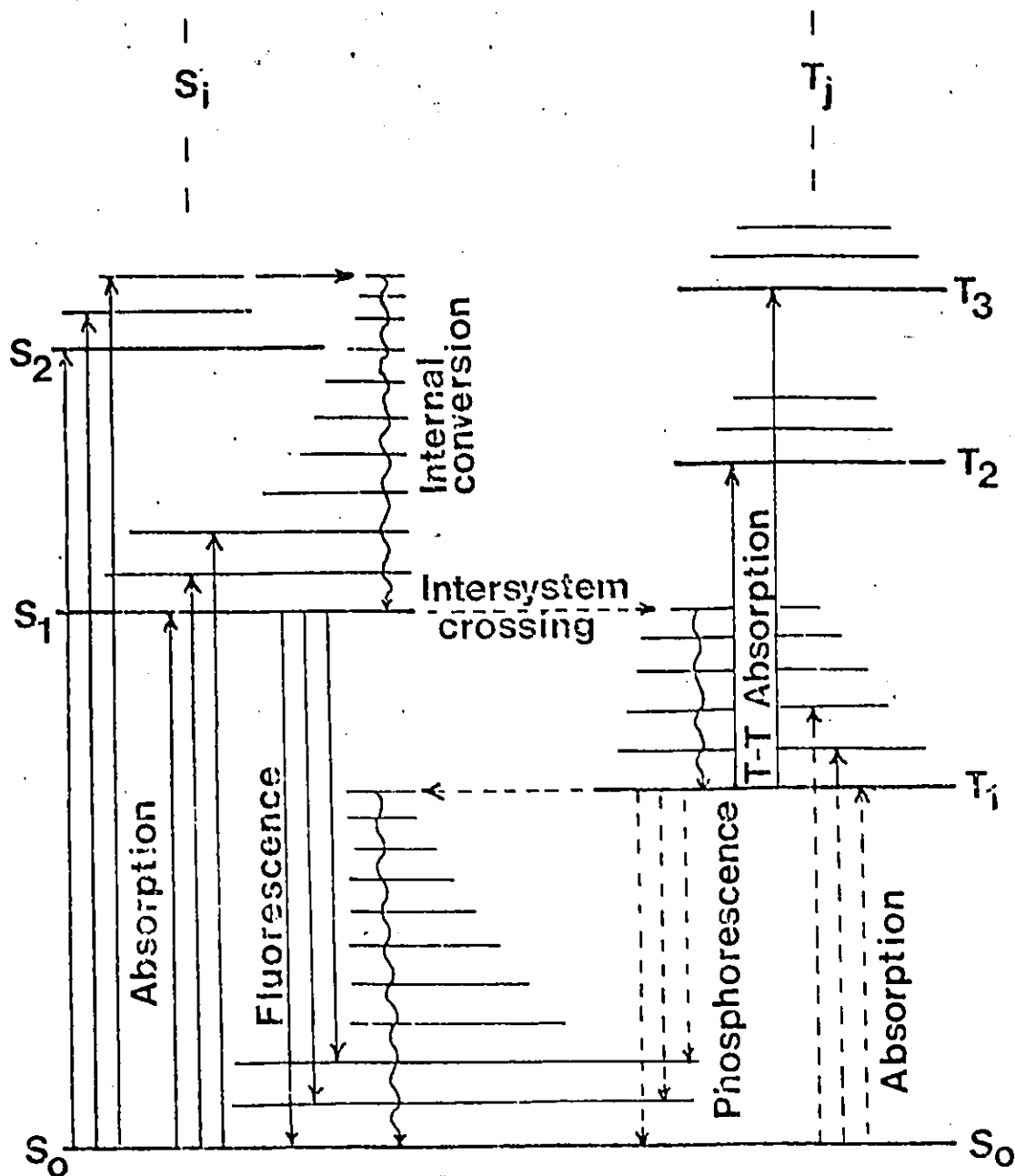


Figure 2.1 Jablonski Diagram Showing Principal Photophysical Processes in Complex Molecules.

deplete the excited state. It follows that

$$\{A^*\} = \{A^*\}_0 e^{-t/\tau} \quad (2.38)$$

where $\{A^*\}_0$ is the initial excited state concentration, and

$$\tau = \frac{1}{\sum_i k_i} \quad (2.39)$$

The quantity τ is known as the mean lifetime of the excited species. When $\{A^*\}$ is a singlet state, τ is commonly known as the fluorescence lifetime. A brief description of the technique used to obtain fluorescence lifetimes in this work is found in Section 2.8.

2.6 Fluorescence Excitation

The total intensity of fluorescence emission is equal to the intensity of light absorbed multiplied by the quantum yield of fluorescence:

$$Q = (I_0 - I_t)\phi_f = \{I_0(1 - 10^{-\epsilon cl})\}\phi_f \quad (2.40)$$

In this equation Q is the total fluorescence intensity in quanta per second, I_0 is the intensity of the exciting light, also in quanta per second, ϵ is the molar extinction coefficient of the solute, c and l are the solution concentration (in moles/litre) and path length (in cm) respectively, and ϕ_f is the quantum yield of fluorescence. For solutions that absorb weakly, i.e. with ϵcl small, Equation 2.40 simplifies to

$$Q = 2.303 I_0 \epsilon cl \phi_f \quad (2.41)$$

It is seen that for a solution containing one solute of a given concentration, the fluorescence intensity is directly proportional to $I_0 \epsilon \phi_f$. If Vavilov's law is obeyed, i.e. if ϕ_f is independent of excitation wavelength, and I_0 is also constant with wavelength, then Q will be proportional to the molar extinction coefficient ϵ , and should closely resemble the absorption spectrum of the solute. Even when I_0 is not constant with wavelength and the solution optical density is large enough that Q is no longer proportional to concentration, a good representation of the solute absorption spectrum can often be obtained as long as these deviations are not too severe.

2.7 Fluorescence Quantum Yields

The fluorescence quantum yield of a solution is defined as that fraction of molecules that emit a photon of fluorescence after direct excitation. The determination of the absolute quantum yield of fluorescence is fraught with a number of experimental difficulties, and so the large majority of quantum yields reported in the literature have been obtained through measurement of fluorescence intensity relative to that emitted by a compound whose fluorescence quantum yield is well known or at least is generally agreed upon.

In the case where the solution optical densities are small, and Equation 2.41 holds, the fluorescence quantum yield of an unknown, $(\phi_f)_s$, is obtained from the quantum yield of the reference compound, $(\phi_f)_r$, by the equation

$$(\phi_f)_s = (\phi_f)_r \cdot \frac{F_s}{F_r} \cdot \frac{I(\lambda_r)}{I(\lambda_s)} \cdot \frac{A_r(\lambda_r)}{A_s(\lambda_s)} \cdot \frac{n_s^2}{n_r^2} \quad (2.42)$$

F in the above Equation refers to the integrated area under the corrected emission spectrum, $I(\lambda)$ is the relative photon output of the light source at excitation wavelength λ , $A(\lambda)$ is the optical density of the solution at wavelength λ , and n is the average refractive index of the solution to the fluorescence. The subscripts r and s refer to the reference and unknown solutions, respectively. The ratio F_s/F_r is used in place of the ratio of the total fluorescence intensities Q_s/Q_r only when the two fluorescence spectra are obtained under identical geometrical conditions with respect to the sample and optics. In the special case where the two solutes are in the same solvent at the same temperature, have the same optical density and are irradiated with the same wavelength of light, Equation 2.42 reduces to

$$(\phi_f)_s = (\phi_f)_r \cdot \frac{F_s}{F_r} \quad (2.43)$$

To obtain corrected emission spectra it is necessary to know how the sensitivity of the detection system varies with wavelength. The sensitivity correction factor S_λ at wavelength λ can be written as

$$S_\lambda = R_\lambda / \frac{dQ}{d\lambda} \quad (2.44)$$

where R_λ is the recorded response from the detection system,

and $dQ/d\lambda$ is the true relative emission intensity at wavelength λ . Correction factors are most often obtained by recording the response of the detection system to a source with a known spectral distribution, such as a standard lamp, or alternatively by obtaining the spectra of compounds that have a known spectral distribution.

A comprehensive review on the measurement of photoluminescence quantum yields has been given by Demas and Crosby⁽⁸⁷⁾.

2.8 Singlet Decay Times

The technique used for the measurement of fluorescence lifetimes was the method of time-correlated single photon counting. This method has found widespread popularity in the last few years, and a number of reviews have been published⁽⁸⁸⁻⁹²⁾. Only a brief outline of the technique will be given here.

The single photon counting technique of lifetime measurement is based upon the concept that the intensity-time profile of all the photons emitted following a single pulse of light can be reproduced by determining the probability distribution for the emission of a single photon following a single excitation pulse. The sample is repetitively excited with a pulsed light source such as a laser or a spark discharge lamp. When the source fires, the pulse is detected either electronically, or alternatively by means of a

photomultiplier tube. This "start" pulse is sent to a time-to-amplitude converter (TAC) where it triggers a voltage ramp, which is linear in time and sets the time reference to zero. The ramp is stopped when a voltage pulse from a photomultiplier tube viewing the sample emission is sent to the "stop" channel of the TAC. The TAC output pulse amplitude is then proportional to the elapsed time between the arrival of the "start" and "stop" pulses. If no "stop" pulse is received by the TAC by the end of its voltage sweep, then no output is generated and the ramp is reset. The output pulses are sent to a multichannel pulse height analyzer (or simply multichannel analyzer, MCA) where they are sorted according to amplitude, and hence time, and stored as counts in the memory. Because the probability of detecting a single photon is directly proportional to the intensity of emission, the detected events will be distributed in the same way as a profile of emission intensity vs time.

Accurate time-correlated single photon data will be obtained only if no more than one emitted photon is detected per excitation pulse. The reason for this is the differential nature of the operation of the TAC. If more than one photon per excitation pulse is incident on the photocathode, the TAC will receive its "stop" pulse when the first photon is detected and the voltage ramp will reset. A second emission photon, detected by the photomultiplier later in time but before the arrival of the next "start" pulse, will not be counted since the TAC is inactive. This phenomenon, called pulse pile-up, discriminates against late arriving photons,

and the apparent lifetime will be shorter than the true value. The simplest method for minimizing error due to pulse pile-up is to attenuate the emission intensity such that the average number of detected emission photons per excitation pulse is ≤ 0.05 ⁽⁹³⁾.

The true fluorescence decay curve for an excited species is that obtained by excitation with a delta function light pulse. In practice, however, excitation pulses have finite widths, and for short lifetimes significant distortion of the true decay curve occurs. In order to recover the true decay function from the experimentally observed curve it is necessary to solve the convolution integral

$$G(t) = \int_0^t I(t')D(t-t')dt' \quad (2.45)$$

where $G(t)$ is the observed time course of the fluorescence intensity, $I(t)$ is the instrumental response function or the lamp time profile distorted by the detection system, and $D(t)$ is the true decay function. Of the several deconvolution techniques available for the analysis of data collected with the single photon counting method^(94,95), perhaps the most widely used is that of reiterative convolution^(96,97). By this method, one assumes a functional form, with adjustable parameters, for the decay law and numerically integrates this $D(t-t')$ with $I(t')$ to obtain a trial curve $G'(t)$ which is compared with the experimentally obtained $G(t)$. The free parameters in the decay law are then adjusted until the best fit (by least squares) between the calculated and observed functions are obtained.

2.9 Polycrystalline Matrices and the Shpol'skii Effect

At room temperature in fluid solution the width of the vibrational bands in a fluorescence emission spectrum is large, typically several hundred wavenumbers. This is due to specific interactions between the solute and solvent. However, Shpol'skii^(98,99) observed that by judicious choice of an n-paraffin solvent, frozen crystalline solutions of aromatic hydrocarbons yield highly resolved luminescence and absorption spectra, with band widths of less than 10 cm^{-1} in favorable cases. The sharpest quasi-linear spectra are obtained when the molecular dimensions of the solute are approximately equal to those of the solvent. In these circumstances, the solute molecule replaces a solvent molecule in the crystal lattice, and can be considered an "oriented gas" molecule to a greater degree than when a rigid glass-forming solvent is used.

Methylcyclohexane, although not an n-paraffin, has been used with success in obtaining resolved low-temperature fluorescence and phosphorescence spectra of a number of substituted benzenes^(8-10,100-102). Evidence has very recently⁽¹⁰³⁾ been put forward to suggest that there are two crystalline modifications of this solvent.

2.10 Triplet-Triplet Energy Transfer in Rigid Solution

The phenomenon of a transfer of energy from a triplet state of a donor D to a triplet state of an acceptor A can be represented by the equation



The asterisk denotes an electronically excited species. That this type of energy transfer occurs was first demonstrated by Terenin and Ermolaev^(104,105) by their observation of naphthalene phosphorescence from a solution containing both naphthalene and benzophenone, but where only the latter species absorbed the incident radiation. These workers found that excitation transfer is efficient only if the triplet energy of the donor is greater than that of the acceptor. The fact that the energy donor is selectively excited rules out singlet-singlet energy transfer, followed by intersystem crossing, as the mechanism that populates the acceptor triplet level. A trivial emission-reabsorption mechanism is also very unlikely due to the very small oscillator strength of singlet-triplet transitions. Triplet-triplet energy transfer is a powerful tool for elucidating the kinetics and mechanisms of photoreactions in solution.

CHAPTER THREE

EXPERIMENTAL

3.1 Chemicals

Styrene-h₈ was purchased from Matheson, Coleman and Bell. Styrene-d₃ was prepared in the following way. To 120 g (6 moles) of refluxing D₂O which contained ~2.1 g of freshly cut sodium metal was added 12 g (0.1 mole) of acetophenone (from Matheson, Coleman and Bell). The reaction was stopped after 22 hours. The acetophenone was extracted from the mixture with ether, and the ether layer removed. The aqueous layer was extracted twice with ether. The ether was removed and combined with the main organic layer, which was then washed twice with water. The organic layer was dried over anhydrous MgSO₄. Evaporation of the ether yielded 10.5 g of C₆H₅COCD₃. Deuterium incorporation was estimated at 94% by ¹H NMR. Ten grams (0.081 mole) of freshly distilled acetophenone-d₃ were added over a period of 20 minutes to ~1.5 g (0.026 mole) of LiAlD₄ (Stohler Isotope Chemicals, 99% D atom) in 50 ml diethyl ether. The mixture was left at mild reflux for four hours, and then quenched with acidified H₂O. After filtering out the inorganic hydroxides, ether was added to the filtrate, the mixture was shaken, and the ether layer removed. The aqueous layer was extracted with ether, and the combined ether layers were dried over anhydrous MgSO₄. After removal of the ether, the crude alcohol was purified by

distillation under reduced pressure. The alcohol, $C_6H_5CDOHCD_3$, was then dehydrated using ~1 g of anhydrous $KHSO_4$ and a trace of copper powder. The mixture was heated with an oil bath whose temperature was gradually raised to $200^\circ C$. Ether was added to the distillate in a separatory funnel. The aqueous layer was drained off and the ether layer was washed first with a saturated Na_2CO_3 solution and then with water. After drying the solution over calcium chloride, the ether was removed by distillation at atmospheric pressure, and the product, $C_6H_5CDCD_2$, was bulb-to-bulb distilled on a vacuum line.

Styrene- d_5 was prepared by synthesis of the corresponding alcohol by a Grignard reaction, followed by dehydration. The Grignard reagent was prepared by adding a crystal of I_2 to 1.48 grams (0.062 mole) of Mg turnings in ~10 ml of ether, and then slowly adding 10 grams (0.062 mole) of bromobenzene- d_5 (Stohler Isotope Chemicals, 99.5% D) in ~50 ml of ether. After most of the magnesium had dissolved, the reaction mixture was cooled to $0^\circ C$ and acetaldehyde (in 10 ml ether) added dropwise over 15 minutes. The reaction mixture was decomposed with careful addition of a saturated NH_4Cl solution. The ether layer was washed with water and dried over anhydrous $MgSO_4$. The crude product, $C_6D_5CHOHCH_3$, was vacuum distilled before dehydration, which was carried out in the same way as in the preparation of styrene- d_3 .

Styrene- d_8 was obtained from Aldrich Chemicals and vacuum distilled, or prepared by the same method as for styrene- d_5 , with acetaldehyde- d_4 (Merck, Sharp and Dohme, 99% D atom) being

used.

Because the styrenes tended to polymerize over a period of months when stored in the dark at -0°C , all stock solutions of the styrenes were made with freshly distilled solute.

Acetophenone (Matheson, Coleman and Bell) was vacuum distilled prior to use. Aldrich Chemical Company 9,10-diphenylanthracene (99+%, GOLD LABEL) was recrystallized from ethanol, m.p. $248-249.5^{\circ}\text{C}$. Biphenyl was first recrystallized from ethanol, and then three times vacuum sublimed, m.p. $69.5-70^{\circ}\text{C}$.

The solvents used, either pure or as components of solvent mixtures, were:

cyclohexane (Matheson, Coleman and Bell, Spectroquality, or Fisher Scientific, ACS Spectroanalyzed), either used as received or passed through a Woelm alumina column;

methylcyclohexane (Matheson, Coleman and Bell, Spectroquality), used without further purification;

diethyl ether (Matheson, Coleman and Bell, Spectroquality), used without further purification;

isopentane (Phillips Pure Grade), which was shaken in Linde 10X molecular sieve;

3-methylpentane (Phillips Pure Grade), which was passed through a Woelm alumina column and repeatedly shaken in Linde 10X or BDH 13X molecular sieve;

ethyl iodide (J.T. Baker Co., "Baker Analyzed" Reagent), stabilized with copper wire, used as received.

The last named solvent was used only in absorption, and was

transparent in the wavelength region of interest, namely 4000 - 5000 Å. The 3-methylpentane exhibited a very slight afterglow when cooled to 77 K and irradiated with broad band excitation centered at 254 nm. This residual luminescence, however, was not significantly above the level of scattered light and so was not considered a problem in fluorescence quantum yield experiments with this solvent, in spite of the fact that the impurity emitted in the same spectral region as the reference compound, 9,10-diphenylanthracene. The latter compound has a quantum yield near unity in many solvents⁽¹⁰⁶⁾ and an extinction coefficient of $\sim 10^5$ at 253.7 nm, the excitation wavelength used in the quantum yield experiments. For all other solvents, no detectible luminescence was observed under the experimental conditions used.

3.2 Spectra

3.2.1. Infrared Spectra

Infrared spectra were recorded on a Perkin-Elmer Model 521 grating spectrophotometer. Samples of the neat liquid styrenes were placed between the two KBr windows of a sealed sample cell of path length 0.025 mm. Weaker bands were developed by employing the 5X ordinate expansion capabilities of the spectrophotometer. The infrared spectra of polystyrene film, and of thin films of indene and 1,2,4-trichlorobenzene were used for calibrating the observed bands of styrene. The accuracy of the band positions is estimated to be $\pm 1 \text{ cm}^{-1}$ for sharp bands and $\pm 2-3 \text{ cm}^{-1}$ for weak or diffuse bands. Spectra

of the vapor phase styrenes were obtained using a 10 cm^{-1} gas cell equipped with a sidearm and fitted with CsI windows.

3.2.2. Raman Spectra

Raman spectra of room temperature and -25°C liquid samples of the styrenes sealed in Pyrex capillary tubes were obtained with excitation from the green 5145 \AA line of a Spectra-Physics Model 164 argon ion laser. The scattered radiation was detected by a photomultiplier (either an ITT Model FW 130 or an RCA C31034 tube) after passing through a Spex Model 1400 Czerny-Turner Monochromator, then amplified and recorded. The lower temperature was attained by passing the cold vapors from liquid nitrogen around the sample, and was measured by means of a copper-constantan thermocouple. Depolarization ratios were measured by placing a rotatable polarizer between the sample and the entrance slit of the monochromator. To avoid polarization effects due to the grating, the scattered radiation was completely depolarized before it entered the monochromator. The Raman spectrum of freshly distilled indene was used for calibration purposes. The estimated accuracy in the Raman bands is $\pm 3\text{ cm}^{-1}$.

3.2.3. Fluorescence and Fluorescence Excitation Spectra

Figure 3.1 shows the basic apparatus used to obtain the emission spectra. Light from an Osram 150 watt xenon lamp, powered by a Bausch and Lomb power supply or an Osram 450 watt xenon lamp powered by an Oriel Optics Corporation Model C-72-50 DC regulated power supply was focused onto the entrance slit of

A LENSES

B DEWAR AND SAMPLE

C PHOTOMULTIPLIER TUBE

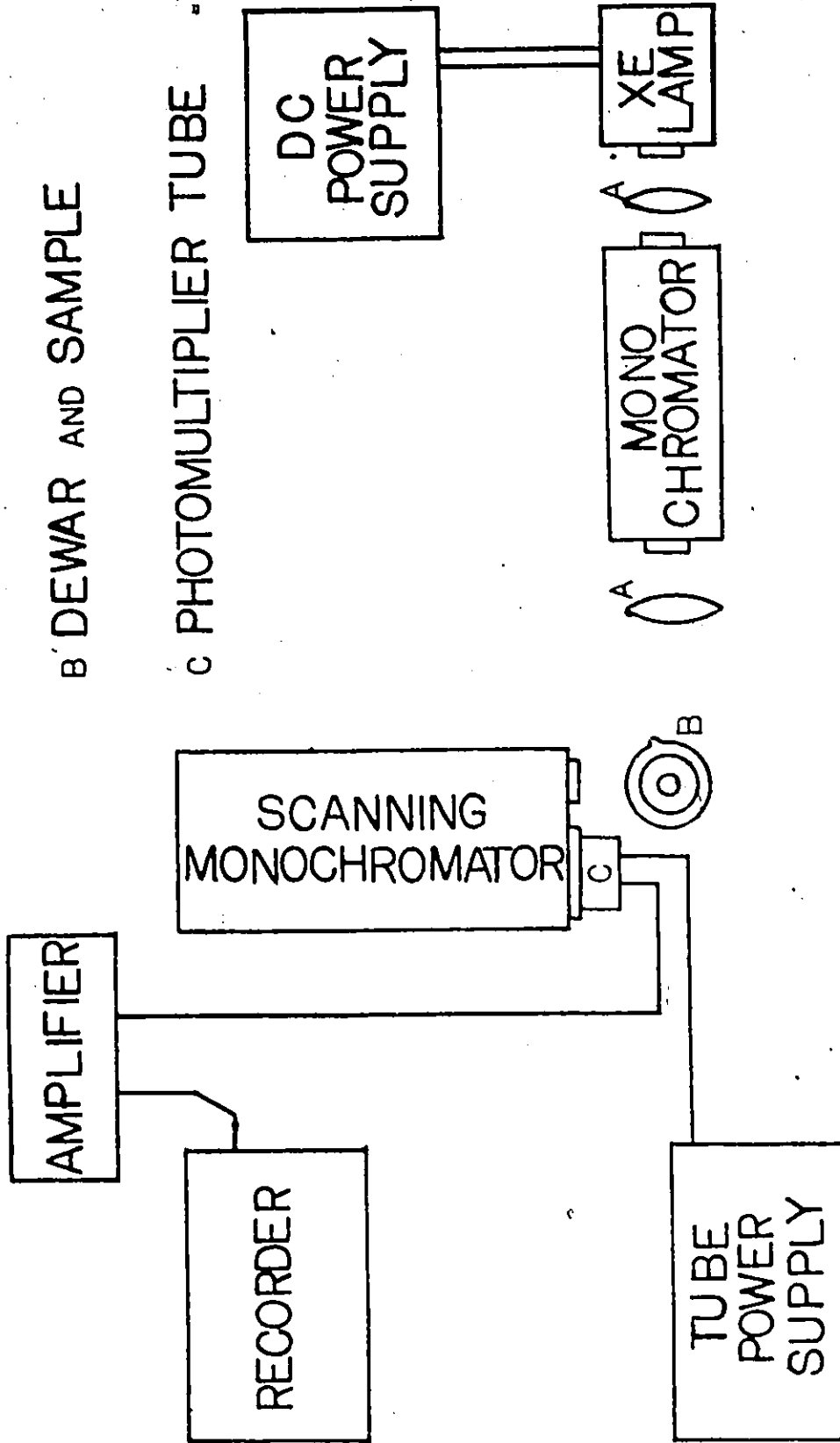


FIG. 3.1 APPARATUS FOR EMISSION EXPERIMENTS

BLOCK
DIAGRAM

either a Jarrell-Ash 0.25 m Ebert monochromator equipped with a 2360 grooves/mm, 300 nm blazed grating, or a Bausch and Lomb 0.25 m monochromator with a 1200 grooves/mm grating. The radiation leaving the monochromator was focused onto the sample, which for low-temperature emission spectra was contained in a 11 mm o.d. quartz tube immersed in a partially silvered dewar containing liquid nitrogen. Emission was observed at 90° to the direction of the incident light by a Jarrell-Ash 0.5 m scanning Ebert monochromator. The dispersive element was a 1180 grooves/mm grating, blazed at 400 nm. The light exiting the monochromator was detected by an RCA 8575 photomultiplier. Amplification was provided by either a Kiethley Model 610C solid State Electrometer, or an Ortec photon counting system consisting of a Model 454 Timing Filter Amplifier, a Model 421 Integral Discriminator, and a Model 441 Ratemeter. The signal from either the electrometer or the ratemeter was fed into a Varian G-2000 strip chart recorder. Fluorescence spectra were usually attained by exciting the $\tilde{B}+\tilde{X}$ transition in the wavelength region 250-260 nm. Spectra were typically run on undegassed samples of concentration 10^{-3} M or less. Slit widths used on the emission monochromator were generally less than 100 μ . The resulting spectra were uncorrected for the varying response of the detection system with wavelength. The wavelengths of the spectral bands were obtained by superimposing the resonance lines from a low-pressure mercury pen lamp. The wavelength accuracy of the bands is $\pm 0.5 \text{ \AA}$.

Fluorescence excitation spectra were obtained using $\sim 10^{-5}$

M solutions of the styrenes by monitoring the highest intensity emission band on the 0.5 m monochromator while varying the wavelength of excitation using the Jarrell-Ash 0.25 m monochromator. Typical slit widths used were 400 μ on the emission monochromator and 150 μ on the excitation monochromator. Wavelength calibration of the fluorescence excitation spectra was performed by the following method. First the emission monochromator was calibrated using a mercury pen lamp. Then the 0.25 m monochromator was set at the wavelength of the maximum intensity band in the excitation spectrum, and the 0.5 m monochromator was scanned through this wavelength. The wavelength dial setting of this monochromator at maximum intensity was recorded, and the wavelengths of all other bands in the spectrum were obtained using the wavelength of the maximum intensity band as the reference wavelength.

The polycrystalline solutions used in obtaining the fluorescence and fluorescence excitation spectra were obtained by one of two methods. In the first method, the tip of the sample tube was placed about one centimeter above the liquid nitrogen level in a dewar (either the sample dewar or an external dewar). When the sample became completely polycrystalline the tube was quickly plunged into the sample dewar. Alternatively, the sample tube was first immersed in liquid nitrogen, the sample becoming a cracked glass. Then the tube was allowed to warm up in the air until a portion of the sample had crystallized. The sample was then quickly placed a short distance above the liquid nitrogen level, and was immersed in the coolant contained

in the sample dewar after complete crystallization had occurred. There was no discernible difference in the emission spectra obtained using the two cooling methods.

3.2.4. Absorption Spectra

All absorption spectra of the styrenes were obtained using a Cary Model 14 recording spectrophotometer. Vapor phase samples were contained in a 10 cm quartz cell. Air was used in the reference beam of the spectrophotometer when recording these spectra. The vacuum wavenumbers of the major peaks were obtained by comparison with the vapor absorption spectrum of $C_6H_5\equiv CH$, which has been thoroughly analyzed by King and So⁽⁶⁾. Almost all solution absorption spectra were obtained using matched one cm absorption cells, with the reference cell containing the pure solvent. The only exception to this was when ethyl iodide was used as the solvent; in this case matched 10 cm liquid cells were used.

3.3 Measurement of Singlet Lifetimes

A brief description of the principles underlying the time-correlated single photon counting method for the determination of fluorescence lifetimes has been given in Section 2.8. The instrument used in this work, illustrated in block form in Figure 3.2, utilized a home-made discharge lamp. The details of the lamp construction are shown in Figure 3.3. The electrodes, which were 1/16" thoriated tungsten welding rod, could be repositioned to the same gap width after cleaning using

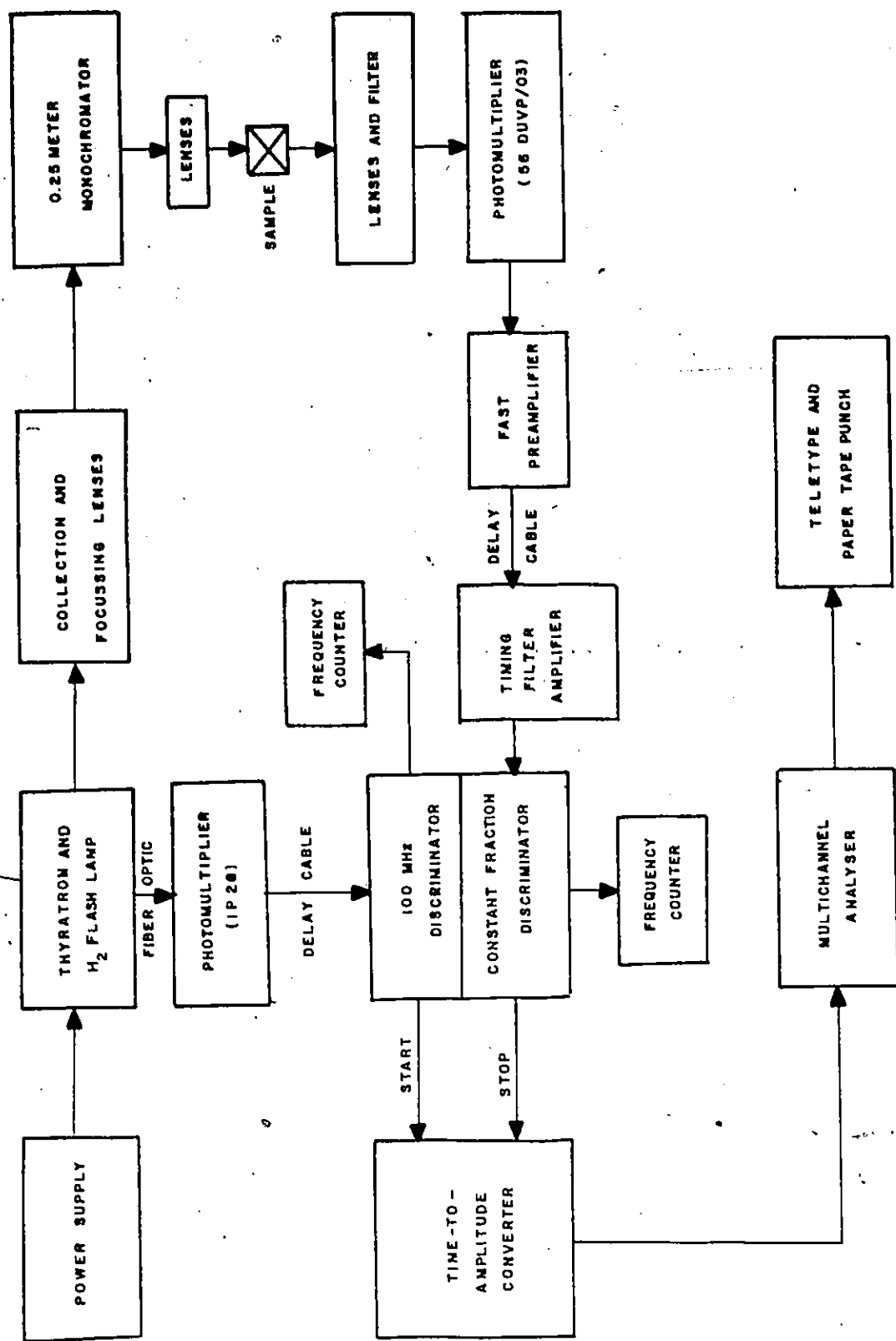


Fig.3.2 Block Diagram of Fluorescence Lifetime Apparatus

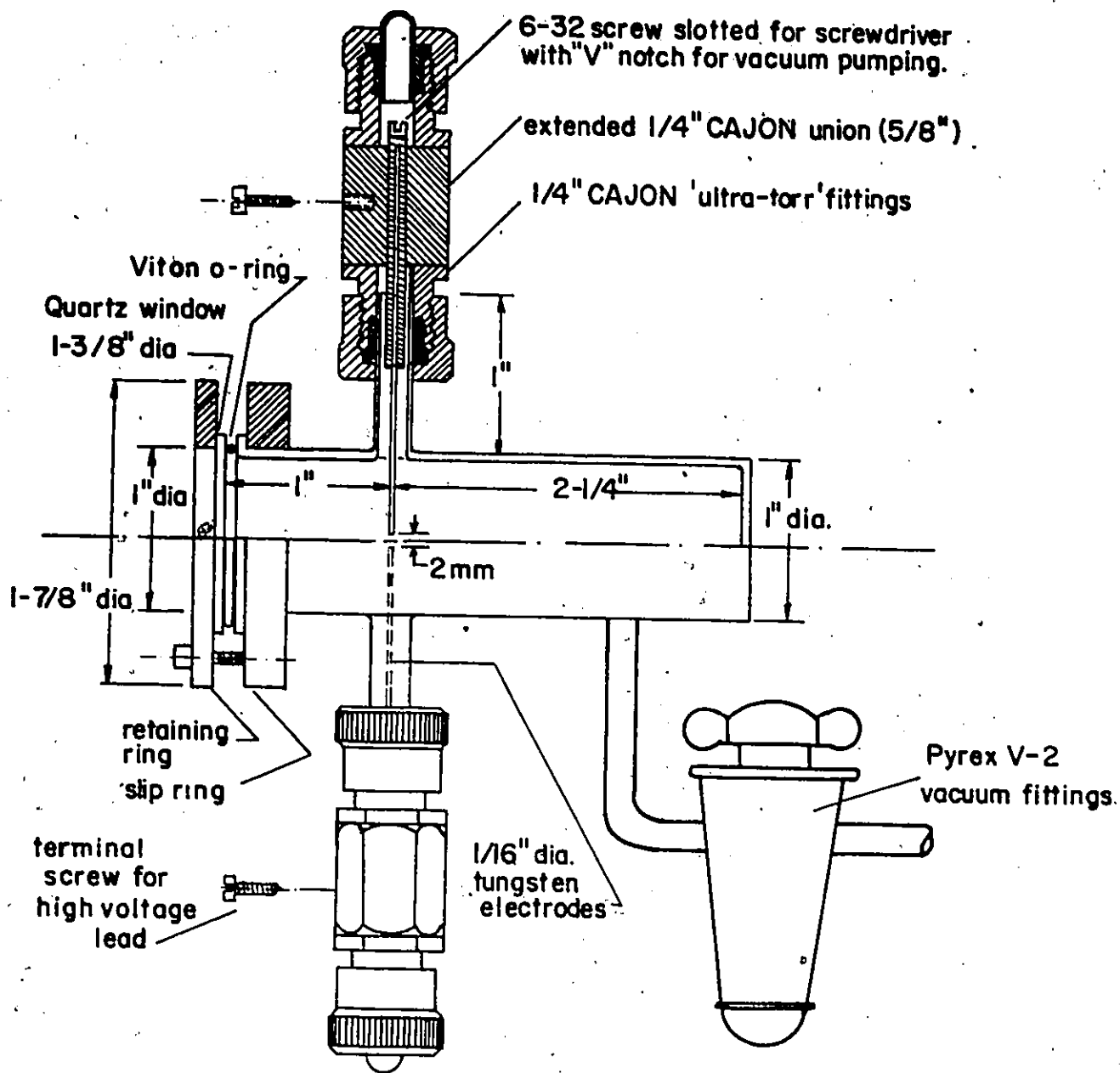


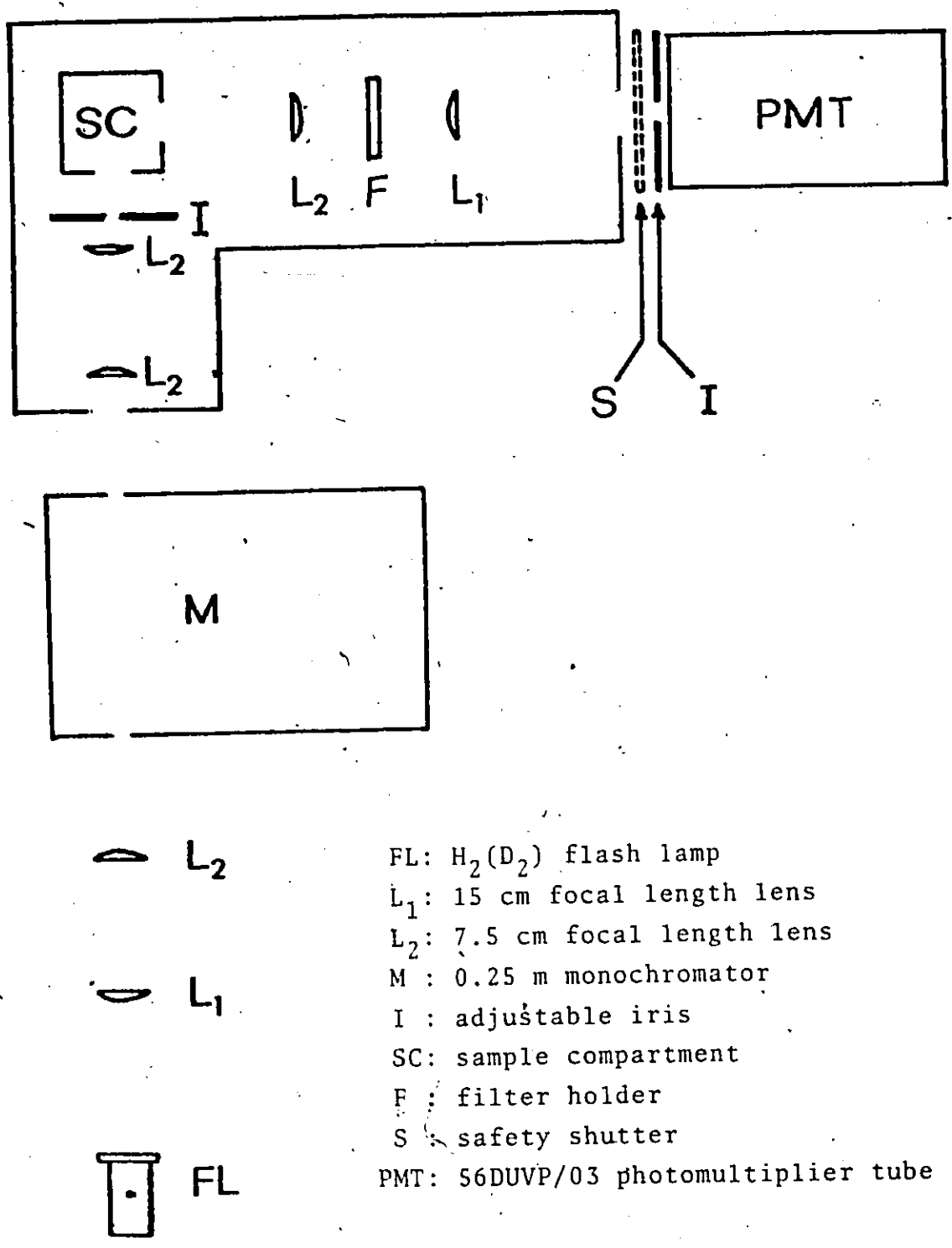
Figure 3.3 Nanosecond Discharge Lamp used for Measurement of Fluorescence Lifetimes.




this design, although the gap could not be changed in situ. The electrode spacing used was 2 mm. The lamp was gated with an EG & G HY-2 ceramic hydride thyratron. The lamp was filled with approximately 0.5 atmosphere of H_2 (or D_2). The voltage applied to the lamp was 7 kV, and the flash repetition rate was typically 18 kHz.

Light from the flash lamp was collimated and focused onto the slit of a Jarrell-Ash 0.25 m Ebert monochromator. The incident radiation and the emission were focused onto the sample and photomultiplier tube respectively by a modified TRW Model 31A Decay Time Fluorometer optical system. The total optical arrangement is depicted in Figure 3.4.

Sample emission was detected at 90° by means of an Amperex 56DUVP/03 photomultiplier tube incorporated in a Photochemical Research Associates, Inc. Model 520 housing. At an operating voltage of -1990 V, the background count rate was 30-40 Hz at ambient temperature.

Anode pulses from the photomultiplier were processed by an Ortec electronics system consisting of a Model 9301 Fast Preamplifier, a Model 454 Timing Filter Amplifier, and a Model 473 Constant Fraction Discriminator operating in the "constant fraction" mode. The latter module's output was a negative-going logic pulse which did not vary with input pulse amplitude. This signal provided the STOP pulse for the Model 457 Time-to-Amplitude Converter (TAC). "START" pulses were derived via an Ortec Model 436 100 MHz discriminator which accepted a pulse from an RCA 1P28 photomultiplier located



-  L₂
-  L₁
-  FL

FL: H₂(D₂) flash lamp
 L₁: 15 cm focal length lens
 L₂: 7.5 cm focal length lens
 M : 0.25 m monochromator
 I : adjustable iris
 SC: sample compartment
 F : filter holder
 S : safety shutter
 PMT: 56DUVP/03 photomultiplier tube

Figure 3.4 Optical System in Fluorescence Lifetime Apparatus

inside the lamp power supply. Light was transmitted to this photomultiplier by means of a 3 ft fiber optic. The TAC output was fed into a Victoreen PIP 400 Multichannel Analyzer (MCA). Data stored in the MCA was converted to a punched tape output and put onto cards. The time base of the TAC was calibrated with an Ortec Model 462 Time Calibrator.

The fluorescence lifetime system was tested, in collaboration with Dr. R.C. Miller, using dilute solutions of compounds that are generally accepted as exhibiting simple exponential decay behaviour. The solutes were purified by recrystallization and/or sublimation and were checked by measurement of their absorption and low temperature emission spectra. Agreement between the lifetimes obtained and those reported in the literature was very good indeed. The results are summarized in Table 3.1.

In a typical decay time experiment an excitation wavelength of 254 nm was used to excite styrene solutions of known optical density (0.45 in cyclohexane and 0.1 in 3-methylpentane in a 1 cm cell). One mm slits were used on the 0.25 m monochromator, resulting in a bandpass of 1.8 nm. A Corning CS7-51 color filter was placed between the sample and the detector to eliminate scattered exciting radiation. Room temperature samples were contained in a cylindrical quartz tube equipped with a Rota-Flo greaseless valve, and deoxygenation was accomplished by several freeze-pump-thaw cycles. 77 K samples were contained in a 2 cm x 2 cm x 2 cm copper block fitted with three 0.75 inch diameter quartz windows

Table 3.1

Singlet Decay Times of some Standard Substances

Solute ^a	Concentration (moles/l)	Measured Lifetime (ns)	Reported Lifetime (ns)	Reference
Pyrene	1.5×10^{-6}	425,442	408	107
			435	108
Naphthalene	1.5×10^{-4}	108,110	96	42
			109	109
			120	110
Phenanthrene	6.3×10^{-5}	56.7	55.8	109
			56.0	111
			57.5	42
Quinine Sulphate in 1N H ₂ SO ₄	1.0×10^{-4}	19.3	19.2	112
			19.2	42
			19.4	113
Fluorene	5.0×10^{-5}	6.65,6.82	6.9±0.5	114
Anthracene	1.07×10^{-4}	5.00,5.07,5.13	4.9	42
			4.94	115
			5.03	116
p-Terphenyl	1.0×10^{-5}	0.92,1.02	0.95	42
			0.93	117

a: The solvent used was Baker GC Spectrophotometric Grade cyclohexane, unless otherwise stated.

(Esco Products, Inc.). The copper block was mounted at the tip of an Air Products Cryo-Tip LC-1-100 liquid nitrogen insert. The samples were degassed by bubbling argon through the solution. To allow thermal equilibrium to be established, accumulation of data began at least one hour after preparation of the low temperature sample. In all decay time experiments at least 10^4 counts in the peak channel were collected. The average fluorescence photon count rate was kept to 3-4% of the flash repetition rate in order to prevent distortion due to pulse pile-up.

The experimental lamp decay profile was obtained using a Ludox SM scattering solution at the same excitation wavelength as that used to excite the sample. The apparent optical density of the scatterer was adjusted to be approximately equal to the absorbance of the sample solution, as advised by Lewis *et al*⁽⁸⁹⁾. Both the lamp profile and sample decay data were required for use in the ITCONV computer program*. This program used the technique of reiterative convolution^(96,97) to solve the convolution integral (Equation 2.45).

3.4 Determination of Fluorescence Quantum Yields

The room temperature fluorescence quantum yields of the four styrenes in cyclohexane solution were obtained using an Aminco-Bowman spectrofluorimeter. The reference solution chosen was biphenyl in cyclohexane, for which a value of the

*A copy of this program was kindly supplied by Dr. T. Nemzek.

fluorescence yield of 0.18 has been reported⁽¹¹⁸⁾. Sample and reference solutions of O.D.=0.45 at 250 nm were contained in stoppered 1 cm quartz cuvettes, and were deoxygenated by argon bubbling. No spectral correction for the response of the emission monochromator-detection system was necessary since there was very good overlap of the sample and reference fluorescence spectra.

Quantum yields at room temperature and at 77 K using 3-methylpentane as solvent were obtained using basically the same apparatus as was used for obtaining the low temperature emission spectra (Section 3.2.3). In these experiments, however, the light source was a low pressure Hg lamp placed at the entrance slit of the 0.25 m monochromator, which was set to pass the 253.7 nm Hg resonance line. Also, a 10 cm path of chlorine gas was placed behind the exit slit of the monochromator to remove the unwanted mercury lines passed as scattered light. The Hg lamp was allowed to warm up for at least three hours before spectra were taken. The reference compound was 9,10-diphenylanthracene, also in 3-methylpentane. Morris, Mahaney and Huber⁽¹¹⁹⁾ have determined a ϕ_f for this solution of 0.93. However, only excitation wavelengths between 357 nm and 380 nm were used. Nevertheless, a ϕ_f of 0.93 was assumed for 254 nm excitation at room temperature, since Heinrich, Schoof and Gusten⁽¹⁰⁶⁾ have found that ϕ_f is the same for both 254 nm and 366 nm excitation for 9,10-DPA in several solvents. Also, since τ_f for 9,10-DPA has the same value at room temperature and at 77 K in 3-MP⁽¹¹⁹⁾, it has been assumed that $\phi_f=0.93$

for 254 nm excitation at 77 K (in EPA solvent, ϕ_f has the same value at both 300 K and 77 K^(120,121)). The copper block sample compartment described in Section 3.3 was used. The absorbance/cm of both sample and reference solutions was 0.10 at 253.7 nm. Since the same apparatus was not used to obtain both the optical density of the solutions and their emission spectra, both the Cary 14 spectrophotometer and the 0.25 m monochromator of the emission apparatus were calibrated using a low pressure Hg lamp.

Corrected styrene and 9,10-DPA fluorescence spectra were obtained by employing a standard quartz-iodine lamp (Electro-Optics Corporation) to calibrate the 0.5 m monochromator-RCA 8575 photomultiplier detection system. A graph of the relative sensitivity correction factor $1/S_\lambda$ (see Equation 2.44) versus wavelength is shown in Figure 3.5. The emission monochromator slit width used to obtain this curve was 300 μ , the slit width used for obtaining the fluorescence spectra. Areas under the corrected fluorescence spectra were obtained by the cut-and-weigh technique.

Room temperature fluorescence quantum yields of the deuterated styrenes, using styrene- h_8 as standard, were obtained using a cylindrical quartz sample tube equipped with a Rota-Flo valve. The emission apparatus, concentration, and deoxygenation procedure were the same as that just described for the experiments using the copper block sample holder and 9,10-DPA as the reference compound. ϕ_f for the styrene- h_8 standard was the value obtained using this latter method. The spectra

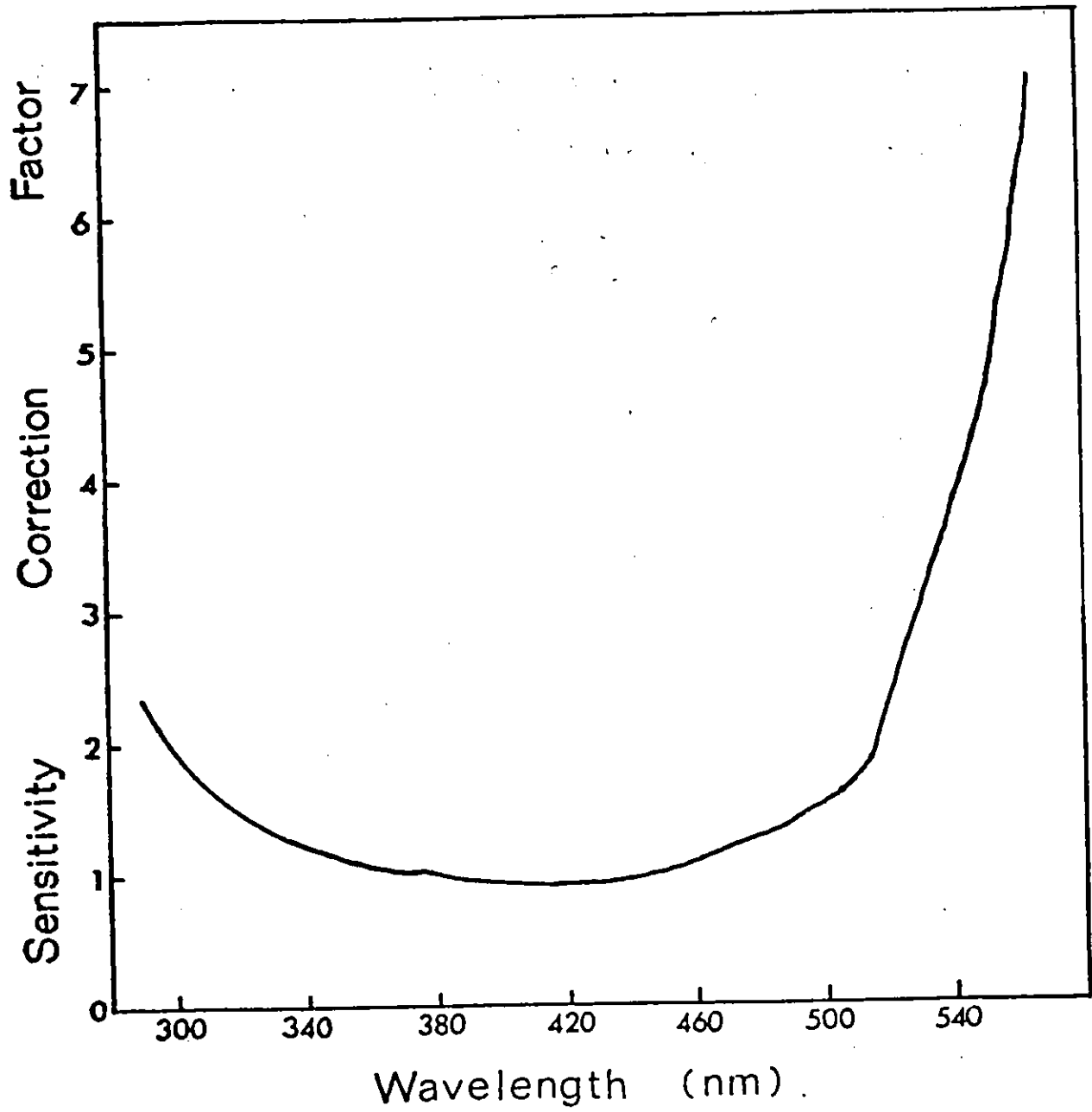


Figure 3.5 Sensitivity Correction Curve for Monochromator-Photomultiplier Combination (normalized to unity at $\lambda=445.0$ nm)

were not corrected¹ for instrumental response variations with wavelength. Areas were obtained by cutting and weighing, as before.

3.5 Triplet-Triplet Energy Transfer Work

The transfer of triplet excitation energy from acetophenone to styrene was observed by monitoring the change in the phosphorescence lifetime of the sensitizer with varying amounts of added styrene. The signal was taken from the electrometer into a Hewlett-Packard 132A Dual Beam Oscilloscope, and the decay was photographed using a Hewlett-Packard 196B Oscilloscope Camera. Excitation was provided by a xenon flash lamp filtered by means of a Corning CS7-51 color filter. The half-width of the flash was ~ 150 μ s. The acetophenone concentration (in a 1:1 by volume diethyl ether-isopentane glass at 77 K) was 2×10^{-2} M, while the concentration of styrene ranged from 0.1 M to 0.5 M. Acetophenone phosphorescence was monitored at $\lambda = 447.5$ nm.

CHAPTER FOUR

ANALYSIS OF THE INFRARED AND RAMAN SPECTRA

4.1 Introduction

The most complete analyses of the vibrational spectra of styrene- h_8 have been given by Pitzer, Guttman and Westrum⁽¹¹⁾, Fateley, Carlson and Dickson⁽¹⁸⁾, and by Mross and Zundel⁽¹⁹⁾, who also studied the corresponding spectra of styrene- d_8 . The last named authors assigned 32 of the normal vibrations of $C_6D_5CDCD_2$, leaving 10 unassigned. The analysis of the vibrational spectra of four isotopic derivatives of styrene, with the help of Raman depolarization ratios and infrared vapor phase band contours, helps to complete the assignment of the normal modes of styrene and also makes changes in previous assignments. The assigned ground state fundamentals of styrene found by the above workers are given in Table 4.1; the designations ν_i of the vibrational modes are explained in Section 4.2.

4.2 Normal Vibrations of Styrene

Styrene has 42 normal modes of vibration. Under the symmetry operations of the C_s point group these vibrations are divided into 29 of species a' and 13 of species a'' . All of these modes are predicted to be infrared and Raman active (Section 2.4.1). The numbering of the fundamentals has been obtained by using Herzberg's notation⁽⁷⁸⁾. By this method, the vibrations are first grouped according to their symmetry types, in the order found in the character table for the point

Table 4.1

Previously Assigned Ground State Fundamentals of Styrene-h₈

Description of Mode ^a	Frequency (cm ⁻¹)		
	<u>Pitzer et al^b</u>	<u>Fateley et al^c</u>	<u>Mross and Zundel^d</u>
<u>a' species</u>			
νC-H	 not assigned 	3092	
ν _{as} =CH ₂			3087
νC-H		3081	3080
νC-H		3060	3059
νC-H			3045
νC-H			3027
ν _β =CH-			3010
ν _s =CH ₂			2981
νC=C		1636	1632
νC-C		1601	1602
νC-C	1581	1578	
νC-C	1495	1495	
νC-C	1320	1450	
β _s =CH ₂	1415	1413	
νC-C		1318	
β=CH-	1301	1305	
βC-H	1280	1290	
X-sens (νC-CHCH ₂)	1204	1203	
βC-H	1181	1182	
βC-H	1155	1156	
βC-H	1070	1083	
β _{as} =CH ₂		1035	
βC-H	1030	1021	
ring	999	1001	
X-sens (αC-C-C)	777	776	
αC-C-C	622	622	
β-C=C	442	440	
X-sens (αC-C-C)	510	555	
			554

Table 4.1 (continued)

Description of Mode ^a	Frequency (cm ⁻¹)		
	<u>Pitzer et al^b</u>	<u>Fateley et al^c</u>	<u>Mross and Zundel^d</u>
<u>a' species</u>			
X-sens (β C-CHCH ₂)	240	242	239
<u>a'' species</u>			
γ =CH-	990	992	991
γ C-H		982	
γ C-H	988		982
γ C-H			909
γ_s =CH ₂	908	909	909
γ C-H	835	840	838
γ C-H	730	776	776
ϕ C-C		698	698
γ_{as} =CH ₂	560		
X-sens (ϕ C-C)	442		440
ϕ C-C	416	440	
X-sens (γ C-CHCH ₂)	212	214	215
torsion		<33	

- a: See Table 4.2 for the approximate descriptions corresponding to these abbreviations.
- b: Reference (11); Wilson notation⁽¹²²⁾ slightly different from that given in Table 4.6.
- c: Reference (18); Wilson notation⁽¹²²⁾ slightly different from that given in Table 4.6.
- d: Reference (19); Schmidt notation⁽¹²³⁾ used.

group to which the molecule belongs, namely a' , a'' for C_s symmetry styrene. For each symmetry type, the frequencies obtained for styrene- h_8 are arranged in descending order, and the vibrations are then labelled $\nu_1, \nu_2, \dots, \nu_{42}$, starting from the totally symmetric modes. The designations of the 42 normal modes of styrene, along with their approximate descriptions and the description abbreviations, are found in Table 4.2.

By treating the substituent as a single unit X, Randle and Whiffen⁽¹²⁶⁾ proposed a set of approximate normal modes in terms of Cartesian displacement vectors for various monosubstituted benzene vibrations. In addition, a number of approximate normal vibrations of the vinyl group in monosubstituted ethylenes have been described⁽¹²⁴⁾. These modes are shown schematically in Figures 4.1 and 4.2 respectively.

4.3 Analysis

As mentioned previously, all of the fundamental vibrations of styrene are predicted to be both infrared and Raman active. In the Raman spectra, the most prominent bands had a' symmetry, and most of these had the expected low depolarization ratio.

Another useful tool in the problem of band assignments is the rotational contour of vapor phase infrared bands. Usually, the individual rotational lines in a rotation-vibration band of a complex molecule are not observed due to the limited spectroscopic resolution of the instrument used. However, if the overall band envelope or contour can be clearly seen, in-

Table 4.2

Approximate Descriptions of the Normal Vibrations of Styrene

Abbreviation	Approximate Description	Normal Mode Designation(s)
ν C-H	ring C-H stretch	$\nu_1, \nu_3, \nu_4, \nu_5, \nu_6$
β C-H	ring C-H in-plane bend	$\nu_{17}, \nu_{19}, \nu_{20}, \nu_{21}, \nu_{23}$
γ C-H	ring C-H out-of-plane bend	$\nu_{31}, \nu_{32}, \nu_{33}, \nu_{35}, \nu_{36}$
ν C-C	ring C-C stretch	$\nu_{10}, \nu_{11}, \nu_{12}, \nu_{13}, \nu_{15}$
α C-C-C	ring in-plane deformation	$\nu_{25}^a, \nu_{26}, \nu_{28}^a$
ϕ C-C	ring out-of-plane deformation	$\nu_{37}, \nu_{39}^a, \nu_{40}$
ring	ring breathing mode	ν_{24}
ν C-CHCH ₂	C-C stretch between the benzene ring and the vinyl group	ν_{18}^a
β C-CHCH ₂	C-C in-plane deformation between the benzene ring and the vinyl group	ν_{29}^a
γ C-CHCH ₂	C-C out-of-plane deformation between the benzene ring and the vinyl group	ν_{41}^a
$\nu_{as}=\text{CH}_2$	antisymmetric C-H stretch of the vinyl =CH ₂ group	ν_2
$\beta_{as}=\text{CH}_2$	antisymmetric in-plane deformation of the vinyl =CH ₂ group	ν_{22}
$\gamma_{as}=\text{CH}_2$	antisymmetric out-of-plane deformation of the vinyl =CH ₂ group ^b	ν_{38}

Table 4.2 (continued)

Abbreviation	Approximate Description	Normal Mode Designation(s)
$\nu_s = \text{CH}_2$	symmetric C-H stretch of the vinyl $=\text{CH}_2$ group	ν_8
$\beta_s = \text{CH}_2$	symmetric in-plane deformation of the vinyl $=\text{CH}_2$ group	ν_{14}
$\gamma_s = \text{CH}_2$	symmetric out-of-plane deformation of the vinyl $=\text{CH}_2$ group	ν_{34}
$\nu = \text{CH}-$	C-H stretch of the vinyl $=\text{CH}-$ group	ν_7
$\beta = \text{CH}-$	C-H in-plane deformation of the vinyl $=\text{CH}-$ group	ν_{16}
$\gamma = \text{CH}$	C-H out-of-plane deformation of the vinyl $=\text{CH}-$ group	ν_{30}
$\nu \text{C}=\text{C}$	C=C stretch in the vinyl group	ν_9
$\beta - \text{C}=\text{C}$	C=C in-plane deformation	ν_{27}
torsion	out-of-plane twist of vinyl group about ring-substituent single bond	ν_{42}

a: These vibrations are ones in which the substituent X (in this case, the vinyl group) moves with appreciable amplitude, and thus the frequencies are sensitive to the mass of X. The abbreviations for these modes will thus be prefixed by the phrase "X-sens".

b: This mode has also been described as a "cis' C-H wag" (124).

c: This mode has also been described as a "trans' C-H wag" (124) and as a "C=C twist" (125).

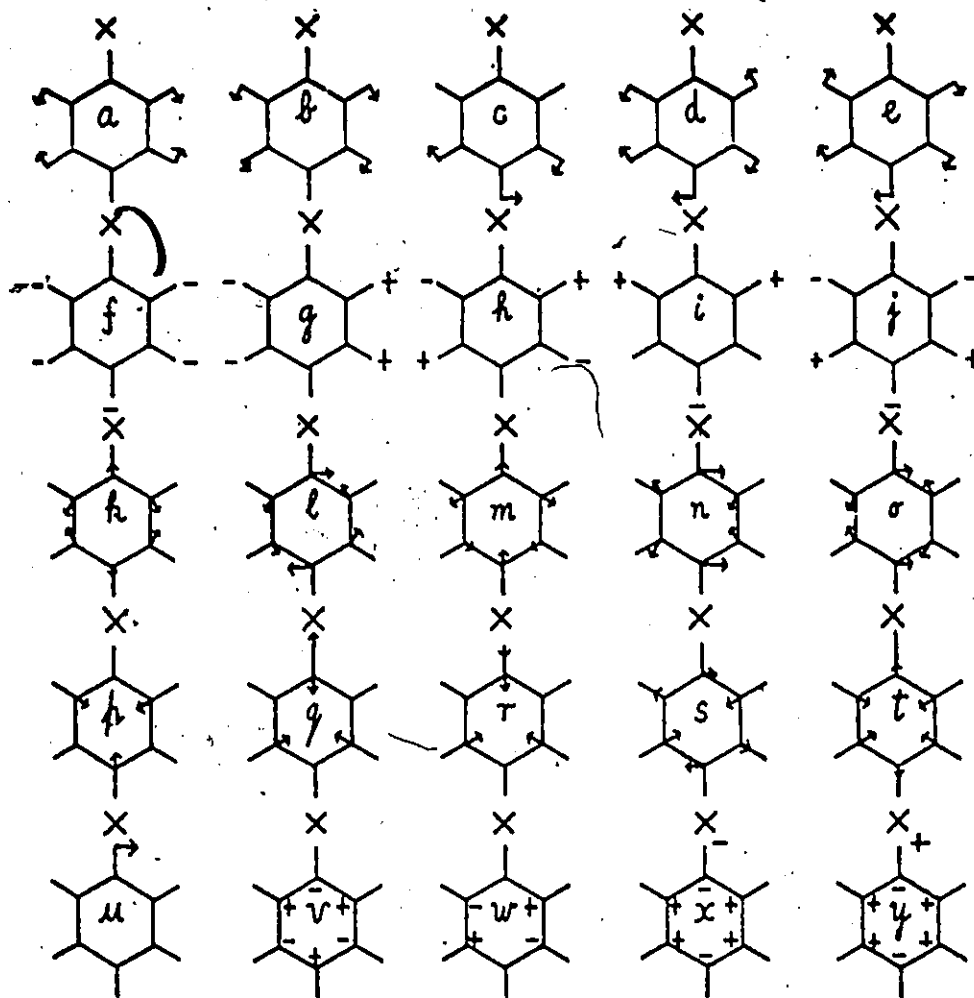


Figure 4.1 Some Normal Vibrations of Monosubstituted Benzenes (from reference 127).

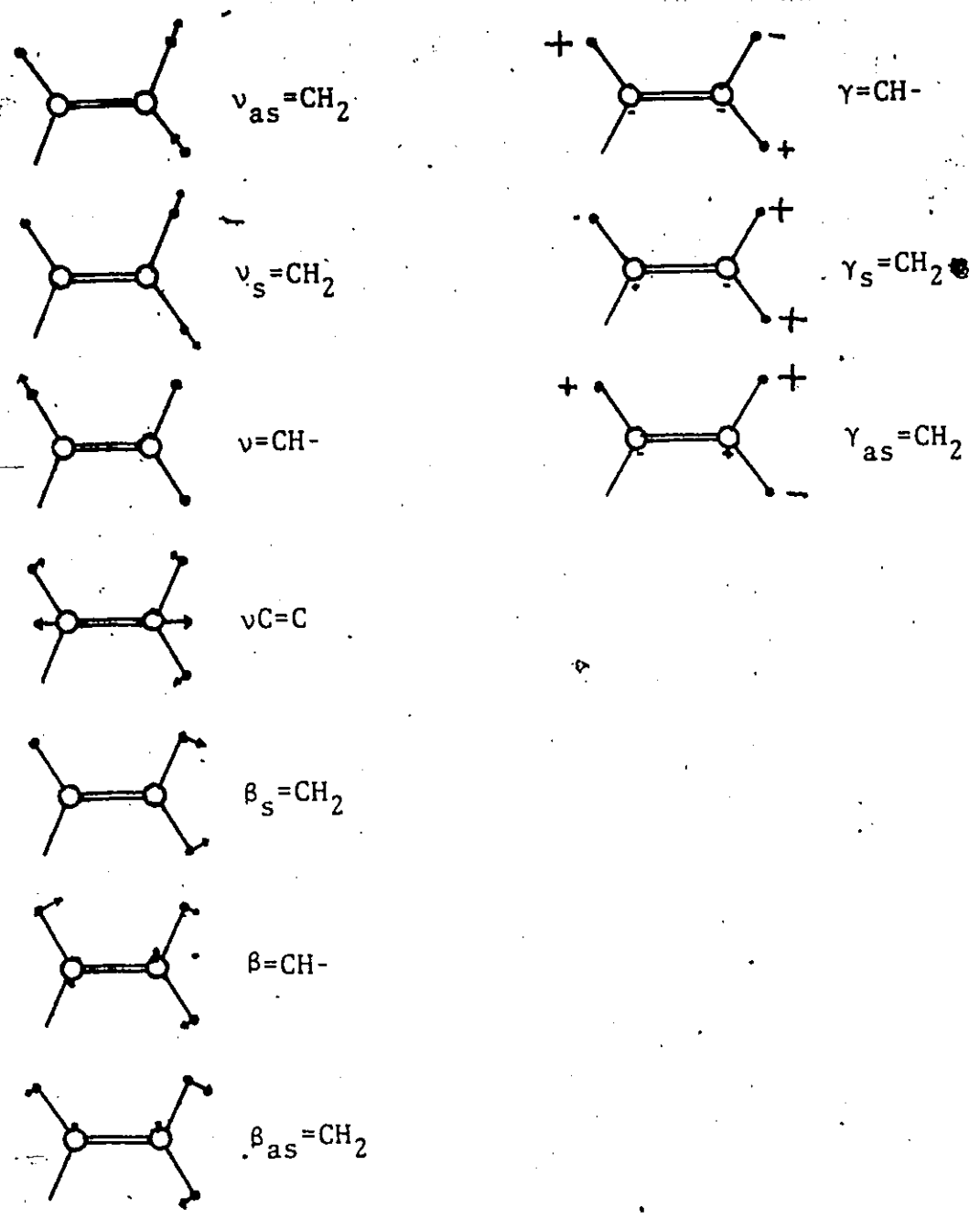


Figure 4.2 Some Normal Vibrations of Monosubstituted Ethylenes (from reference 124).

formation on the direction of the transition moment of the band can be obtained.

The principal moments of inertia for styrene and its three isotopic modifications have been calculated from an assumed molecular geometry (Section 4.4), and the molecule is seen to be an asymmetric top, i.e., $I_c > I_b > I_a$. The subscripts a, b, and c refer to the principal axes of inertia⁽⁷⁸⁾ of the molecule, the a and b axes lying in the symmetry plane and the c axis perpendicular to the plane. For molecules of, say, C_{2v} symmetry (eg. benzonitrile), the transition moment must lie in one of the principal axes, and so a type A, type B, or type C band is obtained, depending on whether the transition moment is parallel to the a, b, or c axis. Styrene, however, has C_s symmetry, and so an in-plane transition moment cannot have a unique direction associated with it. The a' modes, then, will have A/B hybrid contours in the vapor spectra. The out-of-plane vibrations of species a'' should have C-type contours; with very prominent Q branches and weak P and R branches. However, since it was felt that the large majority of the a' vibrations could be satisfactorily assigned from the Raman spectrum, band contour data has been used as confirmatory evidence only for the a'' modes.

The deuterium isotope effect is another valuable aid in the analysis of vibrational spectra. When an atom in a molecule is replaced by an isotopic atom of the same element, then to a high order of approximation the potential function governing the movement of the nuclei is unchanged. The vibrational energy levels are changed, however, because of the

change in the mass of the molecule. The magnitude of the isotopic shift of a particular vibrational frequency depends on the extent to which the substituted atom participates in the normal vibration. For styrene, deuteration of the vinyl group would be expected to lower the frequencies of those normal modes which describe essentially vinyl group vibrations much more than the frequencies of the ring modes. The reverse is expected for ring deuteration.

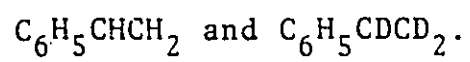
The infrared spectra of the four styrenes are shown in Figures 4.3 and 4.4. The Raman spectra are depicted in Figures 4.5 and 4.6. The band assignments are found in Tables 4.4 and 4.5, and a complete listing of the fundamentals is given in Table 4.6.

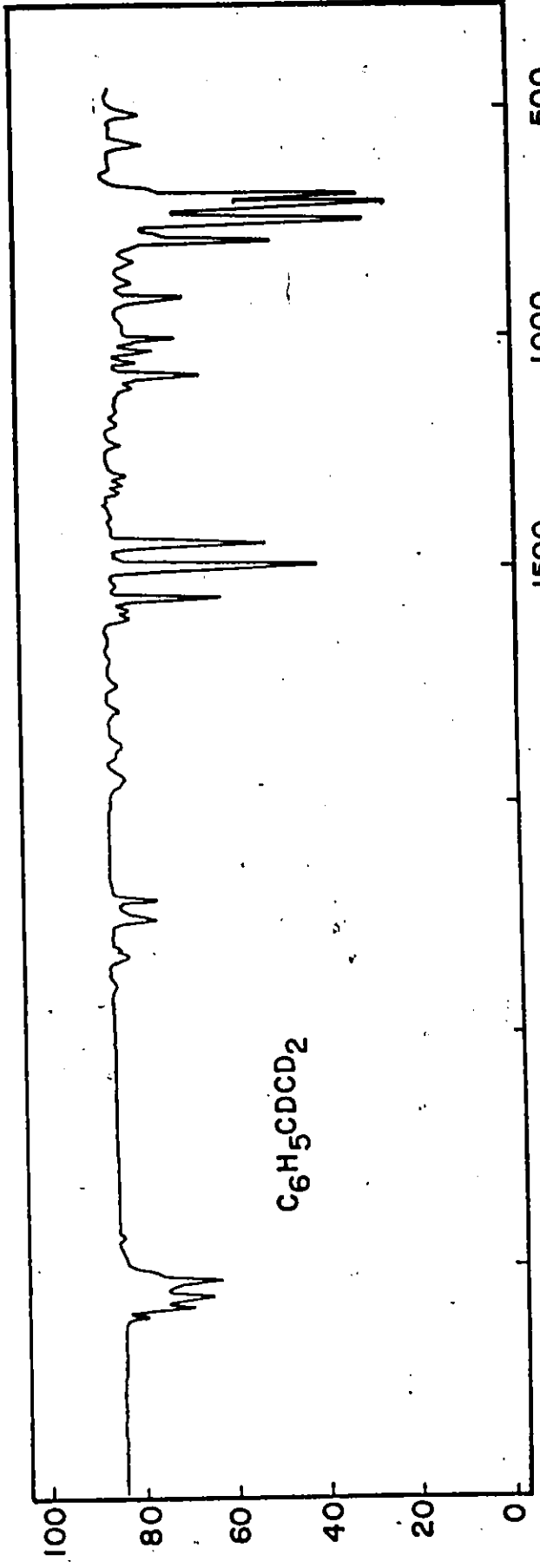
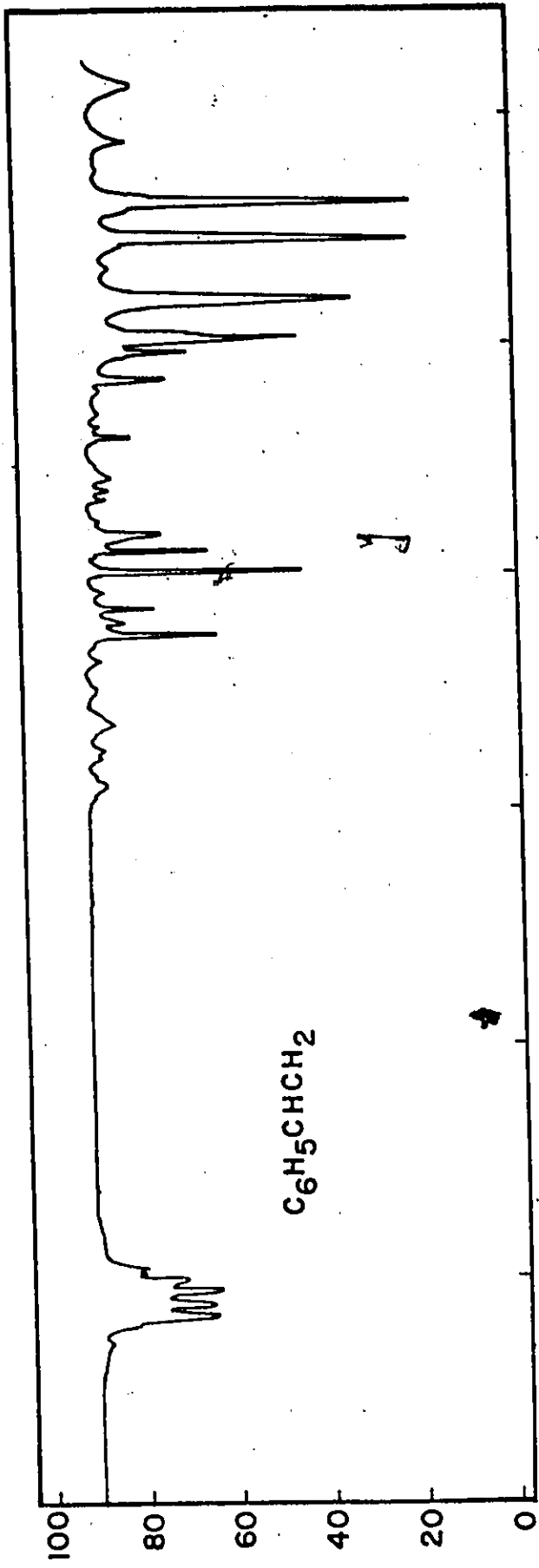
4.3.1 Vibrations Common to Monosubstituted Benzenes

The thirty ring vibrations of monosubstituted benzenes can be grouped into seven categories: C-H stretching, C-H in-plane bending, C-H out-of-plane bending, C-C stretching, ring in-plane deformation, ring out-of-plane deformation, and vibrations mainly involving distortion of the ring-substituent bond. From vibrational studies of various monosubstituted derivatives of benzene⁽¹²⁷⁻¹³¹⁾ it is known that twenty-four of these vibrations are essentially insensitive to the nature of the substituent. Varsanyi⁽¹³²⁾ has compiled a table of expected frequency ranges for monosubstituted benzene ring vibrations which illustrates this fact. Moss and Zundel⁽¹³³⁾ have made a similar list of expected frequency ranges for the ring- d_5 modes, although the number of vibra-

Figure 4.3

The Infrared Absorption Spectra of Liquid





TRANSMITTANCE (PERCENT)

FREQUENCY (cm⁻¹)

Figure 4.4
The Infrared Absorption Spectra of Liquid
 $C_6D_5CHCH_2$ and $C_6D_5CDCD_2$.

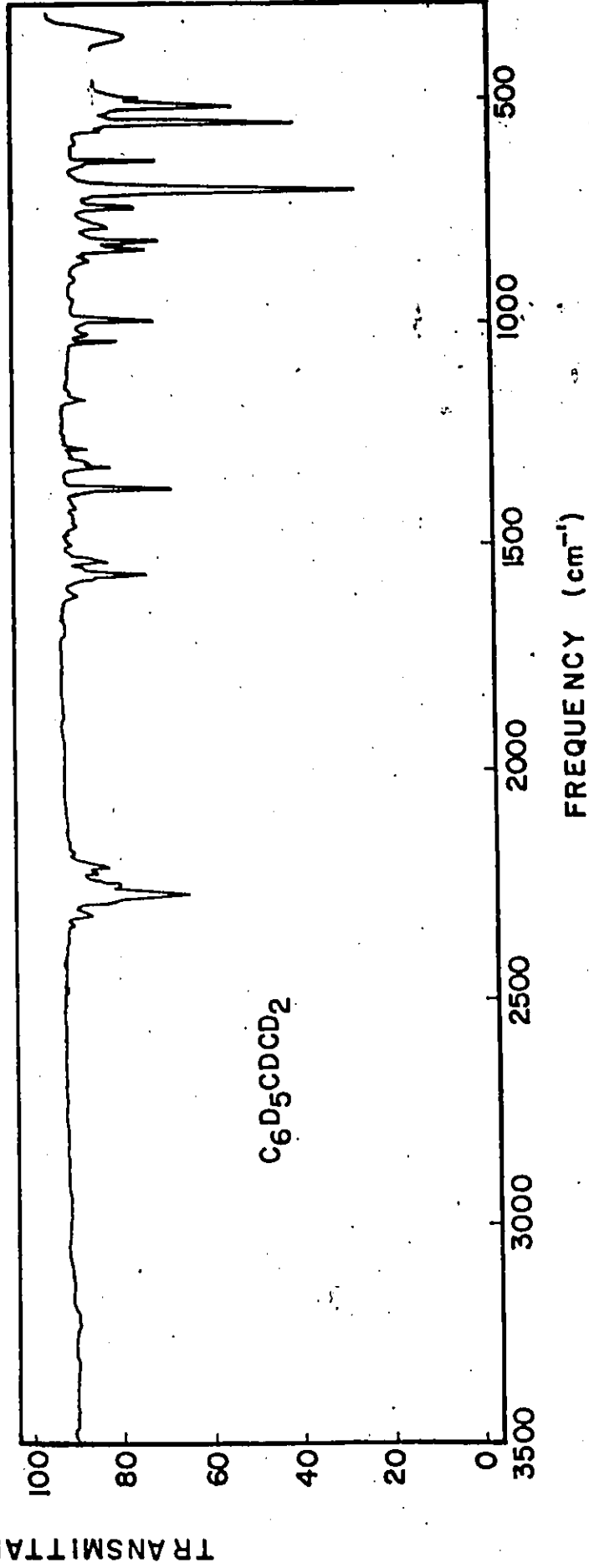
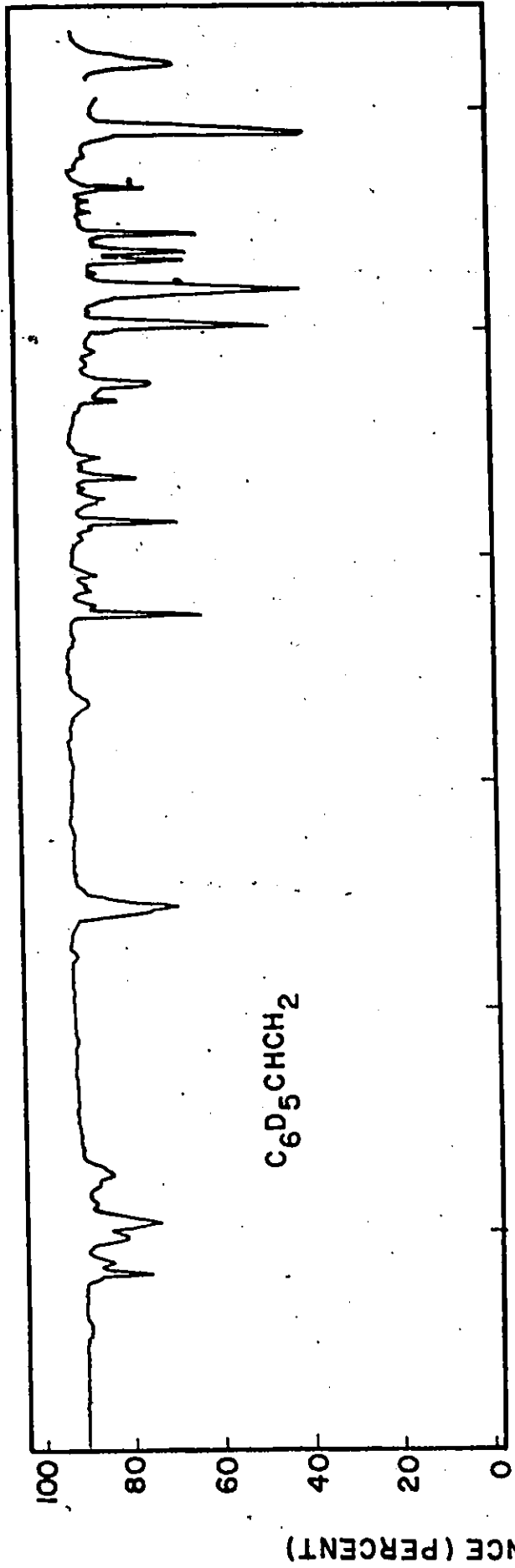
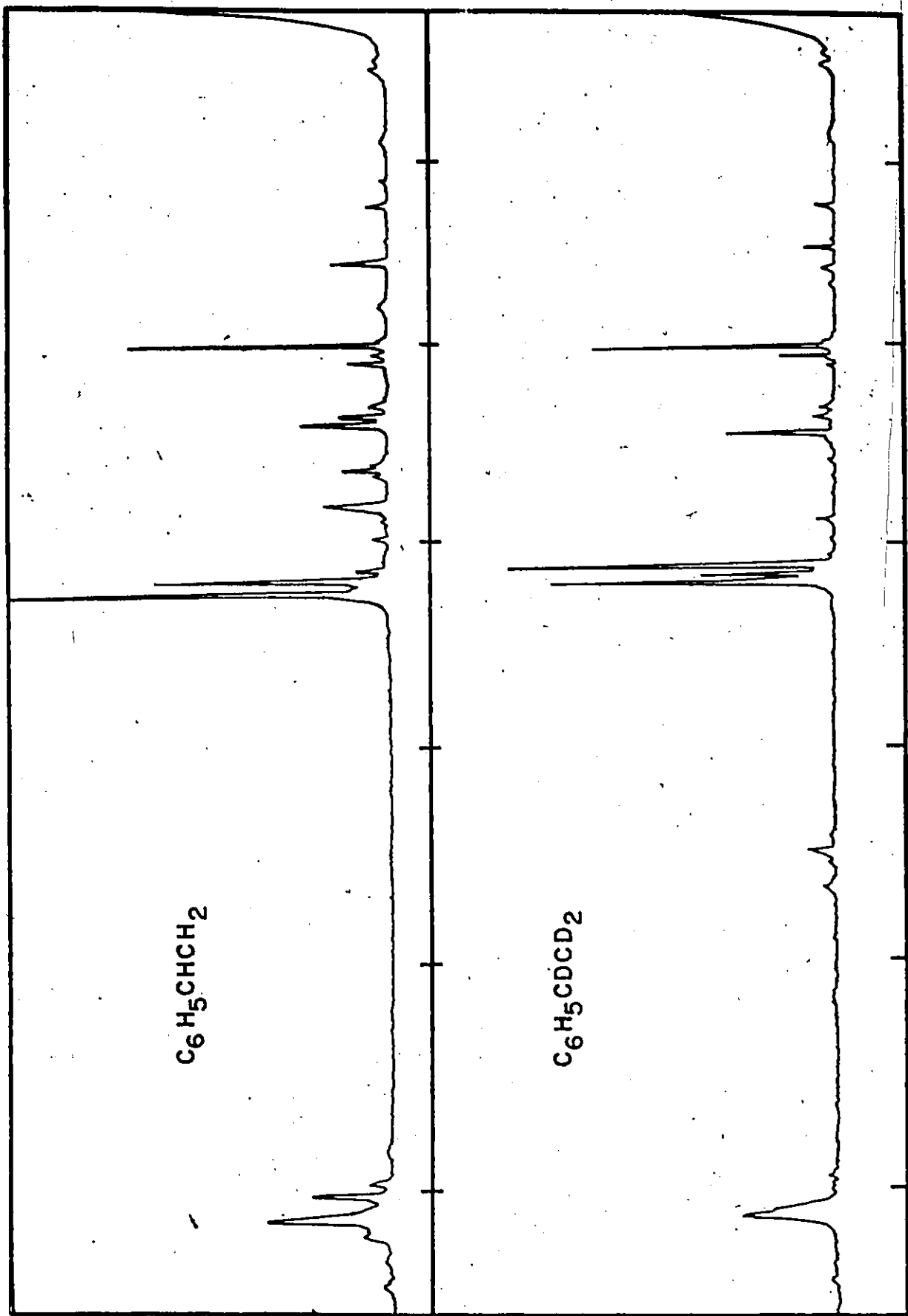


Figure 4.5

The Raman Spectra of Liquid $C_6H_5CHCH_2$ and $C_6H_5CDD_2$.



C6H5CH2CH2

C6H5CD2CD2

INTENSITY

FREQUENCY (cm⁻¹)

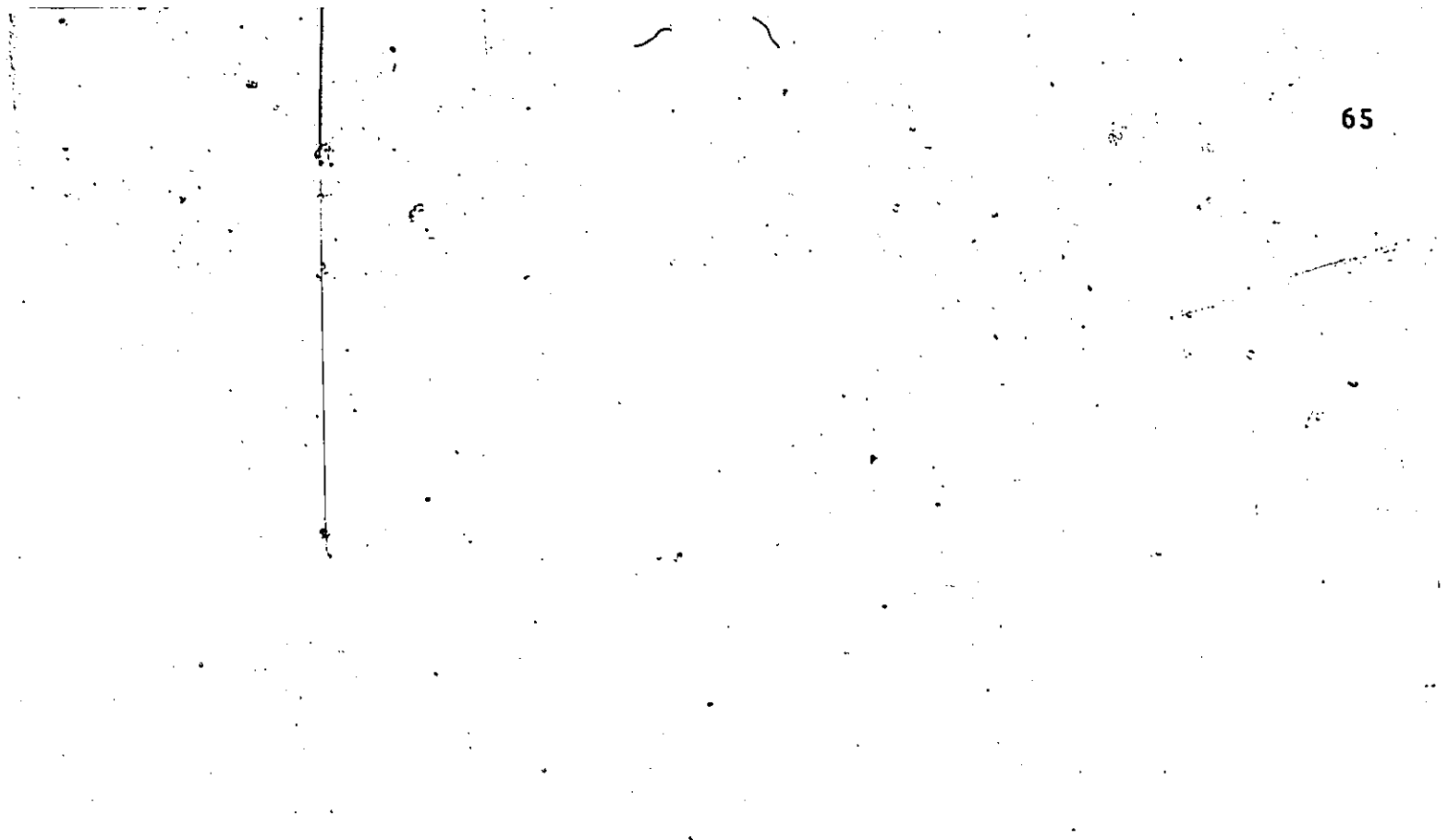
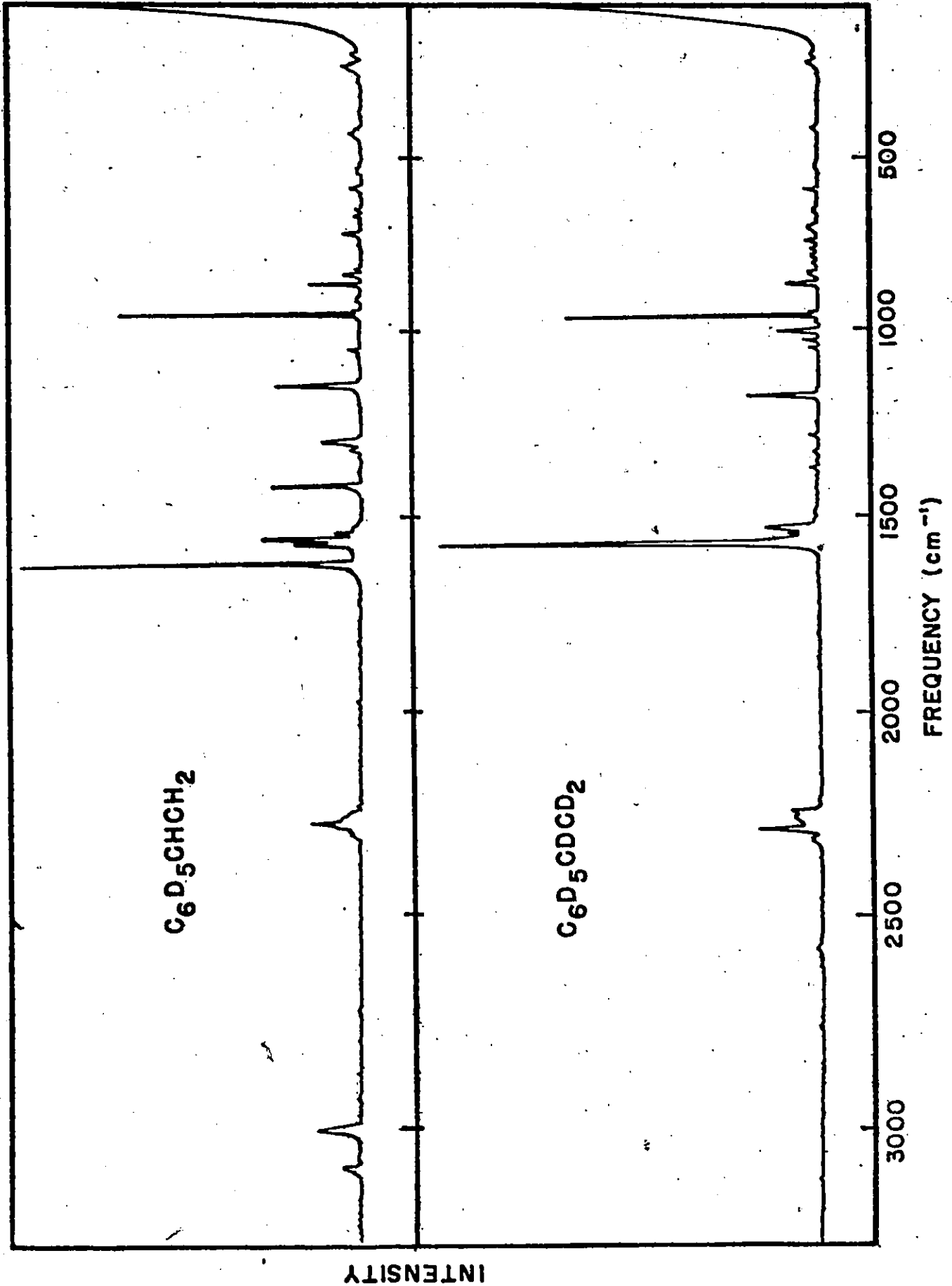


Figure 4.6

The Raman Spectra of Liquid $C_6D_5CHCH_2$ and $C_6D_5CDCD_2$.

6514



tional studies done on ring-deuterated monosubstituted benzenes was, at that time, very small. Both compilations are shown in Table 4.3. Recently, however, more ring-deuterated compounds have been analyzed (129,130,134,135) and these analyses too were useful in assigning the fundamentals of the ring-deuterated styrenes.

The C-H stretching region in monosubstituted benzenes covers the range 3020-3110 cm^{-1} . In the infrared this region can look very complex due to the presence of summation bands involving the ring C-C stretching vibrations (132). In addition, assignment of the five ring C-H stretching vibrations is made more difficult in the case of $\text{C}_6\text{H}_5\text{CHCH}_2$ by the presence of the C-H stretching modes of the vinyl group. Nevertheless, vinyl group deuteration of $\text{C}_6\text{H}_5\text{CHCH}_2$ gives a simpler looking C-H stretching region in the infrared spectrum and the four distinct bands in the 3000-3100 cm^{-1} region of $\text{C}_6\text{H}_5\text{CHCH}_2$, as well as the corresponding bands in $\text{C}_6\text{H}_5\text{CHCH}_2$, have been assigned as C-H stretching vibrations. The fifth ring C-H stretching mode in the ring-protonated styrenes is assigned to the band appearing in the Raman spectrum as a shoulder on the low frequency side of ν_4 , the most intense band in the 3000 cm^{-1} region. Upon ring deuteration the range of frequencies for C-D stretches becomes smaller, resulting in fewer distinct bands in the infrared for $\text{C}_6\text{D}_5\text{CHCH}_2$ and $\text{C}_6\text{D}_5\text{CDCD}_2$. The ring C-H and C-D stretching frequencies given in Table 4.6 are listed merely in order of decreasing frequency (except for ν_4 , which is a strong Raman band for all four molecules), and no correlation is intended among the

Table 4.3

Expected Frequency Regions (cm^{-1}) for the Normal Vibrations
of Monosubstituted Benzenes

Designation and Description of Mode ^a		Frequency Range (cm^{-1})	
		$\text{C}_6\text{H}_5\text{X}^b$	$\text{C}_6\text{D}_5\text{X}^c$
	$\nu\text{C-H}$	3020-3110	2260-2305
a-		1170-1181	860- 880
b-		1018-1031	795- 820
c-	$\beta\text{C-H}$	1150-1160	830- 845
d-		1065-1087	785- 835
e-		1253-1331	1000-1050
f-		720- 830	605- 655
g-		810- 860	655- 695
h-	$\gamma\text{C-H}$	940- 980	760- 795
i-		880- 940	735- 770
j-		970-1000	810- 830
k-		1575-1614	1535-1580
l-		1562-1597	1535-1580
m-	$\nu\text{C-C}$	1470-1515	1320-1390
n-		1440-1470	1305-1330
o-		1300-1350	1260-1295
p-	ring	990-1010	950-965
q-	X-sens ($\nu\text{C-X}$)	1100-1280	990-1230
r-	X-sens ($\alpha\text{C-C-C}$)	620- 830	620- 750
s-	$\alpha\text{C-C-C}$	605- 630	585- 605
t-	X-sens ($\alpha\text{C-C-C}$)	300- 530	260- 530
u-	X-sens ($\beta\text{C-X}$)	160- 410	200- 390
v-	$\phi\text{C-C}$	680- 700	510- 570
w-	$\phi\text{C-C}$	390- 420	350- 380
x-	X-sens ($\phi\text{C-C}$)	430- 560	350- 490
y-	X-sens ($\gamma\text{C-X}$)	140- 250	150- 230

Table 4.3 (continued)

- a: See Figure 4.1 for schematic illustrations of the letter-designated modes. The approximate descriptions corresponding to the abbreviations in the second column under this heading are found in Table 4.2.
- b: From reference (132).
- c: From reference (133).

four styrenes for these modes.

There are five ring C-C stretching modes in monosubstituted benzenes. In the styrenes these are designated as ν_{10} , ν_{11} , ν_{12} , ν_{13} , and ν_{15} . In $C_6H_5CHCH_2$, the strong Raman band at 1600 cm^{-1} has been assigned as ν_{10} , which would be of a_1 symmetry if styrene had strict C_{2v} symmetry. However, the depolarization ratio is rather high (0.46) for an "a₁" mode. It is known, though, that phenylacetylene⁽¹²⁹⁾ and phenylisocyanide⁽¹³⁰⁾ show similar behaviour for this mode. Only the assignment of one more mode in $C_6H_5CHCH_2$, ν_{15} , deserves comment. This mode is expected to appear in the frequency region $1300\text{-}1350\text{ cm}^{-1}$. The Raman spectrum of $C_6H_5CHCH_2$ shows three polarized bands in this spectral region. Of these, the band at 1303 cm^{-1} can be discounted since by comparison with the Raman spectrum of $C_6D_5CHCH_2$ it can be assigned to ν_{16} , a C-H bending mode of the vinyl group. Of the two remaining bands, the one at 1334 cm^{-1} is assigned to ν_{15} by comparison with the $C_6H_5CD_2$ vibrational spectra. This mode is not expected to be substituent-sensitive. In $C_6H_5CD_2$ ν_{11} is assigned to the medium-intensity Raman band at 1585 cm^{-1} (1586 cm^{-1} in the infrared). The frequency of ν_{11} is higher in $C_6H_5CD_2$ than in $C_6H_5CHCH_2$ perhaps due to the perturbing influence of ν_9 (which is a very strong Raman band in all four styrenes). In $C_6D_5CHCH_2$ the infrared and Raman spectra show three bands in the region where ν_{10} and ν_{11} are expected to appear. The weak lowest-frequency Raman band at 1539 cm^{-1} is assigned as ν_{11} ; a band of similar intensity is observed in the Raman spectrum of $C_6D_5CD_2$ at 1535 cm^{-1} .

The stronger of the remaining two bands, at 1564 cm^{-1} (1563 cm^{-1} in $\text{C}_6\text{D}_5\text{CDCD}_2$) is assigned to ν_{10} .

The C-H in-plane bending mode ν_{23} in $\text{C}_6\text{H}_5\text{CHCH}_2$ and $\text{C}_6\text{H}_5\text{CDCD}_2$ is expected to appear in the narrow range $1019\text{-}1032\text{ cm}^{-1}$. Two polarized Raman bands at 1020 and 1032 cm^{-1} are observed in this region for $\text{C}_6\text{H}_5\text{CHCH}_2$. These bands are also seen in the infrared spectrum, the former being of medium intensity and the latter a weak shoulder on this band. The appearance of an infrared band at 1026 cm^{-1} in $\text{C}_6\text{H}_5\text{CDCD}_2$ of comparable intensity to the 1019 cm^{-1} band in the infrared spectrum of $\text{C}_6\text{H}_5\text{CHCH}_2$ enables these bands to be assigned to ν_{23} . The C-H in-plane bending mode ν_{17} has been assigned to bands at 1289 , 1290 , 1054 , and 1028 cm^{-1} for the series $\text{C}_6\text{H}_5\text{CHCH}_2$, $\text{C}_6\text{H}_5\text{CDCD}_2$, $\text{C}_6\text{D}_5\text{CHCH}_2$, and $\text{C}_6\text{D}_5\text{CDCD}_2$. The assignment for $\text{C}_6\text{D}_5\text{CDCD}_2$ has been made on the assumption that ν_{14} , the symmetric bending vibration of the terminal CH_2 group of the vinyl substituent, is insensitive to ring deuteration. This assignment for ν_{17} means that ν_{14} in $\text{C}_6\text{D}_5\text{CDCD}_2$ can be assigned to the polarized Raman band at 1050 cm^{-1} . However, the reverse assignment is equally plausible. One possible reason to favor the first assignment is that the assigned frequency for ν_{17} in $\text{C}_6\text{D}_5\text{CHCH}_2$ is slightly outside the usual frequency range for this mode in ring-deuterated monosubstituted benzenes, and any possibility for vibrational interaction with ν_{22} (the anti-symmetric bending vibration of the $=\text{CH}_2$ Group) is removed by deuteration of the vinyl group. The two C-H in-plane bending modes ν_{20} and ν_{23} are assigned to the same frequency in $\text{C}_6\text{D}_5\text{CHCH}_2$, even though ν_{23} in $\text{C}_6\text{D}_5\text{CHCH}_2$ falls outside its expected range (795

820 cm^{-1}). These two fundamentals are often found in close proximity in ring-deuterated monosubstituted benzenes (129,130,136), but at a higher frequency than ν_{21} , which appears at 824 cm^{-1} in the infrared. There is no evidence that ν_{23} in $\text{C}_6\text{D}_5\text{CHCH}_2$ lies within the frequency range given by Moss and Zundel. Although a weak, polarized Raman band is seen at 810 cm^{-1} in $\text{C}_6\text{D}_5\text{CDCD}_2$, it can reasonably be ascribed to vinyl group mode ν_{22} .

The X-sensitive ring in-plane deformation mode ν_{25} in $\text{C}_6\text{H}_5\text{CHCH}_2$ is expected to have a frequency in the range 620-830 cm^{-1} . A polarized, medium intensity Raman band is seen at 775 cm^{-1} . However, the strong band near 775 cm^{-1} in the infrared spectrum of $\text{C}_6\text{H}_5\text{CHCH}_2$ vapor has a type C band contour. Therefore, it seems probable that ν_{25} is accidentally near-degenerate with a ring C-H out-of-plane bending mode, ν_{36} (the "umbrella" vibration, usually of medium to high intensity and found in the range 720-830 cm^{-1} in monosubstituted benzenes). This suggestion is supported by the analysis of the $\text{C}_6\text{D}_5\text{CHCH}_2$ vibrational spectra. From the approximate descriptions of ν_{25} and ν_{36} (Figure 4.1), ring deuteration is expected to lower the frequency of the latter more, and so the accidental degeneracy should be lifted. Experimentally, a type C band near 680 cm^{-1} in the vapor phase infrared is observed and can be ascribed to ν_{36} , while a weak, but polarized band at 729 cm^{-1} in the Raman spectrum of liquid $\text{C}_6\text{D}_5\text{CHCH}_2$ is assigned as ν_{25} . In the previous vibrational study of $\text{C}_6\text{D}_5\text{CDCD}_2$, ν_{25} was not assigned. However, in this work, a

weak Raman band at 699 cm^{-1} having a low ρ value characteristic of ν_{25} is detected. This assignment for ν_{25} is consistent with the expected isotopic shift for this mode, ie. 776/735/729/699 for the series $\text{C}_6\text{H}_5\text{CHCH}_2/\text{C}_6\text{H}_5\text{CDCD}_2/\text{C}_6\text{D}_5\text{CHCH}_2/\text{C}_6\text{D}_5\text{CDCD}_2$.

In the two most recent studies on the vibrational spectra of styrene^(18,19), the frequency of the X-sensitive ring in-plane deformation mode ν_{6a} has been assigned as approximately 555 cm^{-1} . However, this assignment is thought to be incorrect due to the following evidence. Polarized Raman bands in the series $\text{C}_6\text{H}_5\text{CHCH}_2/\text{C}_6\text{H}_5\text{CDCD}_2/\text{C}_6\text{D}_5\text{CHCH}_2/\text{C}_6\text{D}_5\text{CDCD}_2$ are found at $442/420/433/408\text{ cm}^{-1}$, the isotopic shift being very similar to that seen for vibration 6a in the molecules phenylacetylene⁽¹²⁹⁾, toluene⁽¹³⁷⁾ and aniline⁽¹³⁸⁾. In the fluorescence spectra of the four styrenes, bands red-shifted from the origin bands by frequencies near those mentioned above are observed, and vibration 6a is known to be active in the fluorescence spectra of other nonsubstituted benzenes^(8-10,102). Garg⁽¹³⁹⁾ has reported an empirical formula for the calculation of vibration 6a for monosubstituted benzenes which gives very good agreement for a wide variety of substituents. Using this formula, 443 cm^{-1} is predicted for ν_{6a} (ν_{28} in Herzberg notation) in $\text{C}_6\text{H}_5\text{CHCH}_2$. It is also to be noted that the assignment of 442 cm^{-1} to ν_{28} is consistent with the very recent work of Green and Harrison⁽¹⁴⁰⁾ on benzaldehyde, which is iso-electronic with styrene. In their paper they assign vibration 6a in liquid $\text{C}_6\text{H}_5\text{CHO}$ to a strong, polarized Raman band at 437 cm^{-1} .

The frequency of ν_{18} , the stretching vibration between the ring carbon atom and the substituent, is assigned to bands at 1203/1225/1154/1179 cm^{-1} for the series $\text{C}_6\text{H}_5\text{CHCH}_2/\text{C}_6\text{H}_5\text{CDCD}_2/\text{C}_6\text{D}_5\text{CHCH}_2/\text{C}_6\text{D}_5\text{CDCD}_2$. As in the case of ν_{28} , the activity of this mode in the fluorescence spectra of the styrenes lends credence to this assignment. Vinyl group deuteration seems to increase the frequency of ν_{18} . An increase in the frequency of the C-X stretching vibration upon replacing hydrogen for deuterium in the substituent has also been observed in the vibrational spectra of toluene⁽¹⁴¹⁾ and benzaldehyde⁽¹⁴⁰⁾. This effect could be attributed to an increase in the contribution of the C-H stretching symmetry coordinates to the normal coordinate upon deuteration⁽¹⁴²⁾.

Either of the two strong bands at 788 and 742 cm^{-1} in the liquid phase infrared spectrum of $\text{C}_6\text{H}_5\text{CDCD}_2$ can be assigned to the ring C-H out-of-plane bending mode ν_{36} , the other being ν_{30} , a C-H out-of-plane bending mode in the vinyl group. The vapor phase spectrum shows only the band near 740 cm^{-1} to have a strong type C contour, the band at 790 cm^{-1} being weak. The infrared spectrum of $\text{C}_6\text{D}_5\text{CDCD}_2$ vapor shows a very weak band near 790 cm^{-1} , and the high Raman depolarization ratio for this band, in both substituent-deuterated styrenes indicate that it is of a'' symmetry. A plausible assignment for ν_{30} , then, for the series $\text{C}_6\text{H}_5\text{CHCH}_2/\text{C}_6\text{H}_5\text{CDCD}_2/\text{C}_6\text{D}_5\text{CHCH}_2/\text{C}_6\text{D}_5\text{CDCD}_2$ is 992/788/989/789 cm^{-1} , although the strong type C contours for this mode in $\text{C}_6\text{H}_5\text{CHCH}_2$ and $\text{C}_6\text{D}_5\text{CHCH}_2$ seem to be lost on vinyl group deuteration (the published infrared spectra of propylene and

propylene-d₆⁽¹⁴³⁾ show that this band is also not as sharply defined in the deuterated derivative). This assignment for ν_{30} leaves 747 cm⁻¹ for ν_{33} in C₆D₅CDCD₂. This band displays the type C band contour that is seen for ν_{33} in the other three styrenes. However, an alternative assignment whereby ν_{30} and ν_{36} in C₆H₅CDCD₂ and at the same time ν_{30} and ν_{33} in C₆D₅CDCD₂ are reversed, cannot be ruled out.

The ring out-of-plane C-H bending vibration ν_{32} is expected to give, at best, an extremely weak band in the infrared and Raman spectra. It is often not seen at all as a fundamental, but in ring-protonated monosubstituted benzenes can be assigned from combination bands in the 1650-2000 cm⁻¹ region in the infrared⁽¹⁴⁴⁾. This is the method used to assign ν_{32} in both C₆H₅CHCH₂ and C₆H₅CDCD₂, and the observation of a very weak band at 970 cm⁻¹ in C₆H₅CDCD₂ helps to confirm the ν_{32} assignment.

The X-sensitive ring out-of-plane deformation mode ν_{39} is expected to have a frequency in the range 430-560 cm⁻¹. Two bands are seen in this wavenumber region in liquid C₆H₅CHCH₂, one at 554 cm⁻¹ and one at 434 cm⁻¹, with the latter being broad. Jakobsen and Bentley⁽¹⁴⁵⁾ suggest that for monosubstituted benzenes with a $\text{C}=\text{C}$ substituent, the frequency of this mode is near 550 cm⁻¹. Since this mode is of a'' symmetry it should give rise to a type C band in the vapor phase spectrum. However, the vapor spectrum shows a band near 430 cm⁻¹ to have a type C contour, while the band near 550 cm⁻¹ does not. Hence the broad infrared band at 434 cm⁻¹ is assign-

ed to ν_{39} in $C_6H_5CHCH_2$. (That this band is broad can be explained by the fact that the frequency of in-plane mode ν_{28} is close to that of ν_{39} , and so the band at 434 cm^{-1} may be comprised of two superimposed bands.) It is interesting to note that Green and Harrison⁽¹⁴⁰⁾ obtained a value of 449 cm^{-1} for this mode in the liquid phase infrared spectrum of benzaldehyde. This number agrees well with the value obtained in this work for styrene.

The out-of-plane ring deformation mode ν_{40} is usually very weak or absent in the infrared spectra of monosubstituted benzenes. This mode is often found at about 400 cm^{-1} . It has been assigned to a very weak band at 407 cm^{-1} in the Raman spectrum of $C_6H_5CHCH_2$ liquid. This frequency had not been detected by the earlier workers. In $C_6H_5CDCD_2$ there are two weak Raman bands appearing as shoulders to the low frequency side of in-plane ring mode ν_{28} . The first, at 407 cm^{-1} can be assigned to ν_{39} by way of this mode's expected isotopic shift pattern upon ring and substituent deuteration. The second shoulder, at 398 cm^{-1} , is tentatively assigned to ν_{40} .

The out-of-plane ring deformation mode ν_{37} is generally very strong in the infrared spectrum and occurs within the narrow frequency range $680\text{-}700\text{ cm}^{-1}$. Its assignment in the case of ring-protonated styrenes is straightforward. In $C_6D_5CHCH_2$ liquid a very strong band at 541 cm^{-1} in the infrared is observed. However, in the Raman spectrum a polarized band at 542 cm^{-1} is present. That the infrared band has a "symmetry is shown by the observation of a strong type C band

contour in the vapor phase spectrum near 540 cm^{-1} . Thus, ν_{37} in $\text{C}_6\text{D}_5\text{CHCH}_2$ is accidentally near-degenerate with an in-plane vibration (assigned as ν_{27} , a bending mode of the vinyl group). In $\text{C}_6\text{D}_5\text{CDCD}_2$ there are two type C bands present in the 500-600 cm^{-1} region. Of these, the higher frequency band at 554 cm^{-1} in the liquid is chosen as ν_{37} since, as in $\text{C}_6\text{D}_5\text{CHCH}_2$, its overtone is observed in the Raman spectrum. A further discussion on the 500-600 cm^{-1} region of perdeuterated styrene is given in the analysis of the vinyl group modes.

4.3.2 Vinyl Group Modes

There are 12 vibrations associated with the vinyl group, eight of which are in-plane (3 C-H stretching, 1 C=C stretching, 3 C-H deformation, and the -C=C deformation modes), and four of which are out-of-plane (3 C-H bending modes and the torsional mode). Eight of these modes have been well characterized^(124,146,147) and consequently assignments for some of these vibrations in the styrenes were quite readily made.

Fateley et al⁽¹⁸⁾ gave assignments to only two of the three vinyl C-H stretching modes. Moss and Zundel⁽¹⁹⁾ found frequencies for all three modes, although one assignment was in doubt due to the observation of a depolarized band where one of low ρ value was expected. The $\text{C}_6\text{D}_5\text{CHCH}_2$ spectra confirm the assignments of Moss and Zundel, although a polarized band at 2981 cm^{-1} in the Raman spectrum of $\text{C}_6\text{H}_5\text{CHCH}_2$ is seen, contrary to their observation.

The C=C stretching vibration in alkyl substituted ethylenes

gives rise to a characteristically strong and highly polarized band in the Raman spectrum in the range 1630-1680 cm^{-1} (147). This mode, ν_9 in styrene, has been assigned to the very strong Raman bands at 1630 and 1629 cm^{-1} for $\text{C}_6\text{H}_5\text{CHCH}_2$ and $\text{C}_6\text{D}_5\text{CHCH}_2$ respectively. Vinyl group deuteration lowers the frequency of this mode to 1563 and 1574 cm^{-1} in $\text{C}_6\text{H}_5\text{CDCD}_2$ and $\text{C}_6\text{D}_5\text{CDCD}_2$.

The antisymmetric bending mode of the terminal $=\text{CH}_2$ group, ν_{22} , is usually weak in both the infrared and Raman spectra of alkyl monosubstituted ethylenes, and since its frequency lies in the frequency range of the C-C skeletal deformation modes of the substituent, a characteristic frequency is not associated with this vibration. In $\text{C}_6\text{H}_5\text{CHCH}_2$ this mode has been assigned to weak infrared and Raman bands at 1032 cm^{-1} , in agreement with the work of Fateley *et al* (18) and with that of Singh and Jaiswal (148,149), who recorded and assigned the Raman spectra of the isomeric fluoro- and bromo- styrenes. In $\text{C}_6\text{H}_5\text{CDCD}_2$ a polarized Raman band at 831 cm^{-1} can reasonably be ascribed to ν_{22} . The corresponding frequencies for ν_{22} in $\text{C}_6\text{D}_5\text{CHCH}_2$ and $\text{C}_6\text{D}_5\text{CDCD}_2$ are 1006 and 810 cm^{-1} respectively. The styrene- d_8 value had previously been assigned to ν_{23} by Moss and Zundel. However, this assignment is rejected because no band near this frequency is seen in either the infrared or Raman spectrum of $\text{C}_6\text{D}_5\text{CHCH}_2$.

The C=C in-plane bending mode ν_{27} in $\text{C}_6\text{H}_5\text{CHCH}_2$ and $\text{C}_6\text{D}_5\text{CHCH}_2$ is readily assigned to the polarized Raman bands at 554 and 542 cm^{-1} respectively. Both Fateley *et al* and Moss and Zundel have considered the 554 cm^{-1} band to be ring mode ν_{28} .

The reasons for disagreeing with this assignment have been mentioned in the ν_{28} discussion. Upon vinyl group deuteration, the frequency of ν_{27} drops to 510 cm^{-1} for $\text{C}_6\text{H}_5\text{CDCD}_2$ and to 498 cm^{-1} for $\text{C}_6\text{D}_5\text{CDCD}_2$. For these two isotopic species the Raman band attributed to ν_{27} has a much larger ρ value compared to the substituent-protonated molecules. Nevertheless, the vapor phase infrared spectrum of $\text{C}_6\text{H}_5\text{CDCD}_2$ shows a type A/B hybrid band near 510 cm^{-1} , indicative of in-plane polarization. Although no corresponding band appears in the spectrum of $\text{C}_6\text{D}_5\text{CDCD}_2$ vapor, the assigned frequency of 498 cm^{-1} in the liquid is consistent with the isotopic behaviour of ν_{27} in the other three styrenes.

Only two of the three C-H out-of-plane deformations in the vinyl group give rise to characteristically strong bands in the infrared. One of these, ν_{30} , has been discussed previously; the other, ν_{34} , the symmetric wagging vibration of the $=\text{CH}_2$ group, is well known in both protonated^(125,146,150) and deuterated⁽¹⁵¹⁻¹⁵³⁾ vinyl-containing compounds. The third C-H out-of-plane deformation, an antisymmetric twisting vibration of the $=\text{CH}_2$ group (Figure 4.2), is weaker and has a more variable intensity. It has been found around 630 cm^{-1} in the infrared and Raman spectra of some n-alkyl monosubstituted ethylenes⁽¹⁴⁶⁾, and has been calculated to appear at 613 cm^{-1} for a substituent of infinite mass⁽¹⁵⁴⁾. Fateley et al⁽¹⁸⁾ tentatively assigned ν_{38} to the 554 cm^{-1} infrared band in $\text{C}_6\text{H}_5\text{CHCH}_2$, but the vapor phase spectrum shows that this band is in-plane polarized, and hence cannot be attributed to ν_{38} . However, in

the Raman spectrum a very weak band at 640 cm^{-1} just emerges to the high frequency side of the medium intensity band at 620 cm^{-1} . This observation is more easily seen in the Raman spectra taken at the lower temperature, and perhaps this is the reason why no Raman band at 640 cm^{-1} has been reported in the past. This band, then, is assigned to ν_{38} . A weak infrared and a very weak Raman band at 571 cm^{-1} in $\text{C}_6\text{H}_5\text{CDCD}_2$ are also attributed to ν_{38} , although the corresponding vapor phase band is weak and has an indeterminate profile. The frequency of ν_{38} is expected to change little upon ring deuteration. However, no band attributable to ν_{38} is seen in the 640 cm^{-1} region of $\text{C}_6\text{D}_5\text{CHCH}_2$ (a weak depolarized Raman band at 657 cm^{-1} is also seen in the Raman spectrum of $\text{C}_6\text{D}_5\text{CDCD}_2$, and so can be reasonably assigned to ring mode ν_{35}). In addition, it is interesting to note that ν_{36} appears at 679 cm^{-1} , far outside the frequency range $605\text{-}655\text{ cm}^{-1}$ found for this mode in ring-deuterated monosubstituted benzenes. One possible explanation of these two observations is that vibrational interaction has occurred between ν_{36} and ν_{38} . There is no evidence of any vibrational band in the $600\text{-}650\text{ cm}^{-1}$ region that could be assigned to ν_{38} . Therefore, ν_{38} has been assumed to lie under ν_{26} , the medium intensity depolarized Raman band at 595 cm^{-1} . This assignment is, of course, very tentative. In the spectra of $\text{C}_6\text{D}_5\text{CDCD}_2$ three bands appear which could possibly be ν_{38} . The first of these is a strong infrared band at 516 cm^{-1} . This band has a strong type C contour in the vapor phase spectrum. The second, an intense infrared band at 554 cm^{-1} and which also

has a type C vapor phase contour, has already been assigned to ν_{37} . The third band appears weakly in the infrared at 571 cm^{-1} , and considering its similarity in intensity and frequency to the 571 cm^{-1} band in $\text{C}_6\text{H}_5\text{CDCD}_2$, no doubt is associated with a vibration of the vinyl moiety. It is this band that is assigned as ν_{38} . If the intense 516 cm^{-1} band is chosen as ν_{38} , one is then faced with the problems of a large deuterium shift of a vinyl group vibration upon ring deuteration, and a great intensity enhancement for this mode in $\text{C}_6\text{D}_5\text{CDCD}_2$ compared to the remaining styrenes. The 516 cm^{-1} band is not easily assigned to a summation band, so its assignment as a difference band was investigated. An assignment of this band as $\nu_{25} - \nu_{41}$ would be of the correct frequency and symmetry, but it is difficult to explain why a difference band would be so intense. Another possible rationale, one that would explain the unexpectedly high intensity of the 517 cm^{-1} band, is that ν_{37} has interacted via Fermi resonance with the difference band $\nu_{33} - \nu_{29}$. This would place the unperturbed levels near 535 cm^{-1} . The reason for assigning ν_{37} to the 554 cm^{-1} band has been outlined in the previous analysis of the ring modes.

The frequency of the torsional mode ν_{42} in styrene vapor, recently determined from Raman studies, is 64 cm^{-1} (22). For the liquid, there is no direct spectral evidence that would establish a frequency for this mode, the Rayleigh wing presumably obscuring any bands that could be assigned to the torsional fundamental or its overtone. A liquid phase value can be esti-

mated, however, by adding approximately 20% to the vapor phase value. It is known⁽¹⁵⁵⁾ that for vibrational frequencies less than $\sim 300 \text{ cm}^{-1}$, $\nu_{\text{liquid}} > \nu_{\text{vapor}}$. In addition, studies of torsional vibrations about the C-C single bond in substituted benzaldehydes⁽¹⁵⁶⁾ indicate that the percentage increase in torsional frequency upon going from gas to liquid phase is about 20%. This approximation leads to an estimated value for ν_{42} in $\text{C}_6\text{H}_5\text{CHCH}_2$ of 76 cm^{-1} . Torsional frequencies for the other three styrenes can then be estimated by use of the Teller-Redlich product rule. By this method, ν_{42} is assigned as $76/66/72/59 \text{ cm}^{-1}$ for the series $\text{C}_6\text{H}_5\text{CHCH}_2/\text{C}_6\text{H}_5\text{CDCD}_2/\text{C}_6\text{D}_5\text{CHCH}_2/\text{C}_6\text{D}_5\text{CDCD}_2$.

4.4 Teller-Redlich Product Ratios

The Teller-Redlich product ratios for the a' modes in the styrenes are presented in Table 4.7. The observed ratios are all greater than the calculated ones, as is expected if anharmonicity corrections are neglected. In calculating the product ratios for the styrenes, the required moments of inertia were computed based on the following bond lengths^(24,157,158): ring C-C, 1.399 Å; ring C-H, 1.101 Å; vinyl C=C, 1.344 Å; vinyl C-H, 1.10 Å; ring-substituent C-C, 1.467 Å. All bond angles were assumed to be 120° . The observed product ratios for the a'' modes cannot, of course, be compared with calculated values without experimental data on the frequency of ν_{42} . For comparison, some product ratios of isotopic pairs for some related monosubstituted benzenes are given in Table 4.8.

Table 4.4

Frequencies (cm^{-1}) and Assignments for Infrared and Raman Bands of
 $\text{C}_6\text{H}_5\text{CHCH}_2$ and $\text{C}_6\text{H}_5\text{CDCD}_2$

$\text{C}_6\text{H}_5\text{CHCH}_2$			$\text{C}_6\text{H}_5\text{CDCD}_2$		
IR	RAMAN (ρ)	Assignment	IR	RAMAN (ρ)	Assignment
	212 (0.85)	ν_{41}	192	(0.86)	ν_{41}
	241 (0.53)	ν_{29}	220	(0.51)	ν_{29}
	407	ν_{40}	398 sh		ν_{40}
434 w C	431 sh	ν_{39}	407 sh		ν_{39}
	442 (0.17)	ν_{28}	420	(-0.2)	ν_{28}
554 w	554 (0.32)	ν_{27}	510	(-0.7)	ν_{27}
623 vw	620 (0.75)	ν_{26}	527 vw		$\nu_{40} + 2\nu_{42}?$
	640 dp	ν_{38}	571 w		ν_{38}
683 sh		$\nu_{28} + \nu_{29}$	624 vw	(0.76)	ν_{26}
698 vs C	700	ν_{37}	678 sh		
776 vs	775 (0.17)	ν_{25}, ν_{36}	692 vs C		ν_{37}
841 vw	841 (0.82)	ν_{35}	709 vs C	(-0.7)	ν_{34}
909 vs C	909 (0.77)	ν_{33}, ν_{34}	735	(0.06)	ν_{25}
983 sh	987	ν_{31}	742 vs		ν_{36}

Table 4.4 (Continued)

$C_6H_5CHCH_2$				$C_6H_5CDCD_2$			
IR	RAMAN	(ρ)	Assignment	IR	RAMAN	(ρ)	Assignment
992 s C			ν_{30}	775 sh			$\nu_{34} + \nu_{42}?$
	999	(0.04)	ν_{24}	788 s C	789	(0.83)	ν_{30}
1019 m	1020	(0.07)	ν_{23}	831 w	831	pol.	ν_{22}
1032 sh	1032	(0.05)	ν_{22}	838 sh	841 sh		ν_{35}
1083 m	1083		ν_{21}	875 w	874		$\nu_{37} + \nu_{41}$
1107 vw			$\nu_{33} + \nu_{41}$	913 m C	912		ν_{33}
1155 vw	1156	(0.89)	ν_{20}	970 vw			ν_{32}
1182 vw	1180	(0.17)	ν_{19}	984 vw	988		ν_{31}
1202	1203	(0.22)	ν_{18}	1003 m	1002	(0.06)	ν_{16}, ν_{24}
1266 sh			$\nu_{35} + \nu_{39}$	1026 w	1027	(0.04)	ν_{23}
1289 w			ν_{17}	1048 w	1048	(0.13)	ν_{14}
	1303	(0.27)	ν_{16}	1081 m			ν_{21}
1317 w	1316	(0.18)	$\nu_{33} + \nu_{40}$	1103 w			$\nu_{33} + \nu_{41}$
1334 w	1334	(0.16)	ν_{15}	1156 w	1156	(0.85)	ν_{20}
1384 vw			$2\nu_{37}$	1182 w	1181	(0.19)	ν_{19}
1412 m	1411	(0.23)	ν_{14}	1226 w	1225	(0.25)	ν_{18}
1419 sh			$\nu_{30} + \nu_{39}$	1241	1241	(0.38)	$\nu_{35} + \nu_{39}$

Table 4.4 (Continued)

$C_6H_5CHCH_2$			$C_6H_5CDCD_2$		
IR	RAMAN (ρ)	Assignment	IR	RAMAN (ρ)	Assignment
1450	1449 (-0.6)	ν_{13}	1290 w	1290 (0.41)	ν_{17}
1494	1495 (0.31)	ν_{12}	1310 w	1311 (0.30)	$\nu_{33} + \nu_{40}$
1538		$\nu_{35} + \nu_{37}$	1324		$\nu_{26} + \nu_{34}$
1575	1575 (0.26)	ν_{11}	1332 w	1332 (0.43)	ν_{15}
1601	1600 (0.46)	ν_{10}	1384 vw		$2\nu_{37}$
1620	1618 sh	$\nu_{24} + \nu_{26}$	1445 s	1444 (0.22)	ν_{13}
1630	1630 (0.19)	ν_9	1492 s	1490 (0.12)	ν_{12}
1690		$\nu_{33} + \nu_{36}$	1535 vw	1537 (-0.3)	$\nu_{35} + \nu_{37}$
1753		$\nu_{33} + \nu_{35}$	1562 m	1563 (0.16)	ν_9
	1772	$\nu_{24} + \nu_{25}$	1586 w	1585 (0.13)	ν_{11}
1808		$\nu_{32} + \nu_{35}$	1602 w	1602 (0.43)	ν_{10}
1824		$2\nu_{34}, \nu_{31} + \nu_{35}$	1659 vw		$\nu_{33} + \nu_{36}$
1879		$\nu_{32} + \nu_{33}$	1699 vw		$\nu_{30} + \nu_{33}$
1892		$\nu_{31} + \nu_{33}$	1736		$\nu_{24} + \nu_{25}$
1949		$\nu_{31} + \nu_{32}$			$\nu_{33} + \nu_{35}$
1962		$2\nu_{31}$			$\nu_{32} + \nu_{35}$
1982		$2\nu_{30}$			$\nu_{31} + \nu_{35}$

Table 4,4 (Continued)

C ₆ H ₅ CHCH ₂			C ₆ H ₅ CD ₂		
IR	RAMAN (ρ)	Assignment	IR	RAMAN (ρ)	Assignment
2572		ν ₁₁ + ν ₂₄	1881 w		ν ₃₂ + ν ₃₃
2605		ν ₁₄ + ν ₁₈	1895 w		ν ₃₁ + ν ₃₃
2780		ν ₁₃ + ν ₁₅	1950 w		ν ₃₁ + ν ₃₂
2830		ν ₉ + ν ₁₈	1964 w		2ν ₃₁
2913	2908	ν ₁₁ + ν ₁₅	2207 m	2208	ν ₈
2941		ν ₁₂ + ν ₁₃	2233 sh		ν ₂₀ + ν ₂₁
2982	2981 (0.19)	ν ₈	2244 m	2244 (0.20)	ν ₇
2992		2ν ₁₂		2273 (0.3)	ν ₁₄ + ν ₁₈
3010	3009 (0.19)	ν ₇	2292 vw		ν ₁₆ + ν ₁₇
3029		ν ₆	2317 vw	2315 (0.65)	ν ₁₇ + ν ₂₃
	3044	ν ₁₀ + ν ₁₃	2329 w	2329 (0.62)	ν ₂
	3055 sh	ν ₅	2392 vw		ν ₉ + ν ₂₂
3061	3061 (0.19)	ν ₄		2446	2ν ₁₈
3084		ν ₃		2581	ν ₁₁ + ν ₂₄
3090	3091 (0.73)	ν ₂		2783	ν ₉ + ν ₁₈
3105	3107 sh	ν ₁	2827 vw		ν ₁₀ + ν ₁₈
3150	3150	2ν ₁₁	2874 vw		ν ₁₁ + ν ₁₇

Table 4.4 (Continued)

$C_6H_5CHCl_2$			$C_6H_5CDCl_2$		
IR	RAMAN (ρ)	Assignment	IR	RAMAN (ρ)	Assignment
	3201	$2\nu_{11}$	2887 vw		$2\nu_{13}$
	3256	$2\nu_9$	2933 vw		$\nu_{12} + \nu_{13}$
			2981 sh	2974 (0.22)	$\nu_7 + \nu_{25}$
					$2\nu_{12}$
			3026 m	2995 (0.26)	$\nu_9 + \nu_{13}$
					ν_6
				3033	$\nu_8 + \nu_{22}$
				3051	ν_5
			3062 m	3060 (0.19)	ν_4
				3063	$\nu_2 + \nu_{25}$
			3084 m		ν_3
			3104 w		ν_1
				3118	$2\nu_9$
			3168 vw	3166	$2\nu_{11}$
				3201	$2\nu_{10}$
			3208 vw		$\nu_8 + \nu_{16}$
			3328 vw		$\nu_2 + \nu_{16}$

Table 4.4 (Continued)

s = strong; m = medium; w = weak; v = very; sh = shoulder; br = broad;

C = type C band contour; ρ = depolarization ratio; pol. = polarized;

dp = depolarized; ? = band assigned using the estimated torsional frequency.

Table 4.5

Frequencies (cm^{-1}) and Assignments for Infrared and Raman Bands of $\text{C}_6\text{D}_5\text{CHCH}_2$ and $\text{C}_6\text{D}_5\text{CDD}_2$

$\text{C}_6\text{D}_5\text{CHCH}_2$			$\text{C}_6\text{D}_5\text{CDD}_2$		
IR	RAMAN (p)	Assignment	IR	RAMAN (p)	Assignment
	205	ν_{41}		182	ν_{41}
	231	ν_{29}		212	ν_{29}
	354	ν_{40}		354	ν_{40}
390 m C	392	ν_{39}	368 m C	370	ν_{39}
	433	ν_{28}		408	ν_{28}
495 w		$\nu_{40} + 2\nu_{42} ?$	498 w	498	ν_{27}
541 vs	542	ν_{27}, ν_{37}	516 s C	518	ν_{33}, ν_{29}
597 vw	594	ν_{26}	554 vs C	554	ν_{37}
	657	ν_{35}	571 w		ν_{38}
679 m C	680	ν_{36}	595 vw	594	ν_{26}
707 vw	706	$2\nu_{40}$	647 m	647	ν_{36}
730 w	729	ν_{25}		656	ν_{35}
780 s C		ν_{33}		699	pol.
	786	ν_{32}	709 vs C	707	ν_{34}
824 s	826	ν_{21}, ν_{31}	747 m C	748	ν_{33}

Table 4.5 (Continued)

$C_6D_5CHCH_2$		$C_6D_5CDCD_2$	
IR	RAMAN (p)	IR	RAMAN (p)
2243 sh	2262	2215 m	2215
2262 sh	2271	2227 w	2227
2277 s		2260 m	2250 (0.25)
2283 sh	2283 (0.24)		2261
	2292 sh	2277 s	2267
	2306	2293 sh	2292 (0.13)
2387 vw	2571	2320 w	2320 (0.67)
			2358
2776 vw		2381 w	
2807 vw			2570
2859 sh		2860 vw	
2868 m	2870	2931 vw	
2899 w		2971 vw	
2932 w	2931	3052 vw	
2981 m	2985 sh	3228 w	
3011 m	3007 (0.18)	3320 vw	

$C_6D_5CHCH_2$		$C_6D_5CDCD_2$	
Assignment	RAMAN (p)	Assignment	RAMAN (p)
$\nu_{14} + \nu_{21}$		ν_8	
ν_6		$\nu_{14} + \nu_{18}$	
ν_5		ν_7	
ν_3		ν_6	
ν_4		ν_5	
ν_1		ν_3	
$2\nu_{18}$		ν_1, ν_4	
$\nu_{12} + \nu_{22}$		ν_2	
$2\nu_{15}$		$2\nu_{18}$	
$\nu_9 + \nu_{18}$		$\nu_9 + \nu_{22}$	
$\nu_5 + \nu_{27}$		$2\nu_{15}$	
$\nu_{11} + \nu_{13}$		$\nu_{11} + \nu_{13}$	
$\nu_3 + \nu_{26}$		$\nu_{13} + \nu_{24} + \nu_{26}$	
$\nu_{13} + 2\nu_{32}$		$\nu_3 + \nu_{25}$	
$\nu_9 + \nu_{16}$		$\nu_8 + \nu_{20}$	
ν_8		$\nu_3 + \nu_{24}$	
ν_7		$\nu_2 + \nu_{16}$	

Table 4:5 (Continued)

IR	C ₆ D ₅ CHCH ₂ RAMAN (ρ)	Assignment	IR	C ₆ D ₅ CDCD ₂ RAMAN (ρ)	Assignment
3069 w		2ν ₁₁			
3092 m	3091 (0.72)	ν ₂			
3227 w		ν ₃ + ν ₂₄			
	3253	2ν ₉			

s = strong; m = medium; w = weak; v - very; sh = shoulder; br = broad;

C = type C band contour; ρ = depolarization ratio; pol. polarized; dp = depolarized;

? = band assigned using the estimated torsional frequency.

Table 4.6

Ground State Fundamentals of the Styrenes

Designation	Description of $C_6H_5CHCH_2$ Mode ^a	Frequency (cm^{-1})			
		$C_6H_5CHCH_2$	$C_6H_5CDCD_2$	$C_6D_5CHCH_2$	$C_6D_5CDCD_2$
ν_1	ν_{C-H}	3106	3104	2292	2292
ν_2	$\nu_{as=CH_2}$	3091	2329	3092	2320
ν_3	ν_{C-H}	3084	3084	2277	2277
ν_4	ν_{C-H}	3061	3061	2283	2292
ν_5	ν_{C-H}	3055	3051	2271	2267
ν_6	ν_{C-H}	3029	3026	2262	2261
ν_7	$\nu_{=CH-}$	3009	2244	3009	2250
ν_8	$\nu_{s=CH_2}$	2981	2207	2983	2215
ν_9	$\nu_{C=C}$	1630	1562	1629	1574
ν_{10}	ν_{C-C}	1600	1602	1575	1563
ν_{11}	ν_{C-C}	1575	1585	1539	1536
ν_{12}	ν_{C-C}	1494	1491	1377	1377
ν_{13}	ν_{C-C}	1450	1445	1328	1327
ν_{14}	$\beta_{s=CH_2}$	1411	1048	1425	1050 ^b
ν_{15}	ν_{C-C}	1334	1332	1284	1285
ν_{16}	$\beta_{=CH-}$	1303	1003	1305	1001
ν_{17}	β_{C-H}	1289	1290	1054	1028 ^b
ν_{18}	X-sens(ν_{C-CHCH_2})	1203	1225	1154	1179

Table 4.6 (continued)

Designation	Description of $C_6H_5CHCH_2$ Mode ^a	$C_6H_5CHCH_2$	Frequency (cm^{-1})		
			$C_6H_5CDD_2$	$C_6D_5CHCH_2$	
<u>a' species</u>					
ν_{19}	BC-H	a 9a	1181	871	870
ν_{20}	BC-H	c 15	1156	841	841
ν_{21}	BC-H	d 18b	1083	825	825
ν_{22}	$\beta_{as}=CH_2$		1032	1006	810
ν_{23}	BC-H	b 18a	1019	841	841
ν_{24}	ring	p 12	999	958	958
ν_{25}	X-sens ($\alpha C-C-C$)	r 1	776	729	699
ν_{26}	$\alpha C-C-C$	s 6b	621	595	594
ν_{27}	$\beta-C=C$		554	541	498
ν_{28}	X-sens ($\alpha C-C-C$)	t 6a	442	433	408
ν_{29}	X-sens ($\beta C-CHCH_2$)	μ 9b	241	231	212
<u>a'' species</u>					
ν_{30}	$\gamma=CH-$		992	989 ^b	789 ^b
ν_{31}	$\gamma C-H$	j 5	985	825	825
ν_{32}	$\gamma C-H$	h 17a	970	786	789
ν_{33}	$\gamma C-H$	i 17b	909	780	747 ^b
ν_{34}	$\gamma_s=CH_2$		909	909	708
ν_{35}	$\gamma C-H$	g 10a	841	657	656
ν_{36}	$\gamma C-H$	f 11	776	679	647
ν_{37}	$\phi C-C$	v 4	699	541	554 ^c

Table 4.6 (continued)

Designation	Description of C ₆ H ₅ CHCH ₂ Mode ^a	Frequency (cm ⁻¹)		
		C ₆ H ₅ CHCH ₂	C ₆ H ₅ CDCD ₂	C ₆ D ₅ CD ₂
ν_{38}	$\nu_{as} = CH_2$	640	571	571
ν_{39}	X-sens(ϕ C-C)	x 16b	407	391
ν_{40}	ϕ C-C	w 16a	398	354
ν_{41}	X-sens(γ C-CHCH ₂)	y 10b	192	205
ν_{42}	torsion	(76) ^d	(66) ^d	(72) ^d

a: The letter notation is that of Whiffen⁽¹²⁷⁾ for monosubstituted benzenes. The number-letter notation is that of Wilson⁽¹²²⁾ for the corresponding mode in benzene. The vinyl group mode descriptions are given in Table 4.2.

b: Alternative assignment possible (see Section 4.3.1).

c: Value uncorrected for Fermi resonance.

d: Bracketed numbers indicate estimated frequencies.

Table 4.7

Teller-Redlich Product Ratios for a' Modes in the Styrenes

<u>Isotopic Pair</u>	<u>Calc.</u>	<u>Obs.</u>	<u>% Error</u>
$-d_3/-h_8$	0.134	0.143	6.7
$-d_5/-h_8$	0.0343	0.0365	6.4
$-d_8/-h_8$	0.00458	0.00502	9.6

Table 4.8

 a_1 b_2 Teller-Redlich Product Ratios for Some Monosubstituted
Benzenes

<u>Isotopic Pair</u>	<u>Calc.</u>	<u>Obs.</u>	<u>% Error</u>
$C_6D_5CCH/C_6H_5CCH^a$	0.0342	0.0361	5.5
$C_6D_5CH_3/C_6H_5CH_3^b$	0.0344	0.0370	7.6
$C_6D_5OH/C_6H_5OH^c$	0.0349	0.0382	9.6

a: Reference (6); gas phase spectra.

b: Reference (135); liquid phase spectra.

c: Reference (131); gas phase spectra.

These ratios have been calculated using the fact that for C_{2v} monosubstituted benzenes, the a_1 and b_2 symmetry species together correlate with a' in C_s symmetry.

CHAPTER FIVE

ANALYSIS OF THE FLUORESCENCE AND FLUORESCENCE EXCITATION SPECTRA

5.1 Vibrational Analysis of the Fluorescence of the Styrenes

The solvent which gave the most highly resolved fluorescence spectra was methylcyclohexane. In this solvent the half-width of the observed bands was 80-100 cm^{-1} . This band width is somewhat larger than that which can often be obtained in spectra exhibiting the Shpol'skii effect. The most likely reason for this is the imperfect "fit" of the styrene molecules in the methylcyclohexane lattice (ethylcyclohexane, which possibly is a better solvent to use due to its more similar size, does not form a polycrystalline matrix). At 77 K, $kT = 54 \text{ cm}^{-1}$, so "hot band" fluorescence is not expected to be observed. Torsional mode ν_{42} may be of the order of kT in the excited state, but the whole of the styrene fluorescence spectrum could be satisfactorily assigned without recourse to ν_{42} activity. It is possible, though, that the presence of this low frequency mode is at least partially responsible for the fairly large band width.

For each isotope the highest frequency fluorescence band increases in intensity with decreasing concentration relative to the rest of the fluorescence spectrum. At concentrations of about 5×10^{-2} M the uncorrected intensity of this band is less than 10% of that of the most prominent band in the rest of the

spectrum, while at concentrations of 10^{-6} M or so, it is about one and one-half times as intense. This is the only band whose relative intensity is altered by changing the styrene concentration. This effect is attributed to reabsorption of the fluorescence. The spectra shown in Figures 5.1 and 5.2 were obtained with 10^{-3} - 10^{-4} M solutions. At these concentrations the positions of the fluorescence bands are identical to those found with more dilute solutions.

The sharpness of the fluorescence spectrum of each isotope increases to some extent with decreasing concentration. Also, the spectra of the vinyl-protonated styrenes were sharper than those of the vinyl-deuterated isotopes. The sharpness of the fluorescence and fluorescence excitation spectra also depended on the quality of the polycrystalline matrix.

Finally, no phosphorescence was detected for any isotope at any concentration, and no excimer emission was observed for any isotope as the concentration was increased.

Styrene-h₈

The strong fluorescence band at $34\,335\text{ cm}^{-1}$ is assigned as the pure electronic transition. The reasons for assigning this band as the 0,0 band will be outlined in Section 5.2. The recent paper by Grajcar and Baudet⁽³³⁾ gives the 0,0 band of styrene in an n-pentane matrix to be at $34\,323\text{ cm}^{-1}$. The first band to the red of the 0,0 band, at 435 cm^{-1} , is weak but well-resolved, and is assigned as the 0, ν_{28} transition. Grajcar and Baudet assigned this band to 0, ν_{27} , ν_{27} being the

in-plane deformation vibration of the vinyl group. However, the analysis of the infrared and Raman spectra of the four isotopic styrenes (Chapter 4) indicates that the 435 cm^{-1} vibration should be assigned to ring vibration ν_{28} . In addition, ν_{28} (t in Whiffen notation) is often active in the fluorescence spectra of monosubstituted benzenes (8-10,102).

The medium intensity band at 620 cm^{-1} is attributed to the $0, \nu_{26}$ transition. This normal mode is derived from the degenerate e_{2g} vibration at 606 cm^{-1} in benzene. This latter vibration serves as a false origin in benzene's fluorescence. The assignment of vibronic origins in an electronic absorption or fluorescence spectrum is often made by observing band polarizations that are not the same as that of the electronic origin or, if the resolution is sufficiently high, observing different rotational band contours from that of the $0,0$ band. However, these methods cannot be used when a totally symmetric vibration is involved in vibronic coupling since the polarization would be identical to that of the origin. Nonetheless, when no overtone of a relatively strong vibration in an allowed electronic transition is observed, it is reasonable to assume that vibronic mixing is occurring through this vibration. The fluorescence spectrum of styrene- h_8 is the one in which the region of the first overtone of the 620 cm^{-1} vibration is least overlapped by other bands, and no band that could be assigned to $0, 2\nu_{26}$ was observed.

The next two bands at 775 cm^{-1} and 985 cm^{-1} in the spectrum to the red of the $0,0$ band, are assigned as transitions

involving the totally symmetric vibrational modes ν_{25} and ν_{24} respectively. The ring breathing mode (ν_{24} in styrene) is a prominent vibration in the fluorescence spectrum of benzene and other monosubstituted benzenes.

The strong band at 1210 cm^{-1} to the red of the 0,0 band is assigned to $0,\nu_{18}$, the totally symmetric stretching vibration between the ring and the vinyl substituent. This frequency is observed in combination with most of the other totally symmetric active fundamentals in the spectrum, and its second quantum is seen as well.

Two very weak bands at 1295 cm^{-1} and 1315 cm^{-1} are assigned to the fundamentals ν_{17} and ν_{16} respectively. These assignments are supported by the analysis of the fluorescence spectra of the other isotopic styrenes. Since these bands are weak, any summation bands involving either ν_{16} or ν_{17} would probably be too weak to be observed or would be masked by the more intense bands.

The weak band found at 1405 cm^{-1} is attributed to $0,\nu_{14}$; mode ν_{14} is the in-plane scissoring motion of the terminal $=\text{CH}_2$ group in the vinyl moiety. The two previous gas phase fluorescence studies and the recent work of Grajcar and Baudet concur in this assignment. A very weak band, at 1475 cm^{-1} , is probably $0,\nu_{13}$. This frequency is approximately 20 cm^{-1} lower than the value obtained from infrared and Raman studies of the pure liquid. However, Grajcar and Baudet⁽³³⁾ also observe a weak band in this spectral region and they assign it to the same mode.

The most intense band in the fluorescence spectrum, other than the 0,0 band, is assigned as 0, ν_9 . This mode is the stretching vibration of the C=C double bond of the vinyl group. It is a very active mode in the spectrum, being observed in its second and third quanta as well as in combination with almost all the other active modes.

The remainder of the spectrum is analyzed up to 6255 cm^{-1} from the origin, with a total of 47 bands being analyzed. The two previous vibrational analyses of the vapor phase fluorescence of styrene- h_8 ^(23,30) extended to less than 3000 cm^{-1} from the origin band, while bands extending to about 4000 cm^{-1} from the origin were reported in frozen ethanolic solution ⁽³²⁾. Grajcar and Baudet ⁽³³⁾ measured 38 and analyzed 21 vibronic bands in their analysis of styrene's fluorescence spectrum in an n-pentane matrix at 77 K. The main progressions in the spectrum involve just two modes, ν_9 and ν_{24} . Each progression is seen up to the third quantum. Bands based on combinations of ν_9 , ν_{18} and ν_{24} make up most of the spectrum to the red of the 0, ν_9 transition. The vibrational analysis of the styrene- h_8 fluorescence spectrum is given in Table 5.1; the spectrum is given in Figure 5.1.

Styrene- d_3

Vinyl group deuteration causes a slight blue shift of the 0,0 band of the fluorescence spectrum compared to $\text{C}_6\text{H}_5\text{CHCH}_2$ of about 25 cm^{-1} . The substituent-sensitive ring modes ν_{18} , ν_{25} and ν_{28} , as well as vinyl group mode ν_9 , have shifted

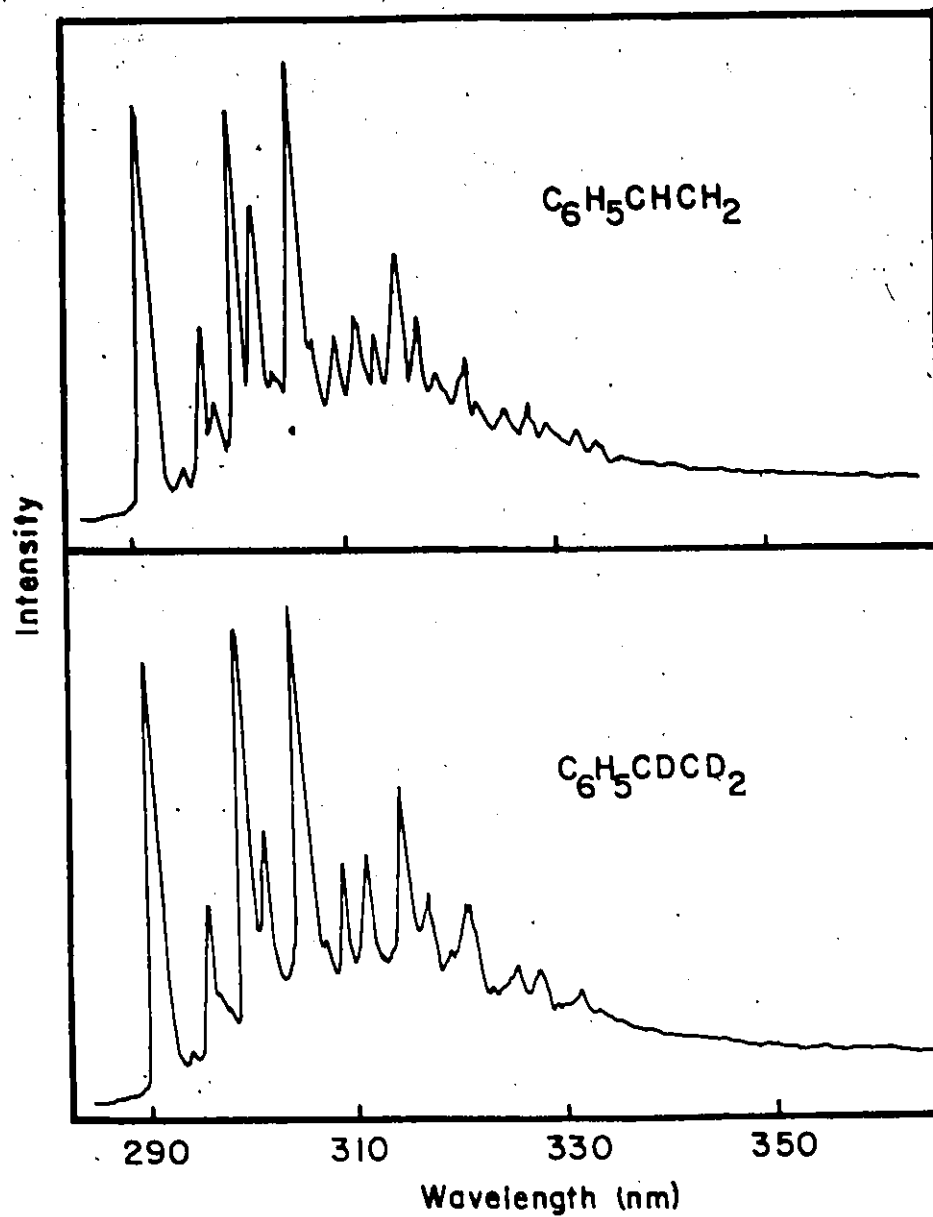


Figure 5.1 The Uncorrected Fluorescence Spectra of 10^{-4} M $C_6H_5CHCH_2$ and $C_6H_5CDCD_2$ in Polycrystalline Methylcyclohexane at 77 K.

Table 5.1

Vibrational Analysis of the Fluorescence Spectrum of 10^{-4} M $C_6H_5CHCH_2$
 and 10^{-4} M $C_6H_5CDCD_2$ in Polycrystalline Methylcyclohexane at 77 K

$C_6H_5CHCH_2$		$C_6H_5CDCD_2$		Assignment
Intensity ^a	$\bar{\nu}(\text{cm}^{-1})$	Intensity	$\bar{\nu}(\text{cm}^{-1})$	$\Delta\bar{\nu}(\text{cm}^{-1})$
vs	34 335	vs	34 360	0, 0
w	33 900	w	33 945	0, ν_{28}
m	33 715	m	33 740	0, ν_{26}
m	33 560	w	33 615	0, ν_{25}
s	33 350	w	33 550	0, ν_{22}
s	33 125	vs	33 360	0, ν_{24}
vW	33 040 sh ^b	s	33 125	0, ν_{16} ; 0, ν_{18}
vW	33 020	vW	33 045 sh	0, ν_{17}
w	32 930	vW	32 995	0, ν_{16}
w	32 905	vW	32 930	0, ν_{25} + ν_{26}
				0, ν_{14} ; 0, ν_{25} + ν_{26}
				0, ν_{24} + ν_{28}

Table 5.1
(Continued)

$C_6H_5CHCH_2$		$C_6H_5CD_2$		Assignment	
Intensity ^a	$\bar{\nu}(\text{cm}^{-1})$	Intensity	$\bar{\nu}(\text{cm}^{-1})$	$\Delta\bar{\nu}(\text{cm}^{-1})$	
vw	32 860		1475	0, ν_{13}	
vs	32 700	vs	32 770	1590	0, ν_9
m	32 565	w	32 635 sh	1725	0, $\nu_{24} + \nu_{25}$
m	32 510	w	32 515	1845	0, $\nu_{18} + \nu_{26}$
m	32 345		1990		0, $2\nu_{24}$
vw	32 270 sh	m	32 350	2010	0, $2\nu_{24}; 0, \nu_9 + \nu_{28}$
m	32 125		2210		0, $\nu_9 + \nu_{28}$
m	32 085 sh	m	32 135	2225	0, $\nu_{18} + \nu_{24}$
m	31 920	m	32 115	2245	0, $\nu_9 + \nu_{26}$
					0, $\nu_{18} + \nu_{24}$
					0, $2\nu_{18}; 0, \nu_9 + \nu_{25}$
vw	31 855 sh	vw	31 900	2460	0, $2\nu_{18}$
m	31 700	s	31 765	2595	0, $\nu_{13} + \nu_{24}$
					0, $\nu_9 + \nu_{24}$

Table 5.1 (Continued)

$C_6H_5ClCH_2$		$C_6H_5CDCl_2$		Assignment		
Intensity ^a $\bar{\nu}(cm^{-1})$	$\Delta\bar{\nu}(cm^{-1})$	Intensity $\bar{\nu}(cm^{-1})$	$\Delta\bar{\nu}(cm^{-1})$			
m	31 490	2845	m	31 540	2820	0, $\nu_9 + \nu_{18}$
w	31 320	3015				0, $3\nu_{24}; 0, 2\nu_{18} + \nu_{26}$
w	31 280 sh	3055				0, $\nu_9 + \nu_{14}$
vW	31 250 sh	3085				0, $\nu_9 + \nu_{14}$
						0, $2\nu_{18} + \nu_{25}$
						0, $\nu_9 + \nu_{22} + \nu_{25}$
						0, $2\nu_9$
w	31 115 sh	3220				0, $\nu_{18} + 2\nu_{24}$
m	31 065	3270				0, $2\nu_9$
w	30 910	3425				0, $2\nu_{18} + \nu_{24}$
w	30 885 sh	3450				0, $\nu_9 + \nu_{18} + \nu_{26}$
						0, $\nu_9 + 2\nu_{24}; 0, 2\nu_9 + \nu_{28}$
w	30 695	3640				0, $\nu_9 + 2\nu_{24}$
vW	30 625 sh	3710				0, $2\nu_9 + \nu_{28}$

Table 5.1 (Continued)

$C_6H_5CHCH_2$		$C_6H_5CDCD_2$		Assignment
Intensity ^a	$\bar{\nu}(cm^{-1})$	Intensity	$\bar{\nu}(cm^{-1})$	
W	30 490	W	30 540	0, $\nu_9 + \nu_{18} + \nu_{24}$; 0, $2\nu_9 + \nu_{26}$
W	30 460 sh			0, $\nu_9 + \nu_{18} + \nu_{24}$
W	30 285			0, $2\nu_9 + \nu_{26}$
VW	30 230 sh	VW	30 355	0, $\nu_9 + 2\nu_{18}$; 0, $2\nu_9 + \nu_{25}$
W	30 065			0, $\nu_9 + 2\nu_{18}$
VW	29 875			0, $\nu_9 + \nu_{13} + \nu_{24}$
VW	29 695			0, $2\nu_9 + \nu_{24}$
VW	29 660			0, $\nu_{18} + 3\nu_{24}$
VW	29 445 sh			0, $2\nu_9 + \nu_{18}$
VW	4845			0, $\nu_9 + 3\nu_{24}$; 0, $\nu_9 + 2\nu_{18} + \nu_{26}$
VW	4890			0, $\nu_9 + 2\nu_{18} + \nu_{26}$
				0, $\nu_9 + \nu_{18} + \nu_{24}$
				0, $3\nu_9$

Table 5.1 (Continued)

$C_6H_5ClCH_2$		$C_6H_5CDCD_2$		Assignment
Intensity ^a	$\bar{\nu}(cm^{-1})$	Intensity	$\bar{\nu}(cm^{-1})$	
vw	29 295	vw	29 310	0, $\nu_9 + 2\nu_{18} + \nu_{24}$
vw	29 080	vw	29 170	0, $2\nu_9 + 2\nu_{24}$
vw	28 880	vw	28 960	0, $2\nu_9 + \nu_{18} + \nu_{24}$
vw	28 675			0, $2\nu_9 + 2\nu_{18}$
vw	28 475	vw	28 610	0, $3\nu_9 + \nu_{24}$
vw	28 270			0, $3\nu_9 + \nu_{18}$
vw	28 080			0, $2\nu_9 + 3\nu_{24}$

a: s = strong; m = moderate; w = weak; v = very

b: sh = shoulder

slightly from their values in $C_6H_5CHCH_2$, as is expected. In the fluorescence spectrum of $C_6H_5CDCD_2$ the band assigned as $0, \nu_{18}$ is not as intense as in $C_6H_5CHCH_2$. In addition, the weak band appearing at 1405 cm^{-1} in the fluorescence spectrum of $C_6H_5CHCH_2$ has disappeared in the $C_6H_5CDCD_2$ spectrum, thereby confirming its attribution to vinyl group mode ν_{14} in the spectrum of the former molecule. The frequency of normal mode ν_{14} , from the analysis of the infrared and Raman spectra, is 1048 cm^{-1} , and so the $0, \nu_{14}$ transition would be expected to be observed to the red of the strong $0, \nu_{24}$ transition. No band is observed here, but the fluorescence spectrum of $C_6D_5CHCH_2$ gives additional evidence supporting the $0, \nu_{14}$ assignment in $C_6H_5CHCH_2$ (see below).

Another difference in the $C_6H_5CDCD_2$ fluorescence spectrum compared to that of $C_6H_5CHCH_2$ is the appearance of a distinct band 810 cm^{-1} to the red of the origin band. It is unlikely that this band is due to a $0, \nu_{28}$ transition for two reasons. First, this transition would probably appear at a higher energy from the $0, 0$ band than the 810 cm^{-1} which is observed. Secondly, no band which could be attributed to this transition is seen in any of the other styrenes studied. The 810 cm^{-1} interval, then, corresponds to a fundamental frequency. The analysis of the infrared and Raman spectra indicates that the transition is probably $0, \nu_{22}$; if so, the corresponding band in $C_6H_5CHCH_2$ is presumably hidden under the strong $0, \nu_{24}$ transition.

As in $C_6H_5CHCH_2$, the majority of the bands can be analyzed in terms of the three fundamental vibrations, ν_9 , ν_{18} and ν_{24} .

Some of the summation bands involving ν_{18} however, are weaker than their counterparts in the $C_6H_5CHCH_2$ spectrum, since the $0, \nu_{18}$ transition itself is weaker. The vibrational analysis of the $C_6H_5CDCD_2$ fluorescence spectrum is given in Table 5.1; the spectrum is shown in Figure 5.1.

Styrene-d₅

Whereas vinyl group deuteration shifted the position of the $0,0$ band 25 cm^{-1} to higher energy in comparison to the fully protonated species, ring deuteration has a much greater effect, shifting the $0,0$ band 140 cm^{-1} to the blue to $34\,475\text{ cm}^{-1}$. The general appearance of the spectrum is very similar to that for $C_6H_5CHCH_2$. Again, the six major bands immediately to the red of the $0,0$ are assigned as $0, \nu_{28}$ (430 cm^{-1}), $0, \nu_{26}$ (580 cm^{-1}), $0, \nu_{25}$ (730 cm^{-1}), $0, \nu_{24}$ (950 cm^{-1}), $0, \nu_{18}$ (1150 cm^{-1}) and $0, \nu_9$ (1620 cm^{-1}). One difference between the two spectra, however, is the appearance of a weak shoulder at 870 cm^{-1} to the red of the origin. This band has been assigned as the $0, \nu_{19}$ transition. The corresponding transition in $C_6H_5CHCH_2$ would presumably be obscured by the much more intense $0, \nu_{18}$ transition.

The appearance of a medium intensity band at 1415 cm^{-1} to the red of the $0,0$ band lends credence to the assignment of the band 1405 cm^{-1} to the red of the origin in $C_6H_5CHCH_2$ as the $0, \nu_{14}$ transition. Also, a new band is now discernable as a shoulder on the $0, \nu_9$ band, at 1550 cm^{-1} to the red of the origin. This band can be assigned to $0, \nu_{24} + \nu_{26}$. This band was not observed in the fluorescence spectrum of $C_6H_5CHCH_2$.

because the intense $0, \nu_9$ band is in the same spectral region. The presence of the $0, \nu_{24} + \nu_{26}$ transition is further evidence that ν_{26} acts as a false origin in the fluorescence spectrum of styrene. Progressions and combinations involving ν_{24} and based on one quantum of ν_{26} can be seen throughout the spectrum. The vibrational analysis of the $C_6D_5CHCH_2$ fluorescence spectrum is given in Table 5.2; the spectrum is shown in Figure 5.2.

Styrene-d₈

The $0,0$ band of perdeuterated styrene is located at $34\,500\text{ cm}^{-1}$, which is 165 cm^{-1} to higher energy than that for $C_6H_5CHCH_2$. This shift is equal to the sum of the $-h_8 \rightarrow -d_3$ and $-h_8 \rightarrow -d_5$ isotopic shifts of the $0,0$ transition. The basic spectrum (Figure 5.2) remains the same as for all the styrenes. The six main active fundamentals are again ν_{28} , ν_{26} , ν_{25} , ν_{24} , ν_{18} and ν_9 , and their frequencies agree well with the vibrational data for $C_6D_5CDCD_2$ given in Chapter 4. As in the spectrum of $C_6D_5CHCH_2$, a weak shoulder on the high energy side of the $0, \nu_{24}$ band, at 880 cm^{-1} to the red of the origin, is assigned as $0, \nu_{19}$. The strong $0, \nu_{24}$ transition, fairly sharp in the spectrum of the other styrenes, is rather broad in this isotope. Spectra run with a large wavelength scale expansion show the presence of two shoulders near the band maximum, at 990 cm^{-1} and 1025 cm^{-1} to the red of the origin. These bands have been assigned as the $0, \nu_{16}$ and $0, \nu_{17}$ transitions respectively.

The $0, \nu_{18}$ transition, a strong band in the fluorescence

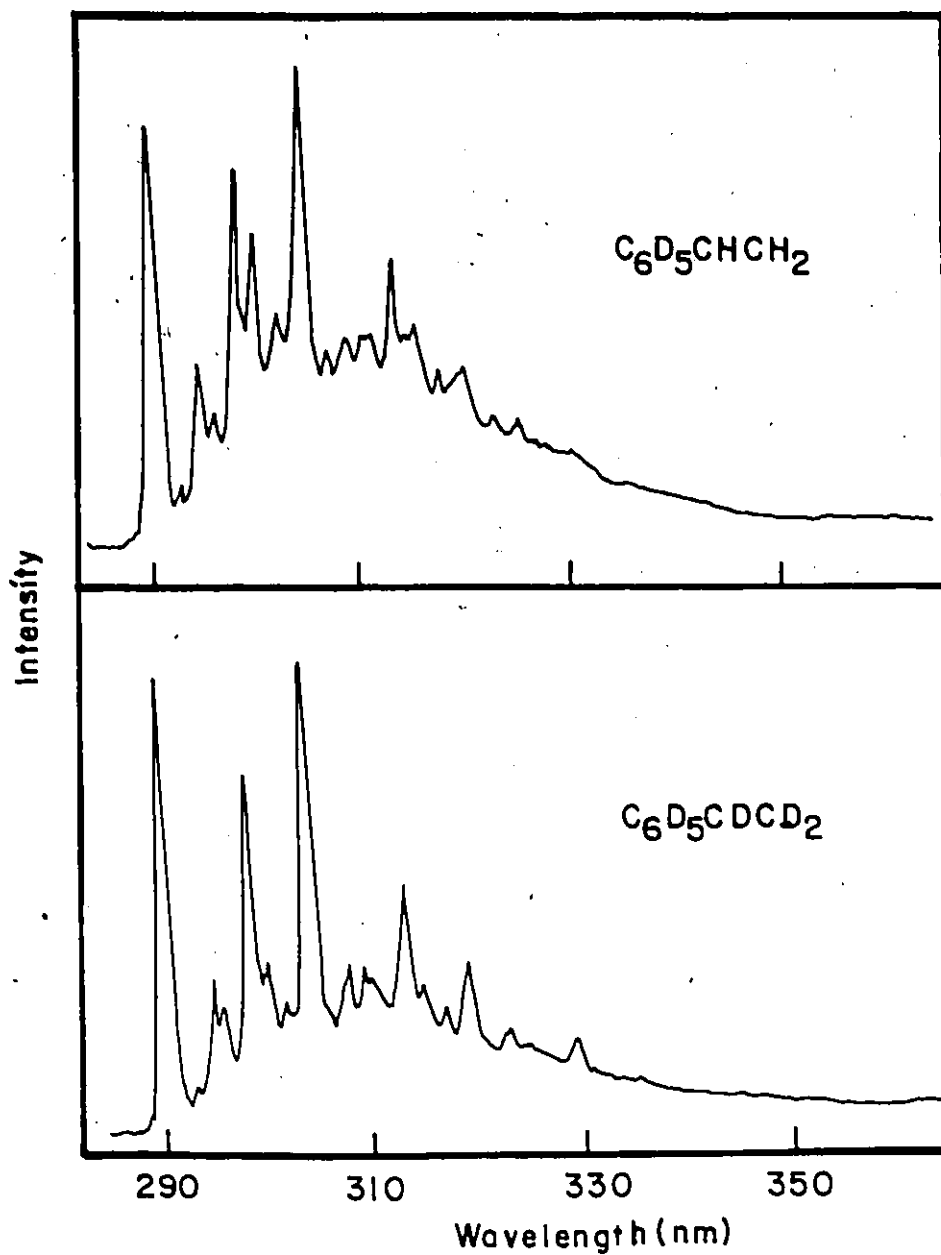


Figure 5.2 The Uncorrected Fluorescence Spectra of 10^{-4} M $C_6D_5CHCH_2$ and $C_6D_5CDCD_2$ in Polycrystalline Methylcyclohexane at 77 K.

Table 5.2
 Vibrational Analysis of the Fluorescence Spectrum of 10^{-4} M $C_6D_5CHCH_2$
 and 10^{-4} M $C_6D_5CD_2$ in Polycrystalline Methylcyclohexane at 77 K

Intensity ^a	$\bar{\nu}(\text{cm}^{-1})$	$\Delta\bar{\nu}(\text{cm}^{-1})$	Intensity	$\bar{\nu}(\text{cm}^{-1})$	$\Delta\bar{\nu}(\text{cm}^{-1})$	Assignment
vs	34 475	0	vs	34 500	0	0, 0
w	34 045	430	w	34 080	420	0, ν_{28}
m	33 895	580	m	33 905	595	0, ν_{26}
m	33 745	730	m	33 785	715	0, ν_{25}
w	33 605 sh ^b	870	w	33 620	880	0, ν_{19}
s	33 525	950	s	33 535	965	0, ν_{24}
			s	33 510 sh	990	0, ν_{16}
			m	33 475 sh	1025	0, ν_{17}
vW	33 440 sh	1035				0, $\nu_{17}; 0, \nu_{22}$
			vW	33 390	1110	0, $\nu_{25} + \nu_{28}$
s	33 325	1150				0, ν_{18}
m	33 300 sh	1175				0, $\nu_{25} + \nu_{28}$
			m	33 315	1185	0, ν_{18}
			vW	33 195	1305	0, $\nu_{25} + \nu_{26}$

Table 5.2 (Continued)

$C_6D_5ClCH_2$		$C_6D_5CDCD_2$		Assignment
Intensity ^a	$\bar{\nu}(cm^{-1})$	Intensity	$\bar{\nu}(cm^{-1})$	
	$\Delta\bar{\nu}(cm^{-1})$		$\Delta\bar{\nu}(cm^{-1})$	
w	33 170		1305	0, ν_{16} ; 0, $\nu_{25} + \nu_{26}$
w	33 085 sh	w	33 100	0, $\nu_{24} + \nu_{28}$
m	33 060		1415	0, ν_{14}
m	32 925		1550	0, $\nu_{24} + \nu_{26}$
vs	32 855	vs	32 920	0, ν_9
m	32 740 sh	w	32 725	0, $\nu_{18} + \nu_{26}$
w	32 565	w	32 570	0, $2\nu_{24}$
vw	32 450		2025	0, $\nu_{14} + \nu_{26}$
vw	32 400 sh	m	32 500	0, $\nu_9 + \nu_{28}$
m	32 360	m	32 355 sh	0, $\nu_{18} + \nu_{24}$
m	32 250	m	32 325	0, $\nu_9 + \nu_{26}$
		m	32 250	0, $\nu_{24} + \nu_{25} + \nu_{26}$
m	32 180	w	32 135 sh	0, $2\nu_{18}$
m	32 130		2345	0, $\nu_9 + \nu_{25}$
w	31 955 sh		2520	0, $2\nu_{24} + \nu_{26}$

Table 5.2 (Continued)

C ₆ D ₅ CHCH ₂		C ₆ D ₅ CD ₂		Assignment
Intensity ^a	$\bar{\nu}(\text{cm}^{-1})$	Intensity	$\bar{\nu}(\text{cm}^{-1})$	
s	31 880	s	31 945	0, $\nu_9 + \nu_{24}$
vW	31 770			0, $\nu_{18} + \nu_{24} + \nu_{26}$
m	31 695	m	31 750	0, $\nu_9 + \nu_{18}$
w	31 615 sh	vW	31 585	0, $3\nu_{24}$
vs	31 485 sh	w	31 530	0, $2\nu_{18} + \nu_{26}$; 0, $\nu_9 + \nu_{24} + \nu_{28}$
w	31 445			0, $\nu_9 + \nu_{14}$
w	31 410			0, $\nu_{18} + 2\nu_{24}$
w	31 280	m	31 350	0, $2\nu_9$
m	31 215	w	31 265 sh	0, $\nu_9 + \nu_{24} + \nu_{26}$
vW	31 110 sh	vW	31 145 sh	0, $2\nu_{24} + \nu_{25} + \nu_{26}$
vW	31 005			0, $2\nu_9$; 0, $2\nu_{18} + \nu_{24}$
w	30 935	w	30 985	0, $3\nu_{24} + \nu_{26}$
				0, $\nu_9 + 2\nu_{24}$

Table 5.2 (Continued)

$C_6D_5ClCHCl_2$		$C_6D_5CDCl_2$		Assignment
Intensity ^a	$\bar{\nu}(cm^{-1})$	Intensity	$\bar{\nu}(cm^{-1})$	
	$\Delta\bar{\nu}(cm^{-1})$		$\Delta\bar{\nu}(cm^{-1})$	
VW	30 810	w	30 935	0, 2 ν_9 + ν_{28}
w	30 730	w	30 755	0, ν_9 + ν_{18} + ν_{24}
VW	30 540	VW	30 560	0, ν_9 + ν_{18} + ν_{24} ; 0, 2 ν_9 + ν_{26}
w	30 490			0, 2 ν_9 + ν_{25}
w	30 315			0, ν_9 + 2 ν_{24} + ν_{26}
w	30 255	w	30 360	0, 2 ν_9 + ν_{24}
VW	30 055	w	30 160	0, 2 ν_9 + ν_{18}
		VW	29 965	0, ν_9 + 2 ν_{18} + ν_{26}
VW	29 800			0, ν_9 + ν_{18} + 2 ν_{24}
		VW	29 780	0, 3 ν_9 ; 0, ν_9 + ν_{18} + 2 ν_{24}
VW	29-590			0, 3 ν_9 ; 0, ν_9 + 2 ν_{18} + ν_{24}
		VW	29 600	0, ν_9 + 2 ν_{18} + ν_{24}
VW	29 310	VW	29 375	0, 2 ν_9 + 2 ν_{24}
VW	29 130	VW	29 170	0, 2 ν_9 + ν_{18} + ν_{24}

Table 5.2 (Continued)

$C_6D_5ClCH_2$		$C_6D_5CDCD_2$		Assignment
Intensity ^a	$\bar{\nu}(cm^{-1})$	Intensity	$\Delta\bar{\nu}(cm^{-1})$	
vW	28 880		5595	0, $2\nu_9 + 2\nu_{18}$
vW	28 650	vW	5825	0, $3\nu_9 + \nu_{24}$
			28 785	5715

a: s = strong; m = moderate; w = weak; v = very

b: sh = shoulder

spectrum of $C_6D_5CHCH_2$, is only of medium intensity in the perdeuterated species. The same effect was seen in the $C_6H_5CHCH_2-C_6H_5CDCD_2$ pair.

The progressions and summation bands in $C_6D_5CDCD_2$ follow the patterns of the other three styrenes. The vibrational analysis of the $C_6D_5CDCD_2$ fluorescence spectrum is given in Table 5.2.

5.2 Analysis of the Fluorescence Excitation Spectra and the Symmetry of the First Excited Singlet State of Styrene

Hepburn and Hollas⁽¹⁵⁹⁾ have put forward arguments favoring assignment of the 288 nm absorption band of styrene vapor as the electronic origin. These workers said that since there is coincidence of the absorption and fluorescence spectra at the 288 nm band, then this band must be the 0,0 and is not vibronically induced, as suggested by King and van Putten⁽⁴⁹⁾. However, it is known that the presence of hot bands in both absorption and fluorescence spectra can make assignments of 0,0 transition based on room temperature vapor phase spectra alone rather tenuous*.

In Figure 5.3 are shown the 77 K fluorescence excitation spectra of $C_6H_5CHCH_2$, $C_6H_5CDCD_2$, $C_6D_5CHCH_2$ and $C_6D_5CDCD_2$ in

*Shashidhar and Rao⁽¹⁶⁰⁾ have completely misassigned the emission spectrum of phenylacetylene vapor by assigning as the origin band the strong band at $36\,370\text{ cm}^{-1}$. This band has been shown by King and So⁽⁶⁾ to be a false origin, the true origin lying at $35\,879\text{ cm}^{-1}$. Also, Singh and Laposa⁽⁹⁾ have given vibrational analyses for the low temperature fluorescence spectra of phenylacetylene and three of its deuterium-substituted analogues which substantiate the work of King and So.

polycrystalline methylcyclohexane. For each of the four isotopes $0, \nu_9$ was the monitored band. In $C_6H_5CHCH_2$ a strong band is observed at $34\ 365\ cm^{-1}$ and is the lowest frequency band in the excitation spectrum. Since the samples were at a temperature of 77 K, it is very unlikely that absorption will occur from excited vibrational levels of the ground state, so that hot bands should not be observed (the only ground vibrational level that would be populated to any appreciable extent is ν_{42} , a non-totally symmetric mode). The $34\ 365\ cm^{-1}$ band is nearly coincident with the very strong highest frequency band at $34\ 335\ cm^{-1}$ in the $C_6H_5CHCH_2$ fluorescence spectrum (see Table 5.1). The observed bathochromic shift of $30\ cm^{-1}$ is very small, and is very similar to the $26\ cm^{-1}$ shift exhibited by the $0,0$ transition of phenylacetylene in isopentane solid solution at $77\ K^{(161)}$. The corresponding $0,0$ shifts for the molecules $C_6H_5CDCD_2$, $C_6D_5CHCH_2$ and $C_6D_5CDCD_2$ are $40\ cm^{-1}$, $30\ cm^{-1}$ and $30\ cm^{-1}$ respectively.

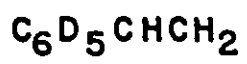
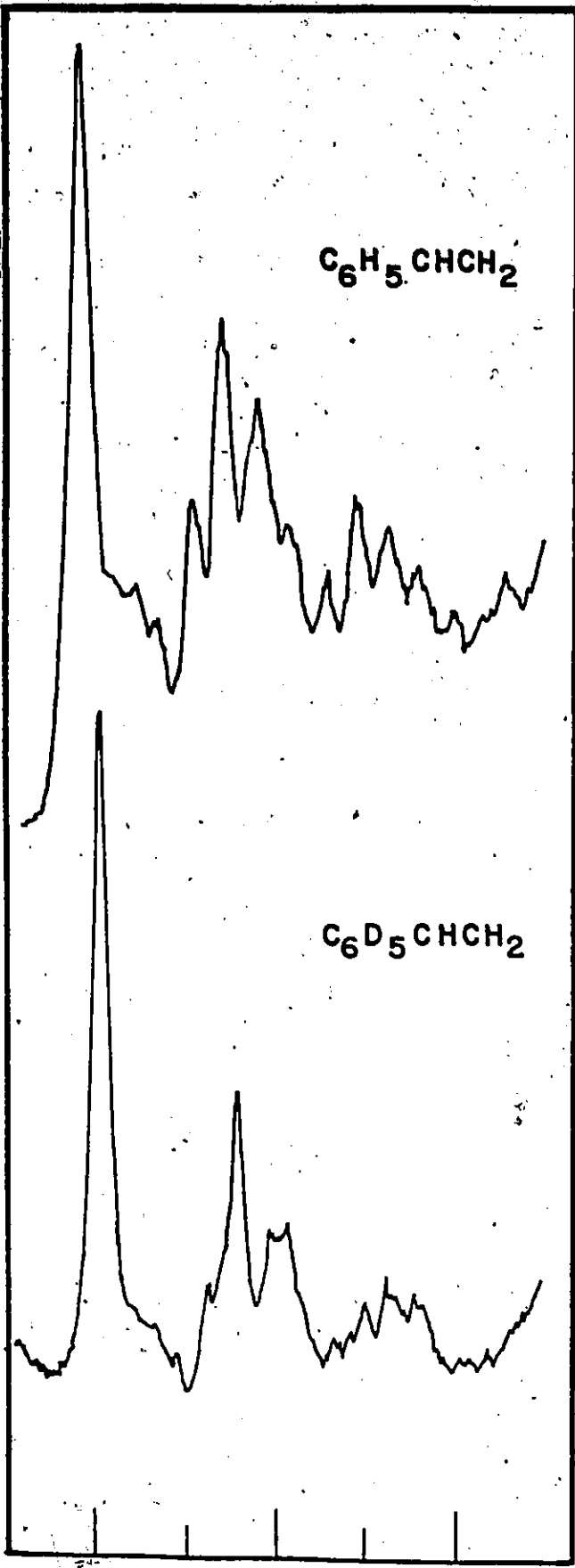
It is clear that the coincidence of two bands in the low temperature fluorescence and fluorescence excitation spectra of styrene and three of its deuterium-substituted analogues rules out the possibility that these bands are false origins produced by an intensity-borrowing mechanism. The $34\ 365\ cm^{-1}$ band in the fluorescence spectra are therefore assigned as the electronic origin bands in polycrystalline methylcyclohexane at 77 K.

Having established the positions of the electronic origin in the low temperature absorption spectra of the four styrenes

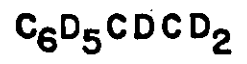
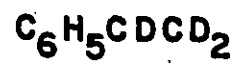
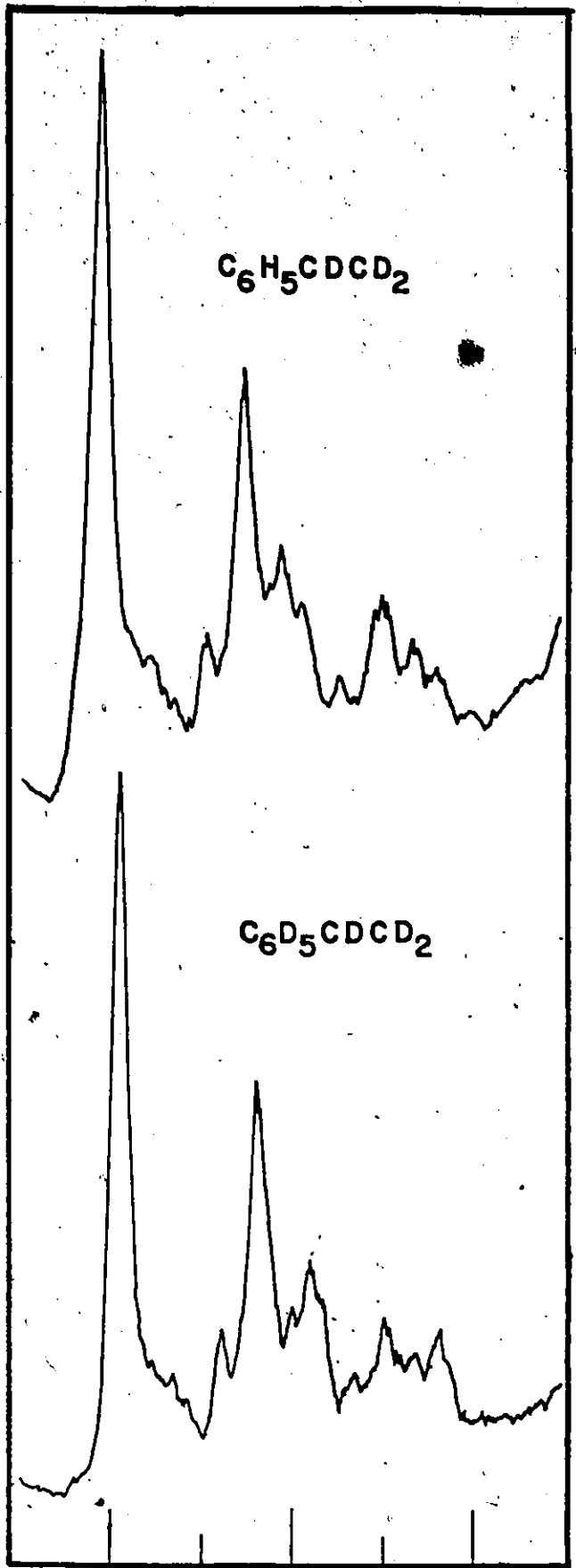
Figure 5.3

The Uncorrected Fluorescence Excitation Spectra of 10^{-3} M
 $C_6H_5CHCH_2$, $C_6H_5CDCD_2$, $C_6D_5CHCH_2$ and $C_6D_5CDCD_2$
in Polycrystalline Methylcyclohexane at 77 K.

Intensity



290 280 270



290 280 270

Wavelength (nm)

this information can now be compared to that obtained from the vapor phase absorption spectra, shown in Figures 5.4 and 5.5. The previously assigned 0,0 band in $C_6H_5CHCH_2$, as determined by Matsen⁽⁵⁾, is at $34\ 761\ cm^{-1}$. Hui and Rice⁽²⁶⁾ reported the origin bands of $C_6H_5CHCH_2$ and $C_6D_5CDCD_2$ to be at $34\ 759\ cm^{-1}$ and $34\ 929\ cm^{-1}$ respectively. From the vapor phase absorption spectra, the frequencies of the corresponding bands for the series $C_6H_5CHCH_2/C_6H_5CDCD_2/C_6D_5CHCH_2/C_6D_5CDCD_2$ are $34\ 760/34\ 780/34\ 910/34\ 925\ cm^{-1}$. The $C_6H_5CHCH_2$ and $C_6D_5CDCD_2$ values are in fair agreement with those of Hui and Rice⁽²⁶⁾. Comparison of these vapor phase "origin bands" with the positions of the origin bands in the 77 K fluorescence excitation spectra shows that there are red shifts from the vapor to solid solution of $395\ cm^{-1}$, $380\ cm^{-1}$, $405\ cm^{-1}$ and $400\ cm^{-1}$ for $C_6H_5CHCH_2$, $C_6H_5CDCD_2$, $C_6D_5CHCH_2$ and $C_6D_5CDCD_2$ respectively. These shifts compare well with those seen for other molecules when going from vapor phase to solid solution (see Table 5.3). Of course the position of the 0,0 band in low temperature absorption and emission spectra is solvent-dependent. The 0,0 shifts given in Table 5.3 are intended only to show that the observed shifts for the styrenes are similar to those of other structurally related molecules.

The observed near-coincidence of two bands in the low-temperature fluorescence and fluorescence excitation spectra of the styrenes, coupled with the shift of these bands from the matrix to vapor phase, lead to the conclusion that the $2877\ \overset{0}{\text{A}}$ band in styrene vapor is indeed the electronic origin,

Figure 5.4
The $\bar{A}+\bar{X}$ Vapor Phase Absorption Spectra of
 $C_6H_5CHCH_2$ and $C_6H_5CD_2$

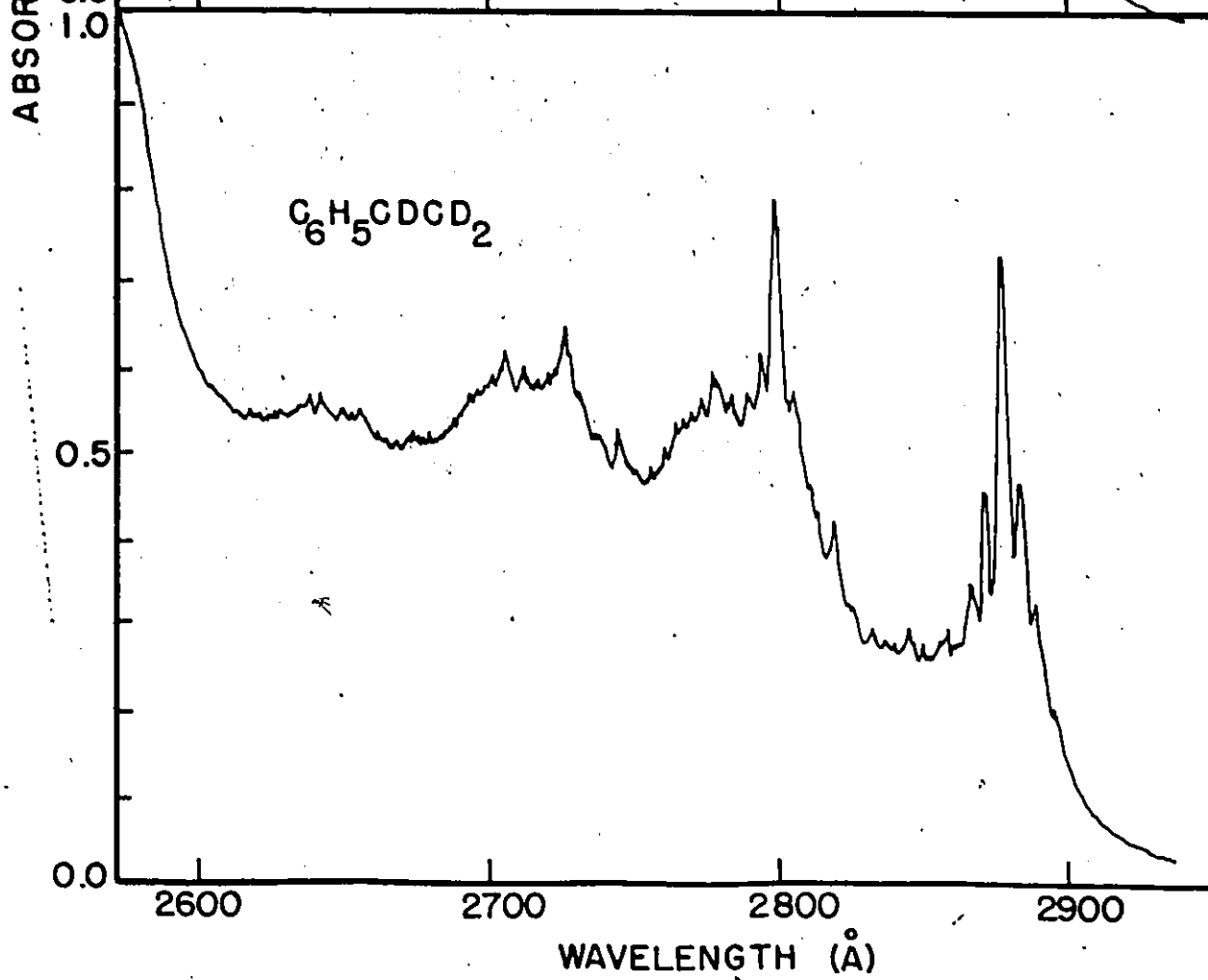
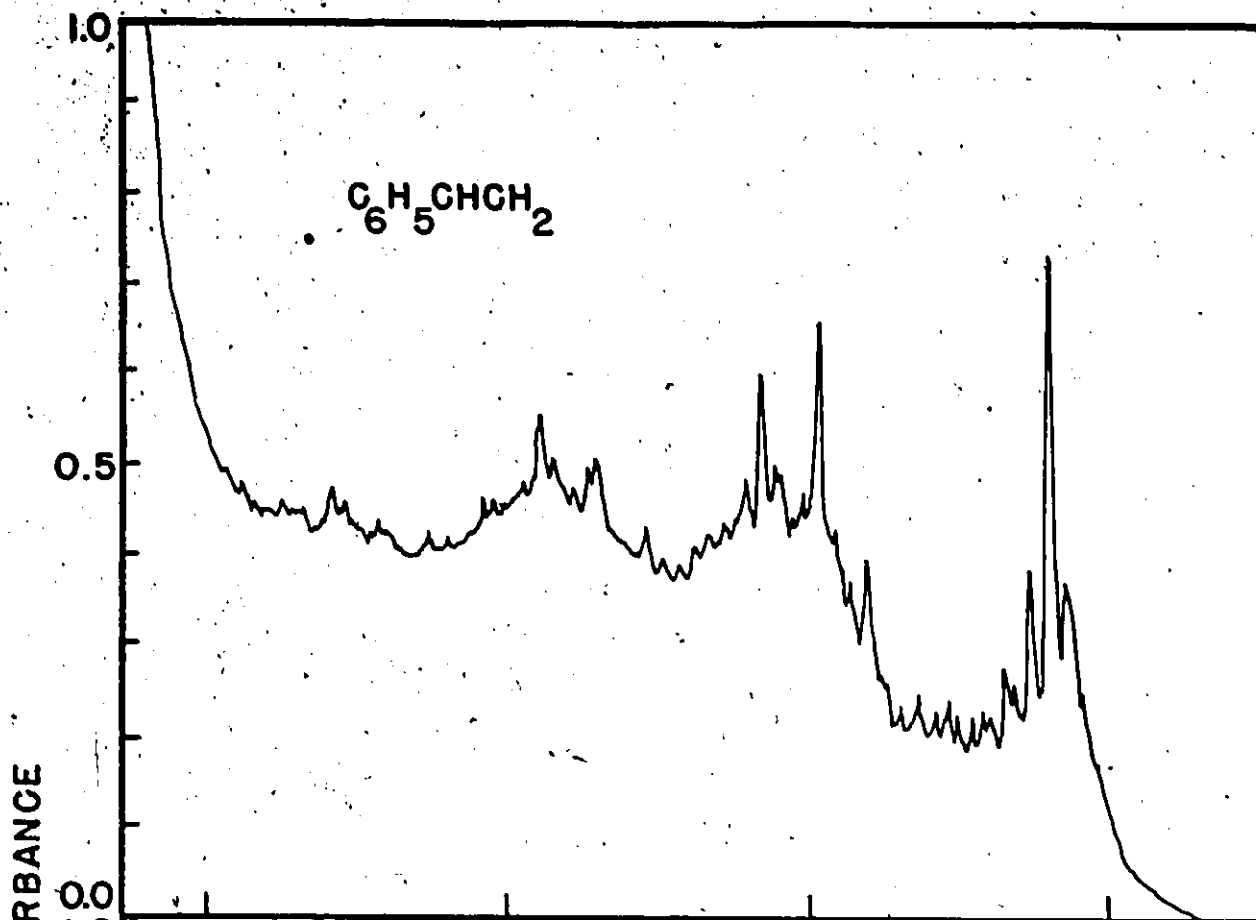


Figure 5.5
The $\tilde{A}-\tilde{X}$ Vapor Phase Absorption Spectra of
 $C_6D_5CHCH_2$ and $C_6D_5CDCD_2$.

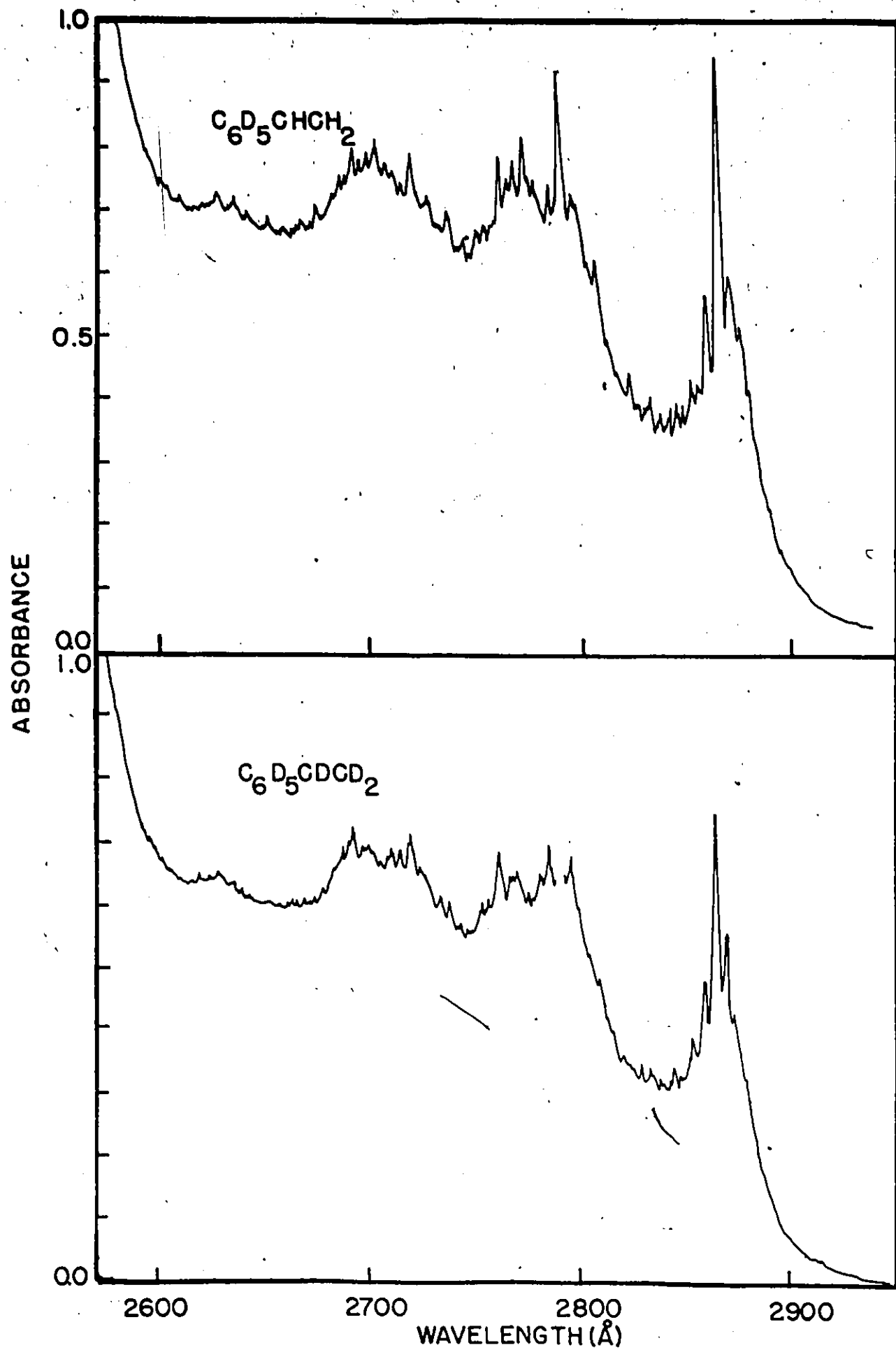


Table 5.3

0,0 Shifts from Vapor to Solid Solution in Some
Substituted Benzenes^a

Molecule	Solvent	Red Shift of 0,0 Band (cm ⁻¹)	References
Toluene	Cyclohexane	313 ^b	162,163
Phenylacetylene	Isopentane	353 ^c	6,161
Benzonitrile	Cyclohexane	445 ^b	164,8
Phenylisocyanide	Methylcyclohexane	291 ^c	7,10
Indene	Decalin	426 ^c	165,166

a: all low temperature spectra at 77 K.

b: Vapor phase emission 0,0 energy used to calculate red shift.

c: Vapor phase absorption 0,0 energy used to calculate red shift.

and is not a false origin produced by vibronic coupling. Rotational analysis of this band⁽²⁴⁾ indicates that the first singlet-singlet transition is a-axis polarized, contrary to the result of other monosubstituted benzenes.

The fluorescence excitation spectra are sufficiently resolved that at least a partial vibrational analysis can be performed. These are found in Tables 5.4 and 5.5. Since not much information exists about the vibrational frequencies of excited singlet states of monosubstituted benzenes, it is difficult to give unambiguous attributions to all the bands seen. Table 5.6 gives a list of some excited state fundamental frequencies in some monosubstituted benzenes. With the aid of this Table, and with a knowledge of expected isotopic shifts, several excited state frequencies can be assigned with confidence. The first two bands to the blue of the 0,0 band in $C_6H_5CHCH_2$ are assigned to the $0, \nu'_{29}$ and $0, \nu'_{28}$ transitions, respectively (the prime indicates an excited state frequency). Evidence for these assignments comes from observation of bands in the deuterated styrenes of similar intensity at frequencies consistent with expected isotopic shifts for these two modes. The fourth band in the $C_6H_5CHCH_2$ spectrum, at 520 cm^{-1} to the blue of the origin, is probably better assigned to ring mode ν'_{26} than to vinyl group mode ν'_{27} , although the evidence of the isotopic shift is ambiguous. The value of 520 cm^{-1} is in good agreement with the frequencies found for this mode in the first excited singlet states

Table 5.4
 Vibrational Analysis of the Fluorescence Excitation Spectrum of
 $10^{-3}\text{M C}_6\text{H}_5\text{CHCH}_2$ and $10^{-3}\text{M C}_6\text{H}_5\text{CDCD}_2$ in Polycrystalline
 Methylcyclohexane at 77 K

$\bar{\nu}(\text{cm}^{-1})$	$\text{C}_6\text{H}_5\text{CHCH}_2$ $\Delta\bar{\nu}(\text{cm}^{-1})$	Assignment	$\bar{\nu}(\text{cm}^{-1})$	$\text{C}_6\text{H}_5\text{CDCD}_2$ $\Delta\bar{\nu}(\text{cm}^{-1})$	Assignment
34 365	0	0,0	34 400	0	0,0
34 625	260 (240) ^a	$\nu_{29}^{\prime b}$	34 600	200 (225)	ν_{29}^{\prime}
34 760	395 (395)	ν_{28}^{\prime}	34 760	360 (375)	ν_{28}^{\prime}
34 885	520 (525)	ν_{26}^{\prime}	34 905	505 (540)	ν_{26}^{\prime}
35 135	770 (750)	ν_{25}^{\prime}	35 130	730 (705)	ν_{25}^{\prime}
35 340	975 (955)	ν_{24}^{\prime}	35 370	970 (960)	ν_{24}^{\prime}
35 520	1155	$\nu_{25}^{\prime} + \nu_{28}^{\prime}$	35 640	1240 (1235)	ν_{18}^{\prime}
35 575	1210 (1205)	ν_{18}^{\prime}	35 790	1390	ν_{13}^{\prime}
35 650	1285	$\nu_{25}^{\prime} + \nu_{26}^{\prime}$	36 065	1665 (1660)	$\nu_{24}^{\prime} + \nu_{25}^{\prime}$
35 785	1420	ν_{13}^{\prime}	36 330	1930 (1910)	$2\nu_{24}^{\prime}$
35 845	1480	$\nu_{24}^{\prime} + \nu_{26}^{\prime}$	36 385	1985	
36 080	1715 (1680)	$\nu_{24}^{\prime} + \nu_{25}^{\prime}$	36 605	2205 (2200)	$\nu_{18}^{\prime} + \nu_{24}^{\prime}$
36 290	1925 (1890)	$2\nu_{24}^{\prime}$	36 765	2365	$\nu_{13}^{\prime} + \nu_{24}^{\prime}$
			36 820	2420	
36 545	2180 (2160)	$\nu_{18}^{\prime} + \nu_{24}^{\prime}$	37 030	2630 (2615)	$2\nu_{24}^{\prime} + \nu_{25}^{\prime}$
36 765	2400	$\nu_{13}^{\prime} + \nu_{24}^{\prime}$	37 320	2920 (2885)	$3\nu_{24}^{\prime}$
37 020	2655	$2\nu_{24}^{\prime} + \nu_{25}^{\prime}$			
37 285	2920 (2865)	$3\nu_{24}^{\prime}$			
	(3120)	$2\nu_{24}^{\prime} + \nu_{18}^{\prime}$			

a: Vapor phase absorption value in parentheses.

b: ' = excited state.

Table 5.5

Vibrational Analysis of the Fluorescence Excitation Spectrum of
 $10^{-3}\text{M C}_6\text{D}_5\text{CHCH}_2$ and $10^{-3}\text{M C}_6\text{D}_5\text{CDCD}_2$ in Polycrystalline
 Methylcyclohexane at 77 K

$\bar{\nu}(\text{cm}^{-1})$	$\text{C}_6\text{D}_5\text{CHCH}_2$ $\Delta\bar{\nu}(\text{cm}^{-1})$	Assignment	$\bar{\nu}(\text{cm}^{-1})$	$\text{C}_6\text{D}_5\text{CDCD}_2$ $\Delta\bar{\nu}(\text{cm}^{-1})$	Assignment
34 505	0	0,0	34 530	0	0,0
34 735	230 (225) ^a	$\nu_{29}^{\prime b}$	34 745	215 (215)	ν_{29}^{\prime}
34 875	370 (385)	ν_{28}^{\prime}	34 885	355 (360)	ν_{28}^{\prime}
35 010	505 (510)	ν_{26}^{\prime}	34 990	460	ν_{26}^{\prime}
35 235	730 (710)	ν_{25}^{\prime}	35 220	690 (665)	ν_{25}^{\prime}
35 340	835	ν_{19}^{\prime}	35 455	925 (915)	ν_{24}^{\prime}
35 430	925 (920)	ν_{24}^{\prime}	35 715	1185	ν_{18}^{\prime}
35 675	1170 (1145)	ν_{18}^{\prime}	35 835	1305 (1300)	ν_{13}^{\prime}
35 790	1285 (1295)	ν_{13}^{\prime}	35 915	1385	$\nu_{24}^{\prime} + \nu_{26}^{\prime}$
35 890	1385		36 130	1600 (1585)	$\nu_{24}^{\prime} + \nu_{25}^{\prime}$
36 140	1635 (1625)	$\nu_{24}^{\prime} + \nu_{25}^{\prime}$	36 255	1725	
36 255	1750	$\nu_{19}^{\prime} + \nu_{24}^{\prime}$	36 375	1845 (1835)	$2\nu_{24}^{\prime}$
36 345	1840 (1845)	$2\nu_{24}^{\prime}$	36 455	1925	
36 525	2020		36 590	2060	
36 730	2225 (2235)	$\nu_{13}^{\prime} + \nu_{24}^{\prime}$	36 765	2235 (2220)	$\nu_{13}^{\prime} + \nu_{24}^{\prime}$
36 880	2375		36 835	2305	
37 075	2570 (2570)	$2\nu_{24}^{\prime} + \nu_{25}^{\prime}$	37 285	2755	$3\nu_{24}^{\prime}$
37 270	2765 (2780)	$3\nu_{24}^{\prime}$			

a: Vapor phase absorption value in parentheses.

b: ' = excited state.

Table 5.6

Excited State Fundamental Frequencies of Some
Monosubstituted Benzenes

Mode ^a	$C_6H_5C\equiv CH^b$	$C_6H_5OH^c$	$C_6H_5NH_2^d$	$C_6H_5N\equiv C^e$	$C_6H_5C\equiv N^f$
t 6a	409.7	475.1	492.0		
r 12	716.7	782.7	797.8	722	702.0
p 1	943.9	934.8	953.3	937	938.1
s 6b	560.3	522.8		547	507.3
q 13	1191.3	1273.2	1307.2	1174	1181.9
a 9a	950.8	957.6			963.4
b 18a	1056.7	975.0			
u 9b	319	395.5			

a: See Table 4.6, footnote "a" for the references for these two notations.

b: Reference (6).

c: Reference (167).

d: Reference (138).

e: Reference (7).

f: Reference (4).

of other monosubstituted benzenes (Table 5.6)*.

The next three intense bands in the $C_6H_5CHCH_2$ excitation spectrum, at 770 cm^{-1} , 975 cm^{-1} and 1210 cm^{-1} to the blue of the origin band, are readily assigned as the $0, \nu'_{25}$, $0, \nu'_{24}$ and $0, \nu'_{18}$ transitions, respectively. The majority of the summation bands observed in the excitation spectrum involve these three modes. Hui and Rice⁽²⁶⁾ have made the same assignments for the corresponding bands in the absorption spectrum of styrene vapor.

The assignment of the band at 1420 cm^{-1} from the origin is more difficult, however. In $C_6H_5CDCD_2$, the vibrational structure of the excitation spectrum is very similar to that of $C_6H_5CHCH_2$, and the band corresponding to the 1420 cm^{-1} band in the latter molecule appears at 1390 cm^{-1} from the origin. A reasonable assignment for these two bands would be $0, \nu'_9$, in keeping with ν'_9 's appearance in the 77 K fluorescence spectrum. Further evidence in support of this assignment comes from the UV absorption spectra of a number of halogen- and methyl-substituted styrenes. Ansari and Sharma⁽¹⁶⁸⁾ have tabulated the assigned excited state C=C stretching frequencies for these substituted styrenes; their average is $\sim 1430\text{ cm}^{-1}$. For styrene itself the listed value of ν'_9 is 1484 cm^{-1} . However, Hui and Rice⁽²⁶⁾ have assigned this band to the $0, 2\nu'_{25}$ transition. A reassignment of this kind cannot

*Hollas et al⁽²⁷⁾ in their recent work on the absorption spectrum of styrene vapor assign $\nu'_{27} = 437.4\text{ cm}^{-1}$ and $\nu'_{26} = 544.6\text{ cm}^{-1}$.

be made for the corresponding bands in the spectra of the substituted styrenes, so that the assignment of these bands as fundamentals is probably correct. In any case, since ν_9 is a vibration associated with the vinyl group, the position of a $0, \nu_9'$ transition should not be greatly affected by ring deuteration. However, there are no prominent bands observed in the fluorescence excitation spectra of $C_6D_5CHCH_2$ and $C_6D_5CDCD_2$ about 1400 cm^{-1} to the blue of the origin. Instead, bands at 1285 cm^{-1} and 1305 cm^{-1} are seen in the spectra of $C_6D_5CHCH_2$ and $C_6D_5CDCD_2$ respectively. It is more likely then, that the bands at $1420/1390/1285/1305\text{ cm}^{-1}$ from the origin arise from a vibration essentially localized in the aromatic ring. An assignment of these bands as the $0, \nu_{13}'$ transition is made for the following reasons. From the recent two-photon excitation spectra of benzene- d_6 (169,170) the frequency of ν_{19}' , the vibrational mode from which ν_{13}' in styrene is derived, is 1209 cm^{-1} . Bands at $\sim 1280\text{ cm}^{-1}$ have been assigned to this mode in the UV absorption spectra of $C_6D_5C\equiv CH$ and $C_6D_5C\equiv CD$ (171). A recent valence force field calculation for the ${}^1B_{2u}$ state of benzene (172) predicts that ν_{19}' in C_6H_6 comes at 1407 cm^{-1} .

The only other band in the excitation spectra that may be assigned as a transition to a fundamental is the weak band appearing as a shoulder 835 cm^{-1} to the blue of the origin band in $C_6D_5CHCH_2$. A possible assignment for this band would be $0, \nu_{23}'$, since this vibration is active in the UV absorption spectra of several monosubstituted benzenes (see Table 5.6). However, the frequency drop upon excitation would then be

anomalously low for a ring C-D bending mode. Instead, this band is tentatively assigned to the $0, \nu_{19}'$ transition. The corresponding transition was also observed in the fluorescence spectrum of $C_6D_5CHCH_2$.

That the ground and first excited singlet state potential energy surfaces are similar is evidenced by the fair mirror-image relationship between the vibrational envelopes of the 77 K fluorescence and fluorescence excitation spectra. There are two main differences in the envelopes:

(i) whereas the $0, \nu_{26}$ band is more intense than the $0, \nu_{25}$ band in emission, the fluorescence excitation spectrum shows $0, \nu_{25}'$ much more intense than the $0, \nu_{26}'$ band. A similar effect is seen in the vapor phase absorption spectra of Hollas *et al*⁽²⁷⁾ when the intensity of the hot bands 25_1^0 and 26_1^0 are compared to those of the cold bands 25_0^1 and 26_0^1 . These authors suggested two possible explanations for this effect but did not pursue the problem further.

(ii) the $0, \nu_9$ band is strong and forms a progression in fluorescence, while it is very weak at best in fluorescence excitation. Perturbation by the solvent is not a factor causing this behaviour, since the same thing is seen in the vapor phase absorption and emission spectra^(27,30).

5.3 Discussion of the Fluorescence of the Styrenes

According to the Franck-Condon principle, if the geometry of the first excited singlet state is significantly different from that in the ground state, progressions are expected in

A these modes converting one state into the other. The work of Carreira and Towns⁽²²⁾ on the torsional potential function of styrene vapor indicates that the molecule is planar in its ground state. The vibrational analysis in Section 5.1 indicates that there is no activity in any out-of-plane vibrations, so it is likely that the first excited singlet state is planar as well. The progression in the totally symmetric ring breathing mode ν_{24} is indicative of a slightly expanded but still planar, aromatic ring. Rotational band contour analysis performed upon styrene vapor⁽²⁴⁾ has shown that there is an overall expansion of the molecule in the excited state, which is to be expected for a $\pi\pi^*$ transition. The other progression, in ν_9 , is interesting in view of the fact that there is only a weak $0, \nu_9'$ transition in the fluorescence excitation spectrum. As previously mentioned, the vapor phase absorption and emission spectra behave similarly. At 77 K, the fluorescence and fluorescence excitation $0,0$ bands coincide, so the absorbing and emitting states are one and the same. The progression in ν_9 is not long (three members) and has its maximum at the $0,0$ band, indicating that in the excited state the vinyl C=C double bond length is not much different from its value in the ground state. This would be the case if the electronic transition is mainly localized on the aromatic ring.

The vibrational analyses of the fluorescence spectra are similar for all four styrenes. Most of the observed bands constitute the allowed component of the spectrum. The false

origin is the $0, \nu_{26}$ transition and the forbidden component of the spectrum makes up ~20% of the total spectral intensity. It is interesting to compare the S_0-S_1 transition of styrene with those of some other exocyclic multiple bond monosubstituted benzenes, namely phenylacetylene, benzonitrile, and phenylisocyanide. It has been found in the UV absorption and fluorescence spectra of phenylacetylene^(6,9) and phenylisocyanide^(7,10) that most of the intensity is vibronic in origin. Benzonitrile, on the other hand, has a very strong allowed component in its spectrum compared to its forbidden component⁽⁸⁾.

One simple explanation that has been used to explain this differing behaviour of these isoelectronic molecules involves an energy gap argument. The amount of vibronic coupling involved in an electronic transition is inversely proportional to the difference in energy between the perturbed and perturbing electronic states (Equation 2.17). Assuming that the second-excited singlet state S_2 acts as the perturbing state, the appropriate energy differences are 0.75 eV for phenylacetylene⁽⁷⁾, 0.83 eV for phenylisocyanide⁽¹⁰⁾, and 1.04 eV for benzonitrile⁽⁷⁾. These energy values correlate well with the amount of forbidden character found in the $\tilde{A}-\tilde{X}$ transitions of these molecules.

Albrecht⁽¹⁷³⁾, using the Herzberg-Teller formalism for vibronic transitions, has found that the amount of "forbidden" character is sensitive to the exact nature of the mixing electronic wavefunctions. He determined that the matrix

element is small when one of the states is of charge-transfer character and the other one is not. When both states are largely non-charge-transfer, the matrix element is large. No simple predictions can be made when both states are charge-transfer. Muirhead et al⁽⁷⁾ have correlated the change in dipole moment upon excitation with the percent allowed character in the $\tilde{A} \leftarrow \tilde{X}$ transitions of several benzene derivatives. Transitions with a large $\Delta\mu$ have a large percentage of allowed character, and vice versa. For example, benzonitrile has a $\Delta\mu$ of 0.31 D and has 80% allowed character in its absorption spectrum, whereas phenylacetylene and phenylisocyanide have $\Delta\mu$ values of 0.14 D and 0.13 D respectively, and each has 25% allowed character. The magnitude of $\Delta\mu$ is a measure of the extent of intramolecular charge transfer occurring on excitation, so that the findings of Muirhead et al are consistent with those of Albrecht so long as one assumes that the perturbing S_2 state is not charge-transfer in character and does not vary much from compound to compound.

Muirhead et al⁽⁷⁾ were of the opinion that the very small value of the change in dipole moment for the styrene molecule ($|\Delta\mu| = 0.13 \text{ D}$ ⁽²⁵⁾) in addition to the small energy separation between the first two excited singlet states ($E_{S_2} - E_{S_1} = 0.55 \text{ eV}$, measured from the first bands of the corresponding transitions) indicate that vibronic coupling plays a large part in the $\tilde{A} \leftarrow \tilde{X}$ absorption system, and that in all likelihood the previously assigned 0,0 band for styrene is really a vibronic origin. The present work has shown that

this is not the case, and that there is only a small amount of vibronic coupling involved in the transition. To get a small forbidden component, two possibilities arise which reinforce each other:

(i) King and van Putten⁽⁴⁹⁾ have calculated that the lowest excited 1A_1 state in styrene results from a transition between two delocalized orbitals, whereas the lowest 1B_2 state results from nearly equal two-way electron traffic which have opposite charge-transfer contributions. The \tilde{A} state has 1A_1 symmetry (in C_{2v}), as suggested in the previous section. Then if the perturbing state is S_2 , with its energy separation from S_1 very favorable for vibronic mixing, the perturbation matrix element $\langle \psi_{S_2}^0 | \hat{H}' | \psi_{S_1}^0 \rangle$ must be small. Following Albrecht⁽¹⁷³⁾, S_2 must have some degree of charge-transfer character.

(ii) Higher energy singlet states S_n are the appropriate perturbing states, but are burdened with unfavorable energy denominators ($E_{S_3} - E_{S_1} = 1.5$ eV, measured from the first bands of the $S_3 \rightarrow S_0$ and $S_1 \rightarrow S_0$ absorption spectra).

Kimura and Nagakura⁽¹⁷⁴⁾ have performed calculations on styrene estimating the degree of charge-transfer character in the \tilde{B} (or S_2) state. They found that charge-transfer configurations contribute 58% to the character of this state. This lends credence to the above possibilities for the small degree of vibronic interaction in the $\tilde{A} \rightarrow \tilde{X}$ fluorescence spectrum of styrene.

CHAPTER SIX

PHOTOPHYSICS OF THE STYRENES

The fluorescence decay times of aerated solutions of styrene in cyclohexane at concentrations of 0.1 and 0.2 ml/liter have been reported as 6.5 and 5.1 ns respectively⁽⁴¹⁾. Berlman⁽⁴²⁾ reported a lifetime of 11.4 ns for 2×10^{-3} M styrene in deoxygenated cyclohexane solution, while Crosby and Salisbury⁽³⁹⁾ give 12.5 ns for the decay time of styrene in cyclohexane, although the concentration the last-named workers used was not given. More recently, Lyons and Turro⁽⁴⁰⁾ reported a lifetime of 21.7 ns for a dilute ($\sim 2 \times 10^{-5}$ M) solution of styrene in cyclohexane. However, this τ_f was obtained just from a plot of the logarithm of the intensity versus time, and was not corrected for the temporal width of the excitation source⁽¹⁷⁵⁾.

The fluorescence lifetimes and quantum yields of the four styrenes are contained in Table 6.1. It was found that room temperature samples of styrene-h₈ exhibited a concentration-dependent lifetime. For example, a 1×10^{-3} M styrene solution has a lifetime which is shorter than that for a 5×10^{-5} M solution by slightly more than one ns. The 11.4 ns lifetime reported by Berlman⁽⁴²⁾ for a 2×10^{-3} M solution is shorter still. The trend toward a shorter decay time with increasing concentration was also observed by Basile in air-saturated cyclohexane solutions⁽⁴¹⁾. What is interesting is

Table 6.1

Fluorescence Lifetimes, Quantum Yields and Rate Constants for the Styrenes

Solvent	Solute ^a	Fluorescence Lifetime (ns)		Fluorescence Quantum Yield	Rate Constants $\times 10^{-7}$ (s ⁻¹)				
		298 K	77 K		k_f	k_{nr}	$k_f + k_{nr}$		
3-Methylpentane	C ₆ H ₅ CHCH ₂	14.6	18.8	0.24	0.46	1.6	2.4	5.2	2.9
	C ₆ H ₅ CDCD ₂	14.8	19.1	0.24(0.26)	0.46	1.7	2.4	5.1	2.8
	C ₆ D ₅ CHCH ₂	14.9	19.4	0.24(0.25)	0.50	1.7	2.6	5.0	2.6
	C ₆ D ₅ CDCD ₂	15.7	19.8	0.23(0.27)	0.52	1.7	2.6	4.7	2.4
Cyclohexane	C ₆ H ₅ CHCH ₂	13.9; 12.5 ^b 11.4 ^c ; 21.7 ^d		0.25; 0.15 ^b 0.22 ^e		1.8			5:4
	C ₆ H ₅ CDCD ₂	14.4		0.28		1.9			5.0
	C ₆ D ₅ CHCH ₂	14.4		0.25		1.7			5.2
	C ₆ D ₅ CDCD ₂	15.0		0.28		1.9			4.8

a: Concentrations are $\sim 1.3 \times 10^{-5}$ M in 3-methylpentane and $\sim 5.5 \times 10^{-5}$ M in cyclohexane.

b: Reference (39); concentration not given.

c: Reference (42); 2×10^{-3} M.

d: Reference (40); apparently the τ_f 's listed in this reference have not been corrected for the temporal width of the excitation source (175). Concentration is about 10^{-5} M.

e: Reference (40); relative to $\phi_f = 0.15$ for biphenyl. If $\phi_f = 0.18$ is used for biphenyl, ϕ_f for styrene becomes 0.26.

that the absorption and emission spectra of styrene overlap, to a fair extent at 77 K as shown in Chapter 5, but also at room temperature, where the separation of 0-0 bands in methylcyclohexane is small, $\sim 270 \text{ cm}^{-1}$. The room temperature absorption and emission spectra in cyclohexane given by Berlman⁽⁴²⁾ also show a region of spectral overlap. With increasing styrene concentration, self-absorption and re-emission of the fluorescence should be more pronounced, but such an effect should lengthen the observed lifetime^(119,176), contrary to the experimental results. It therefore seems that in more concentrated styrene solutions, some degree of self-quenching occurs, although no effects could be observed on the fluorescence spectrum. To obtain lifetime and quantum yield parameters that are approaching their molecular values, then, the styrene concentrations that were used to obtain the data given in Table 6.1 were fairly dilute. In the lifetime measurements, good fits to single exponential decays were obtained in all cases.

In general, the fluorescence lifetimes increased with increasing deuteration. Vinyl group deuteration and ring deuteration had about the same effect. The decay times at 77 K were about 30% longer than those at room temperature. Room temperature ϕ_f 's were essentially independent of both solvent and isotope. At 77 K these yields increased by 100% over their room temperature values. Errors due to polarization effects in the low-temperature quantum yields were not considered to be important. The value of ϕ_f at 77 K for, say, styrene- h_8 relative to its value at room temperature was 0.48, as opposed

to 0.46 when 9,10-DPA at 77 K was the standard. The absorbing and emitting transition moment directions are nearly parallel for styrene but are perpendicular for 9,10-DPA when each is excited into its S_2 electronic state. However, the S_2+S_0 transitions in these molecules are diffuse, and as such the possibility of exciting absorption bands of different degrees of polarization exists, and this increases the emission isotropy.

Biphenyl was chosen as the fluorescence quantum yield standard in cyclohexane solvent because it emits in the same spectral region as do the styrenes. The quantum yield was taken as 0.18 in spite of the fact that the biphenyl concentration used in the present work was about 20-fold more dilute than that used by Berlmán and Steingraber⁽¹¹⁸⁾ in their determination of ϕ_f . If any concentration quenching of fluorescence occurs in biphenyl, which is not too likely because of the very small amount of spectral overlap of the absorption and the fluorescence⁽⁴²⁾, it should be reflected by a distinctly larger fluorescence decay time at the lower concentration. However, the lifetime obtained was 16.1 ns, which is essentially the same as the 16.0 ns value of Berlmán and Steingraber⁽¹¹⁸⁾.

The radiative rate constant k_f and the non-radiative rate constant k_{nr} were calculated using the relationships

$$\phi_f = \frac{k_f}{k_f + k_{nr}} \quad (6.1)$$

and

$$\tau_f = \frac{1}{k_f + k_{nr}} \quad (6.2)$$

and are also contained in Table 6.1. The room temperature results for the styrenes in both cyclohexane and 3-MP indicate that k_f is independent of isotope, as is to be expected for an electronically allowed transition. Also, k_f is independent of solvent after correction for the index of refraction of the medium⁽¹⁷⁶⁾ by the equation

$$k_f^0 = \frac{k_f}{n^2} \quad (6.3)$$

This equation has been verified for several solutes in both hydrocarbon and ethanolic solvents over a wide temperature range⁽¹⁷⁷⁾. Using the average k_f over the four isotopes in each solvent, $k_f^0 = 0.9 \times 10^7 \text{ sec}^{-1}$. A calculation of k_f based on the integrated absorption intensity of the $\tilde{A}+\tilde{X}$ transition was not carried out because of the large amount of overlap this transition has with the more intense $\tilde{B}+\tilde{X}$ transition. However, an oscillator strength of the $\tilde{A}+\tilde{X}$ transition has been reported⁽¹⁷⁴⁾, and an approximate k_f can be calculated using the relationship⁽¹⁷⁸⁾

$$\tau_r = \frac{1}{k_f} = \frac{1.5}{f\bar{\nu}^2} \quad (6.4)$$

where f is the oscillator strength, $\bar{\nu}$ is the wavenumber of the absorption. Taking $f=0.02$ ⁽¹⁷⁴⁾ and $\bar{\nu}=37000 \text{ cm}^{-1}$ (an average absorption frequency), k_f then becomes $1.8 \times 10^7 \text{ sec}^{-1}$, in reasonable agreement with the experimental results.

At first glance the 77 K results in 3-methylpentane in Table 6.1 point to an increase in k_f by about 50% compared

to the room temperature values. Zimmerman et al found a similar result for the structurally similar 1-phenylcycloalkenes^(179,180). Most of this increase, however, can be attributed to the refractive index n of 3-methylpentane increasing from the high to the low temperature. The calculated value of n at 77 K is based on the formula^(120,180)

$$\frac{n^2(T)-1}{\rho(T)\{n(T)+0.4\}} = b \quad (6.5)$$

where the parameter b is evaluated from the room temperature refractive index and density ρ , and the density at low temperature is available from contraction data. The values of n and ρ are 1.3765 and 0.6643 g/ml respectively⁽¹⁸¹⁾. Also, $V(77 \text{ K})/V(293 \text{ K}) = 0.7845 \pm 0.0006$ for 3-methylpentane⁽¹⁸²⁾. Using these data, $n(77 \text{ K}) = 1.489$. The experimentally observed k_f can now be corrected according to Equation 6.3 to give $k_f = 1.1 \times 10^7 \text{ sec}^{-1}$. Comparison with the room temperature value of k_f of $0.9 \times 10^7 \text{ sec}^{-1}$ shows that the temperature variation is not significant. This effect has been observed in other systems^(53,68,183,184).

In general, the non-radiative rate constant k_{nr} can be written as

$$k_{nr} = k_{isc} + k_{ic} \quad (6.6)$$

where k_{isc} represents the intersystem crossing rate constant and k_{ic} is the rate constant for internal conversion. It has

been demonstrated, however, that trans- β -styrene- d_1 undergoes direct trans-cis photoisomerization⁽²⁶⁾. Assuming that the isomerization proceeds through the singlet manifold, as has been demonstrated for trans-stilbene⁽¹⁸⁵⁾, Equation 6.6 can be expressed as

$$k_{nr} = k_{isc} + k_{isom} + k'_{ic} \quad (6.7)$$

with k'_{ic} representing internal conversion pathways other than isomerization. It has also been assumed, as was done by Crosby and Salisbury⁽³⁹⁾, that k_{isc} is relatively unimportant in styrene. The basis of this assumption is the small value of ϕ_{isc} in a series of 1-phenylcycloalkenes^(179,180). Thus the lack of a significant deuterium isotope effect on k_{nr} is interpreted chiefly as the lack of an isotope effect of k_{isom} and k'_{ic} . That the majority of k_{nr} is found in k_{isom} is implied by the work of Crosby and Salisbury⁽³⁹⁾, who suggest that in styrenes with hydrogen atoms on carbons α to the double bond, a photochemical non-radiative pathway exists. Styrene, having no such hydrogen atoms, has the same value of k_{nr} as trans- β -t-butylstyrene, and it is lower than k_{nr} for several vinyl-substituted methylstyrenes.

The rate parameters calculated from the low temperature lifetimes and quantum yields show that non-radiative processes are still important at 77 K. This is in contrast to the results of studies of the temperature dependence of the fluorescence lifetime and quantum yield of trans-stilbene⁽⁶⁸⁻⁷⁰⁾ in which at 77 K, fluorescence is almost completely dominant.

This may indicate that there is a distinct difference in the shape of the torsional potential function, leading to isomerization, between styrene and stilbene. A difference is seen in the theoretical calculation of the lower excited singlet states of these molecules by ab initio-CI methods^(50,66).

For stilbene, excitation to S_1 is predicted to be followed by rotation about the C=C bond to the S_2 surface, which is isoenergetic or even lower than S_1 at rotation angles approaching 90° . Internal conversion is now enhanced since the energy gap has been minimized. In the case of styrene, an S_1 potential curve with a low barrier to torsion is calculated.

An additional factor to be considered is the effect of viscosity on photoisomerization processes. It is known⁽¹⁸⁶⁾ that a dependence of a molecular rearrangement on the viscosity of the medium may be seen if an increase in volume occurs somewhere along the path from the excited singlet state of the reactant to the product's ground state. In the specific case of cis-trans photoisomerization of olefins, it is the rotation about the double bond that provides the increase in molecular volume. If the rotating parts of styrene and stilbene are compared, it can be argued that the increase in volume will be much smaller for rotation in styrene than for rotation in stilbene, due to stilbene's phenyl group. It is possible, then, that the smaller size of styrene makes an increase in viscosity less effective at hindering isomerization, compared to stilbene. To see if a further increase in viscosity would significantly decrease the rate of non-

radiative decay, the fluorescence decay time of a 4×10^{-5} M solution of styrene- h_8 in methylcyclohexane at 77 K was measured. The viscosity of methylcyclohexane glass at 77 K is 1.2×10^{18} p⁽¹⁸⁷⁾ whereas the viscosity of 3-methylpentane glass at 77 K is 2.2×10^{12} p⁽¹⁸⁸⁾. The lifetime obtained was 18.5 ns, indicating that at least in the range of high viscosities, the presence of non-radiative processes at 77K in styrene cannot be accounted for by the effects of viscosity.

In order to try to assess the validity of the assumption that k_{isc} is unimportant in styrene, the intersystem crossing pathway was circumvented by the use of a triplet sensitizer, acetophenone. Observation of phosphorescence following transfer would indicate that k_{isc} from S_1 indeed was small. First the singlet-triplet absorption spectrum of styrene- h_8 in ethyl iodide (1:1 by volume) was obtained. The lowest wavelength band was at 463 nm, in very good agreement with the results of oxygen-enhanced absorption spectra of Evans⁽¹⁸⁹⁾ and Crosby et al⁽¹⁹⁰⁾. Phosphorescence lifetimes of 2×10^{-2} M solutions of acetophenone in diethyl ether-isopentane glass (1:1 by volume) at 77 K were measured as a function of the concentration of added styrene. The results are shown in Figure 6.1. The 14 ms lifetime without styrene addition decreased markedly with increasing styrene concentration, indicating that triplet-triplet transfer was occurring. Also, when steady-state excitation was used, the intensity of phosphorescence was markedly less to the eye when styrene was present. However, no difference was detected in the phos-

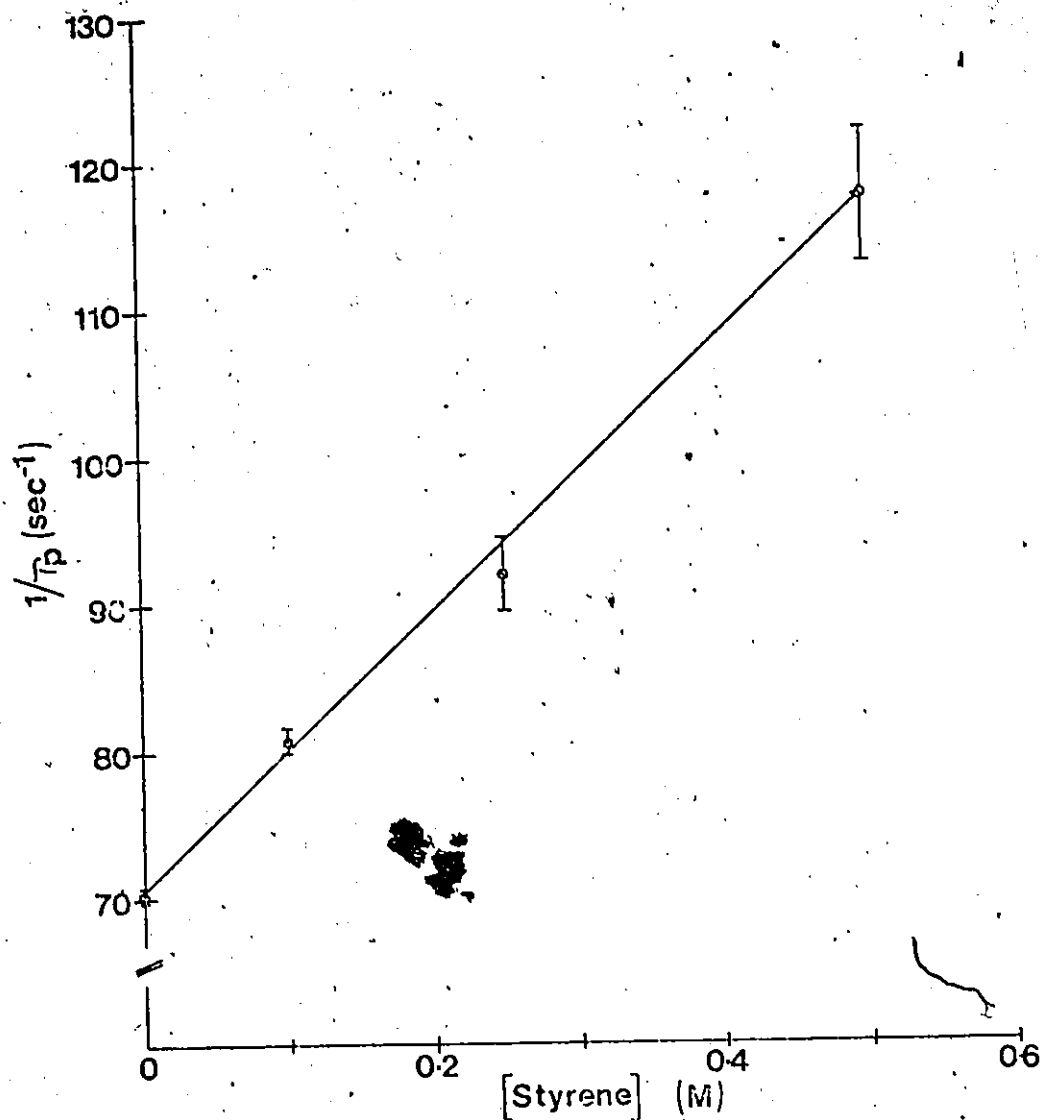


Figure 6.1 Plot of $\frac{1}{\tau_p}$ for Acetophenone vs Styrene Concentration ($\{C_6H_5COCH_3\} = 2 \times 10^{-2}$ M).

phorescence spectrum between samples with and without styrene. Perdeuteration would be expected to reduce the relative contribution of k_{nr} compared to styrene, but no phosphorescence was detected when styrene- d_8 was the acceptor. A possible explanation for the very efficient radiationless deactivation of styrene's triplet state is that there is a deep absolute minimum in the torsional potential function at a rotation angle of 90° , similar to what is thought to exist for triplet stilbene^(63,65). At the perpendicular geometry the S_0 and T_1 states are close in energy, with the result a rapid intersystem crossing and no phosphorescence. Very recently⁽¹⁹¹⁾ absorption from the twisted triplet state of styrene and several of its derivatives has been observed.

CHAPTER SEVEN

SUMMARY

The liquid phase infrared and Raman spectra of styrene- h_8 , $-d_3$, $-d_5$ and $-d_8$ have been investigated, with the aid of Raman depolarization ratios and vapor phase infrared band contours. Changes have been made to the assignments of previous investigators, and plausible assignments made for the large majority of the 42 normal modes of vibration in each molecule.

The fluorescence and fluorescence excitation spectra of dilute solutions of the four isotopic styrenes in polycrystalline methylcyclohexane at 77 K have also been studied. The fluorescence spectra, while they are not a good example of quasi-linearity, are still sufficiently resolved that an analysis of the vibrational sub-structure can be performed, using the ground state fundamental frequencies obtained from the analysis of the vibrational spectra. Qualitative use of the Franck-Condon principle indicates that styrene is fluorescing from a planar excited state configuration. This result has also been found for a number of substituted benzenes.

From the coincidence of bands in the fluorescence and fluorescence excitation spectra of each of the four styrenes, the position of the electronic origin has been established. Using this information in conjunction with the magnitude of the red shift between the origin band proposed from previous vapor phase studies and the low temperature origin, the 1A_1 nature

(in C_{2v} notation) of the \tilde{A} state of styrene has been confirmed.

The fluorescence spectra show the presence of a forbidden component, which is based on one quantum of ν_{26} . Although this vibration is of a' symmetry in C_s symmetry styrene, it is derived from the degenerate e_{2g} vibration in benzene; this latter vibration serves as a false origin in benzene's fluorescence spectrum. The forbidden component contributes to only a minor degree to the total fluorescence intensity. This result is at variance with what would be expected on the basis of a simple inverse energy gap argument that seems to be followed by a number of monosubstituted benzenes.

Analysis of the fluorescence excitation spectra has enabled several excited state fundamental frequencies to be identified for each isotope. There is a fair mirror symmetry relationship between the fluorescence and fluorescence excitation spectra. The resolved nature of the excitation spectra indicate that a Shpol'skii matrix (or also an inert gas matrix) could be used with a source of monochromatic light that can be scanned through a given wavelength range, such as a tunable dye laser, to obtain highly resolved excitation spectra which would be much simpler to analyze than conventional vapor phase absorption spectra.

Fluorescence quantum yield and lifetime data have been obtained for each of the four isotopes of styrene, in cyclohexane and 3-methylpentane at room temperature and in 3-MP at 77 K. There is a constancy of the radiative rate constant with isotope, and also with solvent and temperature after correcting for the change in refractive index with these quantities. There is only a very slight decrease in the non-

radiative rate constant k_{nr} with deuterium substitution. A much larger decrease in k_{nr} is obtained by cooling a room temperature sample to 77 K. The efficiency of non-radiative decay from the \tilde{A} state is still appreciable, however. A hydrocarbon solvent of much higher viscosity at 77 K did not affect the fluorescence decay time appreciably, nor presumably the non-radiative rate. At 77 K non-radiative pathways, principally cis-trans isomerization, can still compete with fluorescence, as opposed to the situation in trans-stilbene, where $\phi_f \approx 1$ at 77 K.

Triplet-triplet electronic energy transfer studies from acetophenone to styrene at 77 K were carried out in an effort to observe phosphorescence from styrene. Although transfer of excitation energy did occur, phosphorescence from the acceptor was not detected. Similar results were obtained when styrene- d_8 was used as the acceptor. These results indicate very efficient radiationless deactivation from triplet styrene.

As for possible future experiments in the areas covered by this work, the fluorescence spectra of the styrenes could be further sharpened by using a perfluorohydrocarbon, for example perfluoromethylcyclohexane, as the low-temperature solvent so as to decrease solute-solvent interactions. A study of the fluorescence lifetimes and quantum yields over a range of temperatures and over a range of viscosities would help to elucidate the effect that each has on the rates of fluorescence and non-radiative decay. A measurement of ϕ_{isc} for styrene itself would quantify the importance of intersystem crossing. Finally the use

of an isotopic species such as trans- β -styrene- d_1 would enable isomerization, either direct or sensitized, to be detected, and the isomerization of styrene under different conditions of temperature, solvent, etc., could be investigated.

BIBLIOGRAPHY

1. J. Stark; Z. Physik. 8, 81 (1907).
2. J. Stark and R. Meyer; Z. Physik. 8, 250 (1907).
3. R.C. Hirt and J.P. Howe, J. Chem. Phys. 16, 480 (1948).
4. H.T. Tan and P.J. Thistlethwaite, J. Chem. Phys. 58, 4408 (1973).
5. W.W. Robertson, J.F. Music and F.A. Matsen, J. Amer. Chem. Soc. 72, 5260 (1950).
6. G.W. King and S.P. So, J. Mol. Spectrosc. 37, 543 (1971).
7. A.R. Muirhead, A. Hartford, K.T. Huang and J.R. Lombardi, J. Chem. Phys. 56, 4385 (1972).
8. G.L. LeBel and J.D. Laposa, J. Mol. Spectrosc. 41, 249 (1972).
9. H. Singh and J.D. Laposa, J. Luminescence 5, 32 (1972).
10. R.A. Nalepa and J.D. Laposa, J. Luminescence 8, 429 (1974).
11. K.S. Pitzer, L. Guttman and E.F. Westrum, J. Amer. Chem. Soc. 68, 2209 (1946).
12. R. Stair and W.W. Coblenz, J. Res. Nat. Bur. Stand. 15, 295 (1935).
13. D. Williams, Physics 7, 399 (1936).
14. M. Bourguel, Compt. Rend. 194, 1736 (1932).
15. M. Bourguel, Compt. Rend. 195, 311 (1932).
16. S. Mizushima, Y. Morino and T. Inoue, Bull. Chem. Soc. Japan 12, 136 (1937).
17. N.K. Roy, Indian J. Phys. 28, 365 (1954).
18. W.G. Fateley, G.L. Carlson and F.E. Dickson, Appl. Spectrosc. 22, 650 (1968).

19. W.D. Moss and G. Zundel, *Spectrochim. Acta* 26A, 1109 (1970).
20. T.R. Gilson, J.M. Hollas, E. Khalilipour and J.V. Warrington, *J. Mol. Spectrosc.* 73, 234 (1978).
21. J.H.S. Green and D.J. Harrison, *Spectrochim. Acta* 33A, 249 (1977).
22. L.A. Carreira and T.G. Towns, *J. Chem. Phys.* 63, 5283 (1975).
23. J.V. Morgan, *J. Amer. Chem. Soc.* 75, 5055 (1953).
24. A. Hartford, Jr. and J.R. Lombardi, *J. Mol. Spectrosc.* 35, 413 (1970).
25. H. Parker and J.R. Lombardi, *J. Chem. Phys.* 54, 5095 (1971).
26. M.H. Hui and S.A. Rice, *J. Chem. Phys.* 61, 833 (1974).
27. J.M. Hollas, E. Khalilipour and S.N. Thakur, *J. Mol. Spectrosc.* 73, 240 (1978).
28. J.K. Marsh, *J. Chem. Soc.* (1923), 3315.
29. R. Titeica, *Ann. Comb. Liquides* 11, 443 (1936).
30. R. N. Singh, *Indian J. Pure Appl. Phys.* 4, 1 (1966).
31. H. Konschin, F. Sundholm and G. Sundholm, *Acta Chem. Scand.* 30B, 262 (1976).
32. I. Penchev and S. Simeonov, *Dokl. Bolg. Akad. Nauk.* 23, 1341 (1970).
33. L. Grajcar and J. Baudet, *J. Mol. Structure* 38, 121 (1977).
34. R.P. Steer, M.D. Swords, P.M. Crosby, D. Phillips and K. Salisbury, *Chem. Phys. Lett.* 43, 461 (1976).
35. K.P. Ghiggino, D. Phillips, K. Salisbury and M.D. Swords, *J. Photochem.* 7, 141 (1977).

36. K.P. Ghiggino, K. Hara, G.R. Mant, D. Phillips, K. Salisbury, R.P. Steer and M.D. Swords, *J. Chem. Soc. Perkin II*, 88 (1978).
37. K.P. Ghiggino, K. Hara, K. Salisbury and D. Phillips, *J. Photochem.* 8, 267 (1978).
38. K.P. Ghiggino, K. Hara, K. Salisbury and D. Phillips, *J. Chem. Soc. Faraday II* 73, 607 (1977).
39. P.M. Crosby and K. Salisbury, *Chem. Commun.* 477 (1975).
40. A.L. Lyons, Jr. and N.J. Turro, *J. Amer. Chem. Soc.* 100, 3177 (1978).
41. L.J. Basile, *J. Chem. Phys.* 36, 2204 (1962).
42. I. B. Berlman, Handbook of Fluorescence Spectra of Aromatic Molecules, Academic Press, New York, 1965.
43. J. Christoffersen, J.M. Hollas and G.H. Kirby, *Proc. Roy. Soc. (London) A* 307, 97 (1968).
44. T. Cvitas, *Mol. Phys.* 19, 297 (1970).
45. G.H. Kirby, *Mol. Phys.* 19, 289 (1970).
46. T. Cvitas and J.M. Hollas, *Mol. Phys.* 18, 101 (1970).
47. J. Christoffersen, J.M. Hollas and G.H. Kirby, *Mol. Phys.* 16, 441 (1969).
48. J.C.D. Brand and P.D. Knight, *J. Mol. Spectrosc.* 36, 328 (1970).
49. G.W. King and A.A.G. van Putten, *J. Mol. Spectrosc.* 44, 286 (1972).
50. G.L. Bendazzoli, G. Orlandi, P. Palmieri and G. Poggi, *J. Amer. Chem. Soc.* 100, 392 (1978).
51. E.W. Schlag, S. Schneider and S.F. Fischer, *Ann. Rev. Phys. Chem.* 22, 465 (1971).

52. E.C. Lim and J.D. Laposa, J. Chem. Phys. 41, 3257 (1964).
53. J.D. Laposa, E.C. Lim and R.E. Kellogg, J. Chem. Phys. 42, 3025 (1965).
54. J.B. Birks, Chem. Phys. Lett. 38, 437 (1976)..
55. E. Heumann, W. Triebel, R. Uhlmann and B. Wilhelmi, Chem. Phys. Lett. 45, 425 (1977).
56. R. Benson and D.F. Williams, J. Phys. Chem. 81, 245 (1977).
57. O. Teschke, E.P. Ippen and G.R. Holtom, Chem. Phys. Lett. 52, 233 (1977).
58. L.A. Brey, G.B. Schuster and H.G. Drickamer, J. Amer. Chem. Soc. 101, 1 (1979).
59. F. Heisel, J.A. Miede and B. Sipp, Chem. Phys. Lett: 61, 115 (1979).
60. B.I. Greene, R.M. Hochstrasser and R.B. Weisman, Chem. Phys. Lett. 62, 427 (1979).
61. O. Teschke, Chem. Phys. Lett. 62, 573 (1979).
62. B.I. Greene, R.M. Hochstrasser and R.B. Weisman, J. Chem. Phys. 71, 544 (1979).
63. G. Orlandi and G.C. Marconi, Chem. Phys. 8, 458 (1975).
64. G. Orlandi and W. Siebrand, Chem. Phys. Lett. 30, 352 (1975).
65. D.A. Luippold, Chem. Phys. Lett. 35, 131 (1975).
66. G. Orlandi, P. Palmieri and G. Poggi, J. Amer. Chem. Soc. 101, 3492 (1979).
67. D.J.S. Birch and J.B. Birks, Chem. Phys. Lett. 38, 432 (1976).
68. M. Sumitani, N. Nakashima, K. Yoshihara and S. Nagakura, Chem. Phys. Lett. 51, 183 (1977).
69. R.H. Dyck and D.S. McClure, J. Chem. Phys. 36, 2326 (1962).

70. S. Malkin and E. Fischer, J. Phys. Chem. 68, 1153 (1964).
71. M. Born and R. Oppenheimer, Ann. Physik. 87, 457 (1927).
72. G. Herzberg and E. Teller, Z. Physik. Chem. B 21, 410 (1933).
73. G.W. King, Spectroscopy and Molecular Structure, Holt, Rinehart and Winston, Inc., New York (1964).
74. D.P. Craig and R.D. Gordon, Proc. Roy. Soc. A 288, 69 (1965).
75. R.M. Hochstrasser and G.J. Small, J. Chem. Phys. 45, 2270 (1966).
76. G.R. Hunt and I.G. Ross, J. Mol. Spectrosc. 9, 50 (1962).
77. E.B. Wilson, J.C. Decius and P.C. Cross, Molecular Vibrations, McGraw-Hill Book Co., Inc. (1955).
78. G. Herzberg, Infrared and Raman Spectra, D. Van Nostrand Co., Inc., Princeton N.J. (1945).
79. W.M. Ralowski, P.J. Mjoberg and S.O. Ljungren, J. Mol. Structure 30, 1 (1976).
80. W.M. Ralowski, P.J. Mjoberg and S.O. Ljungren, J. Mol. Structure 31, 169 (1976).
81. O. Redlich, Z. Physik. Chem. B 28, 371 (1935).
82. M.H. Hui, P. De Mayo, R. Suau and W.R. Ware, Chem. Phys. Lett. 31, 257 (1975).
83. M. Mahaney and J.R. Huber, Chem. Phys. 9, 371 (1975).
84. J.R. Huber and M. Mahaney, Chem. Phys. Lett. 30, 410 (1975).
85. T. Oka, A.R. Knight and R.P. Steer, J. Chem. Phys. 63, 2414 (1975).
86. D.J. Clouthier, A.R. Knight and R.P. Steer, Chem. Phys. Lett. 59, 62 (1978).
87. J.N. Demas and G.A. Crosby, J. Phys. Chem. 75, 991 (1971).

88. W.R. Ware, Creation and Detection of the Excited State, Vol. 1, Part A, Chap. 5, A.A. Lamola, Ed., Marcel Dekker, New York (1971).
89. C. Lewis, W.R. Ware, L.J. Doemeny and T.L. Nemzek, Rev. Sci. Instrum. 44, 107 (1973).
90. A.E.W. Knight and B.K. Selinger, Aust. J. Chem. 26, 1 (1973).
91. L.J. Cline Love and L.A. Shaver, Anal. Chem. 48, 364A (1976).
92. J. Yguerabide, Methods in Enzymology, Vol. 26, Part C, p. 498, S.P. Colowick and N.D. Caplan, Eds., Academic Press, N.Y. (1972).
93. J.B. Birks and I.H. Munro, Progress in Reaction Kinetics 4, 239 (1967).
94. A.E. McKinnon, A.G. Szabo and D.R. Miller, J. Chem. Phys. 81, 1564 (1977).
95. D.V. O'Connor, W.R. Ware and J.C. André, J. Phys. Chem. 83, 1333 (1979).
96. A.E.W. Knight and B.K. Selinger, Spectrochim. Acta 27A, 1223 (1971).
97. A. Grinvald and I.Z. Steinberg, Anal. Biochem. 59, 583 (1974).
98. E.V. Shpol'skii, A.A. Il'ina and L.A. Klimova, Dokl. Akad. Nauk. SSSR 87, 935 (1952).
99. E.V. Shpol'skii and L.A. Klimova, Bull. Acad. Sci. SSSR, Phys. Ser. 18 357 (1954).
100. M. Koyanagi and L. Goodman, J. Chem. Phys. 55, 2959 (1971).
101. J. Olmsted and M.A. El-Sayed, J. Mol. Spectrosc. 40, 71 (1971).

102. V.J. Morrison and J.D. Laposa, *Spectrochim. Acta* 32A, 443 (1976).
103. S.H. Hankin, O.S. Khalil and L. Goodman, *Chem. Phys. Lett.* 63, 11 (1979).
104. A.N. Terenin and V.L. Ermolaev, *Dokl. Akad. Nauk. SSSR* 85, 547 (1952).
105. A.N. Terenin and V. Ermolaev, *Trans. Faraday Soc.* 52, 1042 (1956).
106. G. Heinrich, S. Schoof and H. Gusten, *J. Photochem.* 3, 315. (1974/75).
107. A. Nakajima, *Bull. Chem. Soc. Japan* 46, 2602 (1973).
108. J. B. Birks, D.J. Dyson and I.H. Munro, *Proc. Roy. Soc. A* 275, 575 (1963).
109. T.L. Nemzek, Ph. D. Thesis, University of Minnesota (1975).
110. N. Mataga, M. Tomura and N. Nishimura, *Mol. Phys.* 9, 367 (1965).
111. C.D. Amata, M. Burton, W.P. Helman, P.K. Ludwig and S.A. Rodemeyer, *J. Chem. Phys.* 48, 2374 (1968).
112. ORTEC, Inc., Application Note AN 35, Oak Ridge, Tenn. (1971).
113. W.R. Ware and B.A. Baldwin, *J. Chem. Phys.* 40, 1703 (1964).
114. P. di Marco and G. Giro, *Physica Status Solidi* 30A, K143 (1975).
115. P.R. Hartig, K. Sauer, C.C. Lo and B. Leskovar, *Rev. Sci. Instrum.* 47, 1122 (1976).
116. D.M. Rayner, A.E. McKinnon, A.G. Szabo and P.A. Hackett, *Can. J. Chem.* 54, 3246 (1976).
117. M.G. Badea and S. Georghiou, *Rev. Sci. Instrum.* 47, 314 (1976).

118. I.B. Berlman and O.J. Steingraber, *J. Chem. Phys.* 43, 2140 (1965).
119. J.V. Morris, M.A. Mahaney and J.R. Huber, *J. Phys. Chem.* 80, 969 (1976).
120. W.W. Mantulin and J.R. Huber, *Photochem. Photobiol.* 17, 139 (1973).
121. J.R. Huber, M.A. Mahaney and W.W. Mantulin, *J. Photochem.* 2, 67 (1973/74).
122. E.B. Wilson, *Phys. Rev.* 45, 706 (1934).
123. E.W. Schmidt, J. Brandmuller and G. Nonnenmacher, *Z. Elektrochem.* 64, 726 (1960).
124. N.B. Colthup, L.H. Daly and S.E. Wiberley, Introduction to Infrared and Raman Spectroscopy, 2nd ed., p. 247, Academic Press, New York (1975).
125. W.J. Potts and R.A. Nyquist, *Spectrochim. Acta* 15, 679 (1959).
126. R.R. Randle and D.H. Whiffen, Molecular Spectroscopy, pp. 111-23, Institute of Petroleum, London (1955).
127. D.H. Whiffen *J. Chem. Soc.* (1956), 1350.
128. J.H.S. Green, *Spectrochim. Acta* 17, 607 (1961).
129. G.W. King and S.P. So, *J. Mol. Spectrosc.* 36, 468 (1970).
130. R.A. Nalepa and J.D. Laposa, *J. Mol. Spectrosc.* 50, 106 (1974).
131. H.D. Bist, J.C.D. Brand and D.R. Williams, *J. Mol. Spectrosc.* 24, 402 (1970).
132. G. Varsanyi, Vibrational Spectra of Benzene Derivatives, Academic Press, New York (1969).

133. W.D. Mross and G. Zundel, *Spectrochim. Acta* 26A, 1097 (1970).
134. D.A. Condit, S.M. Craven and J.E. Katon, *Appl. Spectrosc.* 28, 420 (1974).
135. A.P. Hitchcock and J.D. Laposa, *J. Mol. Spectrosc.* 54, 223 (1975).
136. R.J. Jakobsen, *Spectrochim. Acta* 21, 127 (1965).
137. V.J. Morrison, M. Sc. Thesis, McMaster University (1975).
138. J.C.D. Brand, D.R. Williams and T.J. Cook, *J. Mol. Spectrosc.* 20, 359 (1966).
139. S.N. Garg, *Current Sci.* 23, 150 (1954).
140. J.H.S. Green and D.J. Harrison, *Spectrochim. Acta* 32, 1265 (1976).
141. G. Varsanyi, Assignments for Vibrational Spectra of Seven Hundred Benzene Derivatives, Adam Hilger, London (1974).
142. W.H. Fletcher, C.S. Shoup and W.T. Thompson, *Spectrochim. Acta* 20, 1065 (1964).
143. R.C. Lord and P. Venkateswarlu, *J. Opt. Soc. Amer.* 43, 1079 (1953).
144. D.H. Whiffen, *Spectrochim. Acta* 7, 253 (1955).
145. R.J. Jakobsen and F.F. Bentley, *Appl. Spectrosc.* 18, 88 (1964).
146. N. Sheppard and D.M. Simpson, *Quart. Rev. (London)* 6, 1 (1952).
147. F.R. Dollish, W.G. Fateley and F.F. Bentley, Characteristic Raman Frequencies of Organic Compounds, John Wiley and Sons, New York (1974).

148. B. Singh and R.M.P. Jaiswal, *Indian J. Pure Appl. Phys.* 9, 64 (1971).
149. B. Singh and R.M.P. Jaiswal, *Indian J. Pure Appl. Phys.* 9, 199 (1971).
150. L.J. Bellamy, *The Infrared Spectra of Complex Molecules*, 3rd ed., Halsted Press, New York (1975).
151. M. Farina and M. Peraldo, *Gazz. Chem. Italiana* 90, 973 (1960).
152. H. Hunziker and Hs. H. Gunthard, *Spectrochim. Acta* 21, 51 (1965).
153. S. Pinchas and I. Lauicht, *Infrared Spectra of Labelled Compounds*, Academic Press, London (1971).
154. J.K. Brown and N. Sheppard, *Trans. Faraday Soc.* 51, 1611 (1955).
155. W.G. Fateley, I. Matsubara and R.E. Witkowski, *Spectrochim. Acta* 20, 1461 (1964).
156. F.A. Miller, W.G. Fateley and R.E. Witkowski, *Spectrochim. Acta* 23A, 891 (1967).
157. K. Kuchitsu, *MTP International Review of Science, Physical Chemistry, Series 1, Vol. 2, Chap. 6*. G. Allen ed., Medical and Technical Publishing Co., Ltd., Oxford (1972).
158. K. Tamagawa, T. Iijima and M. Kimura, *J. Mol. Structure* 30, 243 (1976).
159. P.H. Hepburn and J.M. Hollas, *Mol. Phys.* 26, 377 (1973).
160. M.A. Shashidhar and K.S. Rao, *Current Sci.* 44, 154 (1975).
161. T.S. Zhuravleva, R.N. Nurmukhametov, Y.I. Kozlov and D.N. Shigorin, *Opt. and Spectrosc.* 22, 489 (1967).
162. L. Watmann-Grajcar, *J. Chim. Phys.* 66, 1023, (1969).

163. J. Kahane-Paillous and S. Leach, *J. Chim. Phys.* 55, 439 (1958).
164. A.M. Bass, *J. Chem. Phys.* 18, 1403 (1950).
165. A. Hartford, Jr. and J.R. Lombardi, *J. Mol. Spectrosc.* 34, 257 (1970).
166. B. Brocklehurst and D.N. Tawn, *Spectrochim. Acta* 30A, 1807 (1974).
167. H.D. Bist, J.C.D. Brand and D.R. Williams, *J. Mol. Spectrosc.* 24, 413 (1970).
168. B.J. Ansari and D. Sharma, *Indian J. Pure Appl. Phys.* 6, 614 (1968).
169. L. Wunsch, H.J. Neusser and E.W. Schlag, *Chem. Phys. Lett.* 31, 433, (1975).
170. L. Wunsch, F. Metz, H.J. Neusser and E.W. Schlag, *J. Chem. Phys.* 66, 386 (1976).
171. S.P. So, Ph. D. Thesis, McMaster University (1970).
172. M.J. Robey and E.W. Schlag, *J. Chem. Phys.* 67, 2775 (1977).
173. A.C. Albrecht, *J. Chem. Phys.* 33, 156 (1960).
174. K. Kimura and S. Nagakura, *Theor. Chim. Acta* 3, 164 (1965).
175. A.L. Lyons, Jr., private communication.
176. J.B. Birks, Photophysics of Aromatic Molecules, Wiley-Interscience, New York (1970).
177. R.B. Cundall and L.C. Pereira, *J. Chem. Soc. Faraday II* 68, 1152 (1972).
178. J.N. Murrell, The Theory of the Electronic Spectra of Organic Molecules, Chapman and Hall, Ltd., London (1963).
179. H.E. Zimmerman, K.S. Kamm and D.P. Werthemann, *J. Amer. Chem. Soc.* 96, 7821 (1974).

180. H.E. Zimmerman, K.S. Kamm and D.P. Werthemann, J. Amer. Chem. Soc. 97, 3718 (1975).
181. Handbook of Chemistry and Physics, 49th edition, R.C. Weast, ed., The Chemical Rubber Co. (1968).
182. K. Rosengren, Acta Chem. Scand. 16, 1421 (1962).
183. W.R. Dawson and J.L. Kropp, J. Phys. Chem. 73, 693 (1969).
184. J.L. Kropp, W.R. Dawson and M.W. Windsor, J. Phys. Chem. 73, 1747 (1969).
185. J. Saltiel, J. D'Agostino, E.D. Megarity, L. Metts, K. Neuberger, M. Wrighton and O.C. Zafiriu, Organic Photochemistry, Vol. 3, p. 1. O.L. Chapman, ed., Marcel Dekker, Inc., N.Y. (1973).
186. D. Gegiou, K.A. Muszkat and E. Fischer, J. Amer. Chem. Soc. 90, 12 (1968).
187. A.C. Ling and J.E. Willard, J. Phys. Chem. 72, 3349 (1968).
188. A.C. Ling and J.E. Willard, J. Phys. Chem. 72, 1918 (1968).
189. D.F. Evans, J. Chem. Soc. (1957), 1351.
190. P.M. Crosby, J.M. Dyke, J. Metcalfe, A.J. Rest, K. Salisbury and J.R. Sodeau, J. Chem. Soc. Perkin II, 182 (1977).
191. R. Bonneau, J. Photochem. 10, 439 (1979).